

MCG 4322[A]

FSAE Analysis Report

FSAE 2

by

AbdalAziz AlGhoul (300005268)

Hasan Shahzad (300001167)

Hisham Ali (300010128)

Peter Saroufim (300015864)

Munir Alsafi (300013845)

University of Ottawa
Department of Mechanical Engineering
November 33, 2021

Professor: Mihaita Matei
Design TA: Nathaniel Mailhot
Marking TA: Ahmed Taimah

Table of Contents

List of Figures	ix
1 Project Charter	1
1.1 Mandate	1
1.2 Requirements	1
1.3 Constraints	2
1.4 Criteria	3
1.5 Parameterization Outline	3
2 System Modelling	5
2.0.1 Suspension Geometry	5
2.0.2 Assumptions and Working Environment	9
2.1 Kinematics and Applied Forces	9
2.1.1 Dynamic Applied Forces	9
2.1.2 Impacts and Collisions	14
2.1.3 Aerodynamics	16
2.1.4 Steering	17
2.1.5 Steady State Low Speed Cornering Geometry and Vehicle Turning Radius	18
2.1.6 Pedals	19
2.1.7 Braking	22
2.1.8 Powertrain	25

3 Analysis	28
3.1 Chassis	28
3.1.1 Description of Inputs and Outputs	28
3.1.2 Assumptions and Materials	28
3.1.3 Stress Analysis	29
3.2 Suspension	37
3.2.1 Forces acting on Suspension Components	37
3.3 Steering Knuckle	43
3.3.1 Description of Inputs and Outputs	43
3.3.2 Constants and Safety Factors	43
3.3.3 Assumptions and Materials	44
3.3.4 Sketch of component and FBD	44
3.3.5 Stress Analysis	45
3.3.6 Critical Review	46
3.3.7 Flowchart for parameterization	47
3.4 Steering Arm Heim Joint	47
3.4.1 Description of Inputs and Outputs	47
3.4.2 Constants and safety factors	47
3.4.3 Assumptions, simplifications and materials	47
3.4.4 Sketch of component and FBD	48
3.4.5 Stress Analysis	48
3.4.6 Critical Review	49
3.4.7 Flowchart for parameterization	49

3.5	Tie Rod	49
3.5.1	Description of Inputs and Outputs	49
3.5.2	Constants and safety factors	49
3.5.3	Assumptions, simplifications and materials	49
3.5.4	Sketch of component and FBD	50
3.5.5	Stress Analysis	50
3.5.6	Critical Review	51
3.5.7	Flowchart for parameterization	51
3.6	Rack Pin	51
3.6.1	Description of Inputs and Outputs	51
3.6.2	Constants and safety factors	51
3.6.3	Assumptions, simplifications and materials	52
3.6.4	Sketch of component and FBD	52
3.6.5	Stress Analysis	52
3.6.6	Critical Review	53
3.6.7	Flowchart for parameterization	53
3.7	Rack	53
3.7.1	Description of Inputs and Outputs	53
3.7.2	Constants and safety factors	53
3.7.3	Assumptions, simplifications and materials	54
3.7.4	Sketch of component and FBD	54
3.7.5	Stress Analysis	54
3.7.6	Critical Review	55

3.7.7	Flowchart for parameterization	55
3.8	Pinion	55
3.8.1	Description of Inputs and Outputs	55
3.8.2	Constants and safety factors	56
3.8.3	Assumptions, simplifications and materials	56
3.8.4	Sketch of component and FBD	56
3.8.5	Stress Analysis	57
3.8.6	Critical Review	58
3.8.7	Flowchart for parameterization	58
3.9	Pinion Key	58
3.9.1	Description of Inputs and Outputs	58
3.9.2	Constants and safety factors	58
3.9.3	Assumptions, simplifications and materials	58
3.9.4	Sketch of component and FBD	58
3.9.5	Stress Analysis	59
3.9.6	Critical Review	60
3.9.7	Flowchart for parameterization	60
3.10	Universal Joint	60
3.10.1	Description of Inputs and Outputs	60
3.10.2	Constants and safety factors	60
3.10.3	Assumptions, simplifications and materials	60
3.10.4	Sketch of component and FBD	61
3.10.5	Stress Analysis	61

3.10.6 Critical Review	62
3.10.7 Flowchart for parameterization	62
3.11 Brake Rotors	62
3.11.1 Safety Factors	63
3.11.2 Assumptions, simplifications, and materials	63
3.11.3 Sketch of component and FBD	63
3.11.4 Stress analysis	63
3.11.5 Critical review	63
3.12 Powertrain	64
3.12.1 Analysis Outline	64
3.12.2 Inputs and Outputs	64
3.12.3 Assumptions and Materials	64
3.12.4 Stress Analysis	65
3.13 Battery Mount Analysis	67
3.13.1 Description of Inputs/Outputs	67
3.13.2 Justification of Inputs, Parameters	68
3.13.3 Bolt Analysis	68
3.14 Springs and Dampers	69
3.14.1 Description of Inputs/Outputs	69
3.14.2 Justification of Inputs, constants and Parameters	70
3.14.3 Assumption, Simplifications and Materials	70
3.14.4 Spring and Damper Modelling	70
3.14.5 Fatigue and Safety Analysis	71

3.15 Powertrain	73
3.15.1 Analysis Outline	73
3.15.2 Inputs and Outputs	74
3.15.3 Assumptions and Materials	74
3.15.4 Stress Analysis	74
4 Discussion and Future Work	78
APPENDICES	81
A Design Solution	82
B Chassis	84
B.0.1 Chassis Simulations	91
B.1 Brake Flow	97
B.1.1 Flowchart	97
B.2 Chassis Flowchart	97
B.2.1 Flowchart	97
B.3 Acceleration Equation Derivations	98
B.4 Maximum Achievable Acceleration	99
B.5 Deceleration Equation Derivations	101
B.6 Cornering Calculations and Equation Derivations	104
B.7 Maximum Cornering Speed at different Radii	106
B.8 Aerodynamic Load Distribution Model	109
B.9 Damper Equation Derivations	111

B.10 Suspension Force and Stress Analysis	114
B.10.1 Bolt Analysis	114
B.10.2 Mount Weld Analysis	116
B.10.3 MATLAB program for front suspension	123
B.10.4 MATLAB program for rear suspension	124
B.11 Suspension Geometry Derivation	125
B.11.1 Front Suspension	125
B.11.2 Rear Suspension	133
B.11.3 Description of Inputs and Outputs	141
B.11.4 Justification of Inputs, constants and Parameters	141
B.11.5 Assumptions, Simplifications and Materials	141
B.12 Chassis Impact Analysis Code	144

List of Figures

2.1	Suspension Geometry Front View	5
2.2	Lower Control Arm Dimensions	7
2.3	Upper Control Arm Dimensions	7
2.4	Rocker Dimensions	8
2.5	FBD of an Accelerating Car on a Level Road	9
2.6	Reaction at Wheels Due to Applied Centripetal Force	12
2.7	Illustration of Steering System Geometry	17
2.8	Vehicle Steering Ackermann Method	18
2.9	FBD of the driver exerting his foot onto the acceleration pedal	20
2.10	FBD of the spring mounted onto the pedal	21
2.11	FBD of the driver exerting his foot onto the brake pedal	22
2.12	Tire Free Body Diagram	25
3.1	Nodes and Elements on the Chassis	29
3.2	Element 4 free body diagram	30
3.3	Reaction forces on Element 4 FBD	32
3.4	Front Impact FBD	33
3.5	Rear Impact FBD	34
3.6	FBD of suspension member bolts for mounting	42
3.7	FBD of steering knuckle and wheel	44

3.8	FBD of the bolt connecting the steering arm to the heim joint	44
3.9	FBD of the steering arm heim joint	48
3.10	FBD of the Tie Rod	50
3.11	FBD of steering rack	54
3.12	FBD of the pinion	56
3.13	FBD of the Pinion Key	59
3.14	FBD of the shaft of the U-Joint	61
3.15	FBD of the U-joint pin	61
3.16	Half Axle Shaft Free Body Diagram	65
3.17	Sprocket Free Body Diagram	66
3.18	Chain Shaft Free Body Diagram	67
3.19	FBD of Forces acting on Battery Mounts	68
3.20	FBD of Forces acting on Battery Mount	69
3.21	Half Axle Shaft Free Body Diagram	74
3.22	Sprocket Free Body Diagram	75
3.23	Chain Shaft Free Body Diagram	76
A.1	Updated Solution of the vehicle with labeled components	82
A.2	Updated Solution of the vehicle with dimensions	83
B.1	Frame element FBD	84
B.2	Bar element FBD	84
B.3	Beam element FBD	86
B.4	Rotation of element to the global coordinates	89

B.5	Front Impact Simulation Stress Plot	91
B.6	Front Impact Simulation Safety Factor Plot	92
B.7	Rear Impact Simulation Stress Plot	93
B.8	Rear Impact Simulation Safety Factor Plot	94
B.9	Side Impact Simulation Stress Plot	95
B.10	Side Impact Simulation Safety Factor Plot	96
B.11	Flowchart of the Brake Flow	97
B.12	Flowchart of the Chassis Flow	97
B.13	FBD of an Accelerating Car on a Level Road	98
B.14	FBD of an Accelerating Car on a Level Road	101
B.15	Reaction at Wheels Due to Applied Centripetal Force	104
B.16	FBD for forces acting on the vehicle	109
B.17	FBD of Suspension Member Bolts for Mounting	115
B.18	FBD of Mount and Weld	117
B.19	Welding Profile	118
B.20	Overall front suspension geometry with labeled points	125
B.21	Front suspension track width determination	126
B.22	Front suspension geometry front view	127
B.23	Front control arms geometry determination	129
B.24	Front view of front rocker and pushrod locations in relation to chassis . . .	130
B.25	Front rocker and shock absorber dimensions	131
B.26	Front pushrod location with respect to rocker	132
B.27	Overall rear suspension geometry with labeled points	133

B.28 Rear suspension track width determination	134
B.29 Rear suspension geometry front view	135
B.30 Rear control arm geometry determination	137
B.31 Rear rocker and push rod location with respect to chassis	138
B.32 Rear rocker and pushrod dimensions	138
B.33 Rear pushrod location determination	139
B.34 Rear pushrod dimensions	140
B.35 FBD of Forces acting on spring	142

Chapter 1

Project Charter

1.1 Mandate

Formula SAE (Society of Automotive Engineers) is a series of international competitions in which university teams compete to design and manufacture the best performing race cars. Our design team has been approached by a car manufacturer and contracted to develop a small electric Formula-style race car. The prototype should have high performance and be sufficiently durable to successfully complete all the static and dynamic events at the Formula SAE competitions. The prototype will be evaluated as it must follow all Formula SAE rules and regulations.

1.2 Requirements

1. The tractive system must be completely isolated from the chassis and any other conductive parts of the vehicle.
2. The tractive system motor(s) must be connected to the accumulator through a motor controller.
3. Only electrical motors of any type are allowed and the number of motors is not limited.
4. All accumulator containers must be designed to withstand forces from deceleration in all directions.

5. The accumulator container(s) must be completely closed at all times without the need to install extra protective covers.
6. Exposed high speed final drivetrain equipment must be fitted with scatter shields that may be composed of multiple pieces.
7. Coolant for electric motors and accumulators must be either plain water with no additives or oil.
8. The braking system must be operated by a single control and act on all four wheels. It must have two independent hydraulic circuits that have their own fluid reserve.
9. Vehicles may have either dry or wet tires.
10. The steering wheel must be mechanically connected to the front wheels.
11. The chassis must include both a main hoop and a front hoop.

1.3 Constraints

1. The maximum power drawn from the accumulator must not exceed 80 kW.
2. The maximum permitted voltage that may occur between any two points must not exceed 600 V DC.
3. A maximum of 12 kg is allowed in any accumulator container section.
4. Regenerating energy is allowed and unrestricted when the vehicle speed is more than 5 km/hr.
5. The brake pedal and system must withstand a minimum force of 2000 N
6. Wheels must be 203.2 mm (8.0 inches) or more in diameter.

7. The vehicle must be equipped with an operational suspension system with usable wheel travel of at least 50 mm, with a driver seated.

1.4 Criteria

1. **Performance:** Increase in handling, response, and tractive capability of the steering, suspension, and tires. Increase in acceleration and traction force of the vehicle.
2. **Serviceability:** Ease of repair, subsystems accessibility, parts interchangeability, low manufacturing complexity, and standardization of fasteners across the vehicle.
3. **Safety:** Visibility, cockpit protection, firewall, rollover protection, and scatter shields. Wiring is safely routed, color coded, and marked for function.
4. **Ergonomics:** Driver comfort, arm room, leg room, head restraint, ease of control, seat adjustability, and readability of essential instruments.
5. **Reliability:** Consistent and reliable braking system, drivetrain, and motor.
6. **Aerodynamics:** Drag reduction, lift reduction, noise elimination, and downforce gain.
7. **Cost:** Raw material selection, manufacturing process selection, and design optimizations for simpler solutions.
8. **Efficiency:** Lightweight design, increase in range, and improve in performance and structural integrity.

1.5 Parameterization Outline

The design of the vehicle is driven by the length and weight to be able to accommodate drivers of sizes ranging from 5th percentile female up to 95th percentile male. Accommo-

dation will include driver position, driver controls, and driver equipment. Primarily, the wheel base will be altered to change the length and weight of the vehicle to accommodate the driver. To alter the wheel base, the geometrical properties of the space frame and its members will be adjusted and hence, the overall weight of the vehicle will vary.

Chapter 2

System Modelling

2.0.1 Suspension Geometry

2.0.1.1 Overall Geometry

The main dimensions of both the front and rear suspension geometries can be seen in the figure below. The derivations of all these dimensions are found in Appendix B.11, with some having trigonometric relationships that can be modeled.

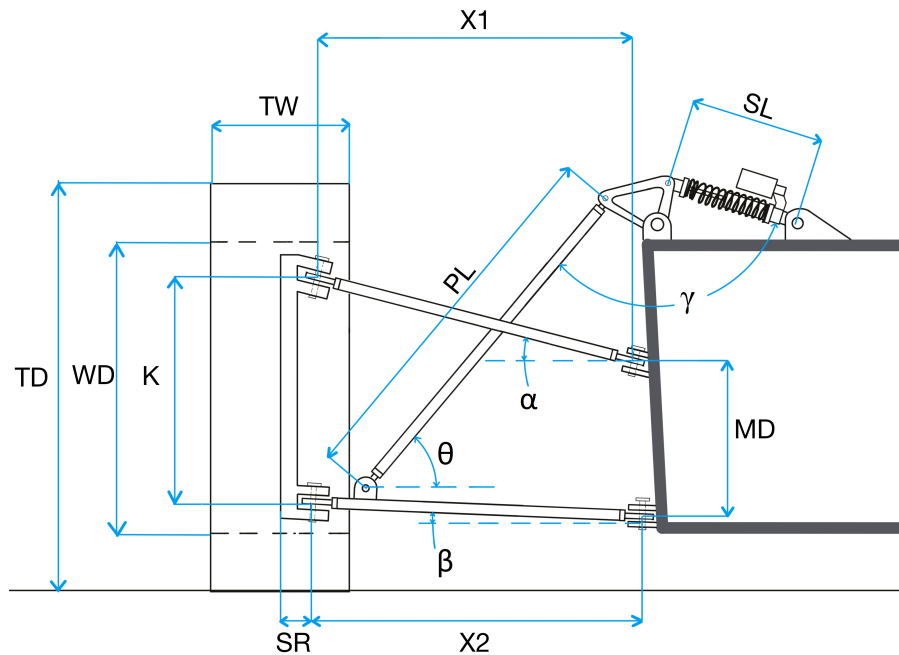


Figure 2.1: Suspension Geometry Front View

For both suspension systems, the following parameters are held the same. Tire diameter (TD) is 510.54 mm, wheel diameter (WD) is 304.8mm, tire width (TW) is 238.76 mm, K is 228.60 mm, scrub radius (SR) is 30 mm, and shock absorbers length (SL) is 190 mm in an uncompressed state.

For the front suspension, the pushrod length (PL) is 575.56mm, pushrod angle (θ) is 69.13° , distance between the upper control arm (UCA) and lower control arm (LCA) chassis mounts (MD) is 175.27mm. For the front LCA, X_{2short} is 302.18 mm and X_{2long} is 325.72 mm (calculated in Appendix B.11). For the UCA, X_{2short} and X_{2long} which have lengths of 302.4 mm and 327.66 mm. The angle of the UCA from the horizontal, α , is 10.25° . The angle of the LCA from the horizontal, β , is 1.45° . The angle between the shock absorber and the pushrod, γ is 99.47° .

For the rear suspension the following dimensions are determined. The pushrod length PL is found to be 368.02 mm. The pushrod angle θ , is found as 69.13° . The distance between the upper and lower control arm chassis mounts, MD, is 189.61 mm. For both control arms, the horizontal distance from the chassis mounting point to the steering knuckle mounting point is the same so, X1 and X2 are found to be 233.68 mm. The angle of the upper control arm from the horizontal, α , is found as 10.93° . The angle of the lower control arm from the horizontal, β , is found as 1.51° . As explained in Appendix B.11, the angle between the shock absorber and the pushrod, γ , falls within the optimal range ($80\text{-}120^\circ$) and is found as 99.47° .

2.0.1.2 Control Arm Geometry

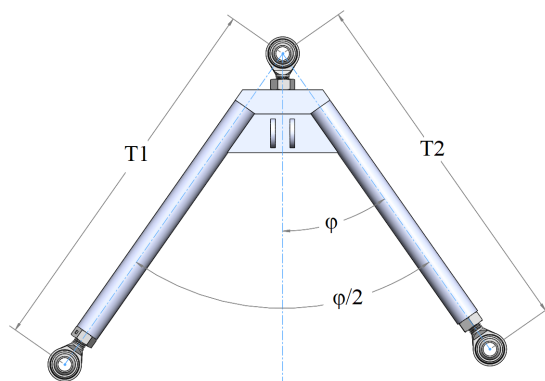


Figure 2.2: Lower Control Arm Dimensions

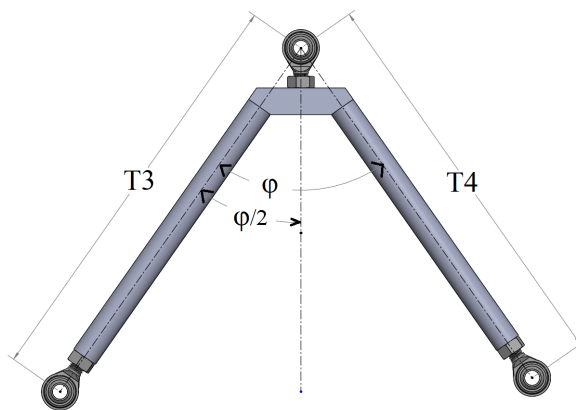


Figure 2.3: Upper Control Arm Dimensions

Unlike the rear suspension, for the front suspension, each control arm has unequal tube lengths. The front lower control arm tube lengths T1 and T2 are 393.04 mm and 373.77 mm respectively. Likewise, the front upper control arm has tube lengths T3 and T4 of 393.70 mm and 377.85 mm respectively. Both front control arms have a wishbone spread angle, ϕ , of 70° where the tubes are evenly spread along the axis of symmetry.

The rear suspension control arms have equal tube lengths. The rear lower control arm has tube lengths of T1 and T2 equal to 270 mm. The rear upper control arm has tube lengths of T2 and T3 equal to 273.66 mm. Both rear control arms have a wishbone spread angle, ϕ , of 60° where the tubes are evenly spread along the axis of symmetry.

For the sake of calculations later in the analysis, the tube lengths for all control arms are estimated as the distance from the knuckle mounting point to the respective chassis points. In reality, all tube lengths are slightly less than the values described above, if the rod ends and weld plate are taken into consideration.

2.0.1.3 Rocker Geometry

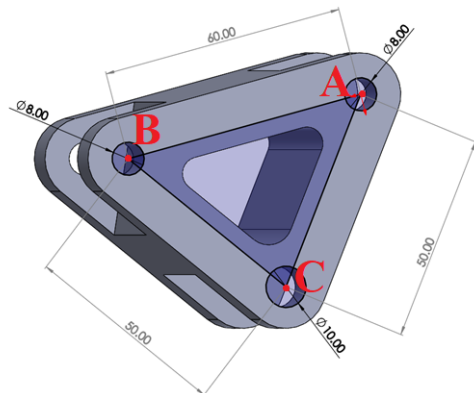


Figure 2.4: Rocker Dimensions

Point A is the connection location of the shock-absorbers to the rocker. Point B is the connection location of the pushrod to the rocker. Point C is the connection location of the rocker to the chassis. Length AB is found to be 60 mm, length BC is found to be 50 mm, and length AC is found to be 50mm. These dimensions are determined in Appendix B.11.

2.0.2 Assumptions and Working Environment

The FSAE vehicle is assumed to operate under clear weather conditions while being susceptible to high impact crashes. The driver of the vehicle is assumed to be a 95th percentile male with a weight of 111.58 kg. The total weight of the vehicle with the driver is calculated to a total of 303.5 kg. The vehicle is assumed to be operating using its maximum speed and acceleration, 105 km/hr and $B.34 \text{ m/s}^2$ respectively.

2.1 Kinematics and Applied Forces

2.1.1 Dynamic Applied Forces

Acceleration on a Level Road An accelerating car on a level road produces reaction forces on the wheels as seen in the figure below. In this situation load is transferred longitudinally shifting the load more to the driven wheels (rear wheels) causing the car to squat. Additionally, the friction force is only considered for the driven wheels since the front wheels are free-rolling and thus friction on them is assumed negligible. [1].

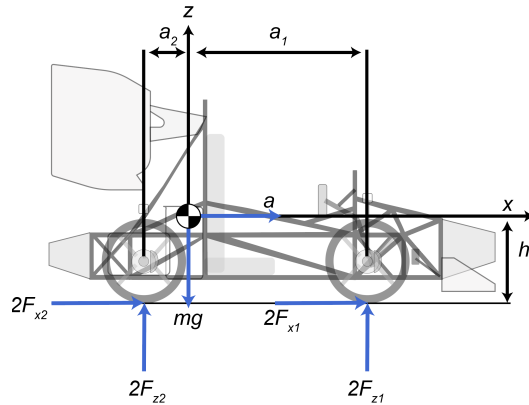


Figure 2.5: FBD of an Accelerating Car on a Level Road

The forces in the FBD above can be found as follows, where it is assumed $\mu_k = 0.9$ [1]:

$$F_{z_1} = \frac{1}{2}(mg)\left(\frac{a_2}{a_2 + a_1}\right) - \left(\frac{h}{a_1 + a_2}\right)\left(\frac{a}{g}\right) \quad (2.1)$$

$$F_{z_2} = \frac{1}{2}(mg)\left(\frac{a_1}{a_2 + a_1}\right) + \left(\frac{h}{a_1 + a_2}\right)\left(\frac{a}{g}\right) \quad (2.2)$$

Provided an acceleration of $a = 4.157 \frac{m}{s^2}$ (refer to appendix B.4 for max acceleration calculation and B.3 for the derivation of equations used.) Thus, the normal forces are calculated as:

$$F_{z_1} = \frac{1}{2}(303.5kg * 9.81 \frac{m}{s^2})\left(\frac{0.789m}{0.813m + 0.789m}\right) - \left(\frac{0.289m}{0.813m + 0.789m}\right)\left(\frac{4.157 \frac{m}{s^2}}{9.81 \frac{m}{s^2}}\right) = 619.65 \text{ N} \quad (2.3)$$

$$F_{z_2} = \frac{1}{2}(303.5kg * 9.81 \frac{m}{s^2})\left(\frac{0.813m}{0.813m + 0.789m}\right) + \left(\frac{0.289m}{0.813m + 0.789m}\right)\left(\frac{4.157 \frac{m}{s^2}}{9.81 \frac{m}{s^2}}\right) = 868.84 \text{ N} \quad (2.4)$$

$$F_{x_2} = \mu_k F_{z_2} = 0.9 * 868.84 = 781.95 \text{ N} \quad (2.5)$$

Deceleration on a Level Road

A decelerating car on a level road produces reaction forces on the wheels as seen in figure 2.5. In this situation load is transferred longitudinally shifting the load more to the front wheels causing the car to dive. Additionally the friction force on all wheels is considered in this section and down-forces produced by the car are taken into account. The maximum deceleration of the car was determined to be: $13.714 \frac{m}{s^2}$ refer to appendix B.5 for the its derivation. Thus, the reaction forces on the car can be determined by the following:

$$F_{zf} = \left(\frac{(mg - F_{Lcar} + F_{Lf} + F_{Lr}) a_2 + mah + F_{Lr}l_r - F_{Lf}l_f}{2a_2 + 2a_1} \right) = 1548.75N \quad (2.6)$$

$$F_{zr} = -\frac{mah - a_1mg + a_1F_{Lcar} - a_1F_{Lf} - F_{Lf}l_f - a_1F_{Lr} + F_{Lr}l_r}{2(a_2 + a_1)} = 763.26N \quad (2.7)$$

Where F_{zf} & F_{zr} are the normal forces at the front wheel and the rear wheel respectively, F_{Lf} & F_{Lr} are the down-forces produced by the front and rear wing. F_{Lcar} is the lift force acting at the center of mass, a is the deceleration, and a_1 & a_2 & h are the dimensions illustrated in the figure.

High Speed Cornering During a turn at a relatively high velocity, a centripetal force is produced which transfers the load laterally to the side of the car inside a turn. For a car moving at a reasonable velocity v , around a corner with a radius of curvature R , there is an applied centripetal force (F_c). The maximum cornering velocity for the vehicle at different cornering radii was determined and can be further explored in appendix B.6. At the maximum turning radius of $R = 50m$, the max velocity which can be achieved is $v = 25.62\frac{m}{s}$, the centripetal force can be calculated as follows below. It should be noted that this radius of curvature is close to the maximum value of R that is allowed in the FSAE guidelines [2].

$$F_C = \frac{mv^2}{R} = (303.5 \text{ kg}) \left(\frac{(25.62\frac{m}{s})^2}{50 \text{ m}} \right) = 3941.31 \text{ N} \quad (2.8)$$

A consequence of F_C when turning, is that the load is transferred laterally from one side of the car to the other. That is, more load is placed on the wheels on the inside of a turn, causing the car to roll. To illustrate this, an FBD for the front wheels during a corner is used, where the load experienced on the front wheels corresponds to the load on the front axle (W_F) and the down-force (F_{Lf}) produced on the front of the car.

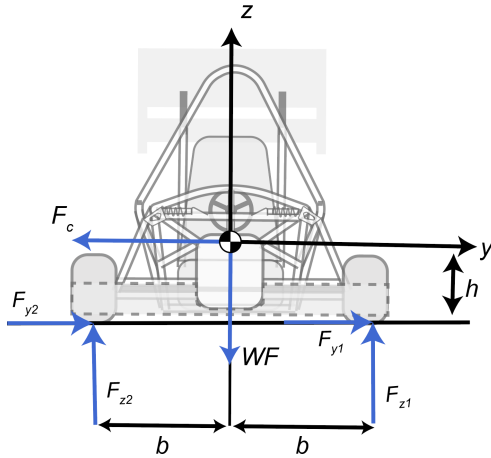


Figure 2.6: Reaction at Wheels Due to Applied Centripetal Force

Refer to appendix B.6 for the derivation of the reaction forces acting on each wheel where it was concluded that the reaction forces can be determined by the following:

$$F_{z1FRONT} = \frac{R_{bias}(b(W_F + F_{Lf}) - hF_C)}{2b} = 519.80 \text{ N} \quad (2.9)$$

Where F_{z1} is the normal force on the front right wheel, F_{Lf} is the down force produced by the vehicle, R_{bias} is the weight distribution between the front and rear end of the car, and F_C is the centripetal force of the car.

$$F_{z2FRONT} = \frac{R_{bias}(b(W_F + F_{Lf}) + hF_C)}{2b} = 1661.65 \text{ N} \quad (2.10)$$

Where F_{z2} is the normal force on the front left wheel.

Assuming a kinetic friction coefficient $\mu_k = 0.9$, its found:

$$F_{x1FRONT} = (\mu_s)(F_{z1FRONT}) = (0.9)(519.80 \text{ N}) = 467.82 \text{ N} \quad (2.11)$$

$$F_{x2FRONT} = (\mu_s)(F_{z2FRONT}) = (0.9)(1661.65 \text{ N}) = 1495.485 \text{ N} \quad (2.12)$$

Similarly, calculating for the normal forces experienced by the rear wheels during a turn uses the same equations as the front. However, the normal forces experienced in the rear wheels correspond to the load on the rear axle (W_R) and the down-force produced on the rear axle (F_{Lr}).

$$F_{z_1REAR} = \frac{R_{bias}(b(W_R + F_{Lf}) + hF_C)}{2b} = 535.10 \text{ N} \quad (2.13)$$

$$F_{z_2REAR} = \frac{R_{bias}(b(W_R + F_{Lf}) + hF_C)}{2b} = 1710.56 \text{ N} \quad (2.14)$$

$$F_{x_1REAR} = (\mu_s)(F_{z_1REAR}) = (0.9)(535.1N) = 481.59 \text{ N} \quad (2.15)$$

$$F_{x_2REAR} = (\mu_s)(F_{z_2REAR}) = (0.6)(1710.56N) = 1539.50 \text{ N} \quad (2.16)$$

Finally, the reaction forces in the y direction can also be determined as they are the reaction forces due to the centripetal force acting on the wheels. However, since this force will not be distributed equally between the left and right side of the car the ratio of force distribution between the two sides must first be determined and then split based on the weight distribution between the front and rear. It was determined that the ratio between the right and left side. $Force_{biasright} = 0.3128$ $Force_{biasleft} = 0.6872$. The following can then be determined:

$$F_{y_1FRONT} = \frac{m * v^2}{R} * R_{bias} * Force_{biasright} = 614.16N \text{ N} \quad (2.17)$$

$$F_{y_2FRONT} = \frac{m * v^2}{R} * R_{bias} * Force_{biasleft} = 1348.79N \text{ N} \quad (2.18)$$

$$F_{y_1REAR} = \frac{m * v^2}{R} * R_{bias} * Force_{biasright} = 632.24N \text{ N} \quad (2.19)$$

$$F_{y_2REAR} = \frac{m * v^2}{R} * R_{bias} * Force_{biasleft} = 1388.85N \text{ N} \quad (2.20)$$

2.1.2 Impacts and Collisions

To mathematically inspect the safety of the driver during the race, external forces that can potentially damage the chassis need to be calculated. External forces during an FSAE race include front, rear, and side impact forces exerted from other vehicles on the track during the case of a collision.

First Case: Front Impact Force

In the case of a front collision, it is assumed that the vehicle is traveling at maximum speed, 105 km/h, in order to assess the worst case scenario. However, it is also reasonable to assume that the driver suddenly pushes the brakes 1 second before the collision. After considering the aforementioned assumptions, the impact velocity can be calculated using the maximum deceleration value calculated in the previous sections, 5.35 m/s^2 .

$$v_f = v_i + at \quad (2.21)$$

Where v_f is the final speed after impact, v_i is the speed before impact, a is the maximum deceleration of the vehicle, and t is the time under maximum deceleration.

$$v_f = 29.4 \text{ m/s} + (-5.35 \text{ m/s}^2)(1 \text{ s}) = 24.05 \text{ m/s} \quad (2.22)$$

Therefore, the FSAE vehicle is going to hit a wall at a speed of 24.05 m/s. The velocity of the vehicle after impact is 0 m/s with the assumption that the crash time is 0.4 s. Considering these assumptions, the impact deceleration and the impact force can be calculated.

$$0 \text{ m/s} = 24.05 \text{ m/s} + (a_{\text{impact1}})(0.4 \text{ s})a_{\text{impact1}} = -60.125 \text{ m/s}^2 \quad (2.23)$$

Where a_{impact1} is the deceleration during impact.

$$F_{impact1} = ma \quad (2.24)$$

Where $F_{impact1}$ is the front impact force and m is the mass of the vehicle.

$$F_{impact1} = 303.645kg(-60.125m/s^2) = -18245.83N \quad (2.25)$$

The front impact force is 18245.83 N towards the front bulkhead of the chassis.

Second Case: Rear Impact Force

In the case of a rear impact, it is assumed that the car is static and a second car collides with it from the rear bulkhead. To get the maximum rear impact force that would result from a rear collision, it is also assumed that the velocity of the second car collides with the first car at maximum speed with an impact time of 0.45 s.

$$0m/s = 29.4m/s + (a_{impact2})(0.45s)a_{impact2} = -65.33m/s^2 \quad (2.26)$$

$$F_{impact2} = 303.645kg(-65.33m/s^2) = -19826.38N \quad (2.27)$$

The rear impact force is 19826.38 N towards the rear bulkhead of the chassis.

Third Case: Side Impact Force

During a side impact scenario, it is assumed that the car is static and a second car collides with it from the side impact protection of the chassis. Similar assumptions as the previous cases will be applied. The second car collides at maximum speed and with a collision time of 0.45 s.

$$0m/s = 29.4m/s + (a_{impact3})(0.45s)a_{impact3} = -65.33m/s^2 \quad (2.28)$$

$$F_{impact3} = 303.645kg(-65.33m/s^2) = -19826.38N \quad (2.29)$$

2.1.3 Aerodynamics

Aerodynamic Effects at Max Speed

The lift forces on the vehicle can easily be calculated. Given a lift coefficient of -2.34 [3] with an aerodynamic package installed, and a coefficient of 0.29 [3] when no aerodynamic packages are installed. Then, the lift forces acting on the car would be:

$$F_{L1} = 0.29 \times 1.54m^2 \times 1.225kg/m^2 \times \frac{(29.16m/s)^2}{2} = 235.59N \quad (2.30)$$

With an aerodynamic package, the lift force acts as a down-force.

$$F_{L2} = -2.34 \times 1.54m^2 \times 1.225kg/m^2 \times \frac{(29.16m/s)^2}{2} = -1876.79N \quad (2.31)$$

Force required to lift car off the ground.

$$F = 303.5kg \times 9.81m/s^2 = 2977.34N \quad (2.32)$$

The Drag Forces acting on the vehicle can be calculated similarly, where the drag coefficient acting on the vehicle is 0.92 when an Aero package is installed. Since, the drag force acting on the vehicle will be the highest when the vehicle is at its maximum velocity, the drag force can be found to be:

$$F_D = .92 \times 1.54m^2 \times 1.225kg/m^2 \times \frac{(29.16m/s)^2}{2} = 737.88N \quad (2.33)$$

2.1.4 Steering

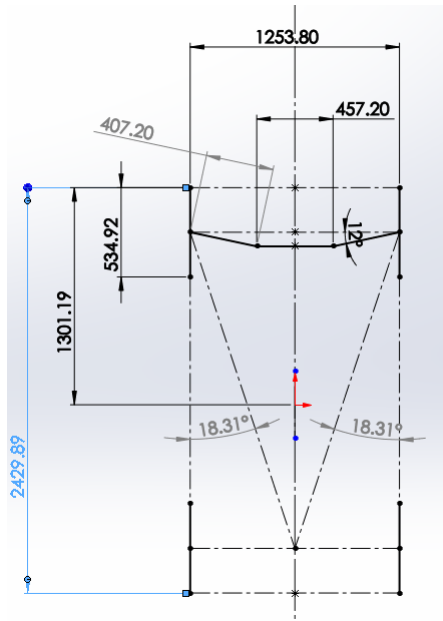


Figure 2.7: Illustration of Steering System Geometry

Figure 2.7 above illustrates the geometry of the steering system when the car is not steering in any direction. The wheel diameter which is 534.92mm are connected to the steering knuckle. The knuckles are represented by the point at which the tie rods connect to the wheel center. Since the distance of these arms is identical, the angle at which they pivot will be at an identical rate. Thus, the angle β will remain constant, and can be determined by extending the point at which the tie rods intersect with the knuckles to the center of the rear axle. The model thus returned an angle $\beta = 18.31\text{degrees}$. This is used later when analysing the forces acting on the Heim joint connections at the knuckle.

2.1.5 Steady State Low Speed Cornering Geometry and Vehicle Turning Radius

The figure below illustrates an Ackermann Geometry also known as a kinematic steering geometry. The Ackermann geometry states that for a basic steering system for a front wheel steering system, the difference of the cotangents of the angles of the outer front wheels to the inner front wheels should equate to the ratio of the width (T) and length (L) of the vehicle.

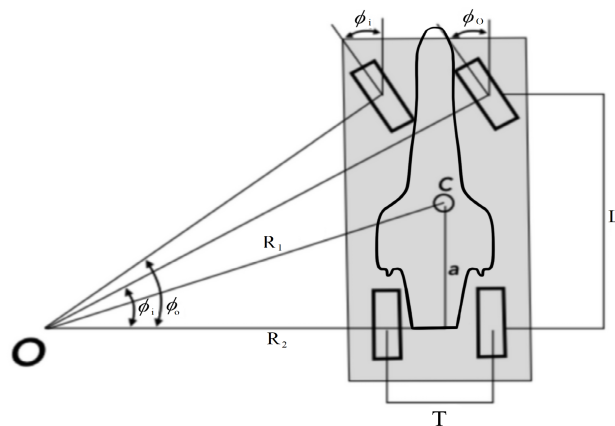


Figure 2.8: Vehicle Steering Ackermann Method

This condition can be simply modeled by the following set of equations:

$$\cot(\phi_i) - \cot(\phi_o) = \frac{T}{L} \quad (2.34)$$

Where, ϕ_i is the steering angle of the inner front wheel, ϕ_o is the steering angle of the outer front wheel, T is the vehicle's track width, and L is the wheelbase of the vehicle.

As seen in figure 2.8 it can be seen that if a normal is drawn from all the wheels they intersect at a point O which is the center of rotation. The vehicle's center of mass will turn with a radius R_1 . This is known as the turning radius, which can be geometrically

defined as follows:

$$R_1 = \sqrt{a^2 + (L^2) \left(\frac{(\cot(\phi_o) + \cot(\phi_i))^2}{2} \right)} \quad (2.35)$$

Where, a is the distance from the rear axle to the center of mass and is 0.739 m. Given that the desired steering angle of for the inner tire will be $\phi_i = 27.5\text{degrees}$, and $L = 1.603m$ and $T = 1.2538m$. Then, the steering angle of the outer wheel and the turning radius of the vehicle can be determined as follows:

$$R_2 = \left(\frac{L}{\tan(\phi_i) \frac{T}{2}} \right) = \left(\frac{1.603}{\tan(0.4815) \frac{1.2538}{2}} \right) = 3.695m \quad (2.36)$$

$$\phi_o = \arctan \left(\frac{L}{R_2 + \frac{T}{2}} \right) = \arctan \left(\frac{1.603m}{3.695m + \frac{1.2538m}{2}} \right) = 0.3552rad \quad (2.37)$$

$$R_1 = \sqrt{(.7899m)^2 + (1.603m)^2 \left(\frac{(\cot(0.3552rad) + \cot(0.4815rad))^2}{2} \right)} = 3.7786m \quad (2.38)$$

Hence, from the above series of equations it can be determined that the turning radius of the center mass of the vehicle would be 3.7786 meters.

2.1.6 Pedals

The following figure describes the forces that are acting on the acceleration pedal. Parameter F_{app} describes the applied force from the drivers foot. The minimum applied force (F_{AppMin}) onto the acceleration pedal was assumed to be 45 N, and the maximum applied force (F_{AppMax}) onto the acceleration pedal is 300 N. The force applied from the acceleration cable onto the pedal (F_c) is 10 N. Variable L represents the length at which the pedal force is applied from. C represents the length at which the cable attaches to the acceleration pedal. θ represents angle of the acceleration pedal. Parameter a represents the horizontal distance from the acceleration pedal to F_{Cy} .

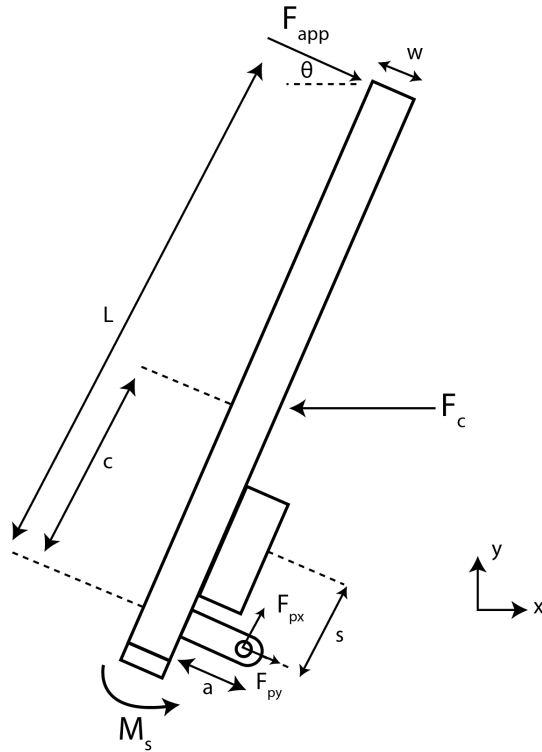


Figure 2.9: FBD of the driver exerting his foot onto the acceleration pedal

The moment that the spring must produce to return the acceleration pedal back to its original position (M_s) can be determined:

$$M_{SMin} = (F_{AppMin} \times L) - (F_c \times \cos(\theta) \times c) - (F_c \times \sin(\theta) \times a) \quad (2.39)$$

$$M_{SMax} = (F_{AppMax} \times L) - (F_c \times \cos(\theta)) - (F_c \times \sin(\theta)) \quad (2.40)$$

When analysing the brake pedal, the F_{App} will be assumed to be 300 N. The force applied onto the master cylinder from the pedal (F_c) can be determined with the following relationship.

$$F_c = L \frac{F_{app}}{c} = 0.0125m \times \frac{300N}{0.037m} = 1013.51N \quad (2.41)$$

The moment needed from the spring to return the pedal to its original position can be determined by analysing figure ??.

$$M_{SBrake} = (F_{App} \times L) - (F_c \times \cos(\theta)) - (F_c \times \sin(\theta)) \quad (2.42)$$

The spring used in the pedal can be modeled in the following figure.

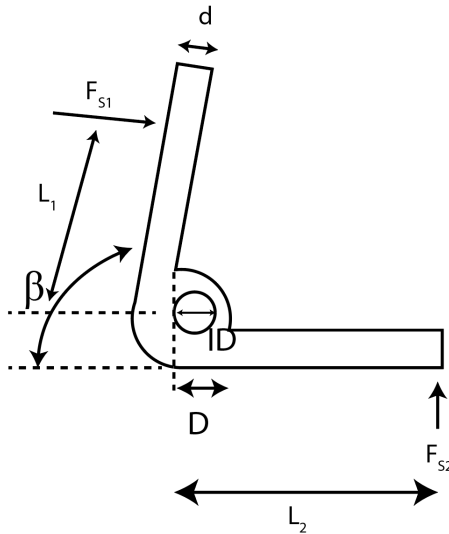


Figure 2.10: FBD of the spring mounted onto the pedal

The spring width (d) is 0.009m and the maximum angle between the horizontal and the spring arm (β) is 180°. The maximum force the spring experiences from the pedal (F_{S1}) is 1854.14 N (equation 2.40). The length of the upper arm of the spring (L_1) is 0.02 m. The outer diameter of the spring hole (D) is 0.029m and inner diameter of the spring hole (ID) is 0.02m. The length of the bottom arm of the spring (L_2) is 0.03 m. The total angular deflection the spring experiences can be determined by the following equation:

$$\theta_{Deflection} = (M_s \times OD) - (F_c \times \cos(\theta)) - (F_c \times \sin(\theta)) \quad (2.43)$$

Assuming the Young's Modulus of the spring to be 2.034E+11 Pa, the spring constant can be determined:

$$k = \frac{M_s}{\theta_{Deflection}} = \frac{5.207 \text{ Nm}}{0.0411 \text{ rad}} = 126.52 \text{ Nm/rad} \quad (2.44)$$

2.1.7 Braking

To start the brake modelling, we will first start with the brake pedal. We will assume that the force to reach maximum acceleration and maximum braking is 300 N. F_{app} is the force that the driver exerts onto the brake pedal. (L) is the length of the brake pedal estimated to be 0.125m , (c) is where the brake master cylinder attaches to the pedal measured to be 0.041m, M_s is the moment produced by pressing onto the brakes, and (F_c) is the reaction force from the master cylinder.

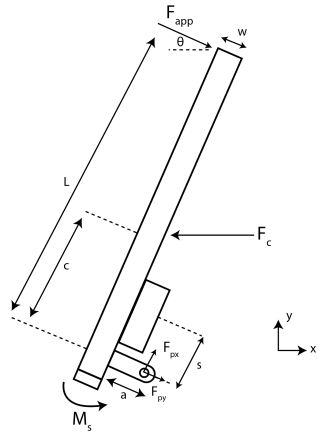


Figure 2.11: FBD of the driver exerting his foot onto the brake pedal

By analysing figure 2.11, it can be determined by the following equation that the relationship between the force on the top of the pedal to the force applied onto the master cylinder is:

$$F_c = L \frac{F_{app}}{c} = 0.0125 \text{ m} \times \frac{300 \text{ N}}{0.041 \text{ m}} = 914.63 \text{ N} \quad (2.45)$$

The force experienced from the master cylinder is then transferred to the bias bar. The bias bar is able to split the force into the two master cylinders. For this vehicle the bias bar will be split 58% to the front brakes and 42% to the rear brakes. The chosen brake calipers have 4 pistons. The radius of each caliper piston ($R_{\text{Caliper Piston}}$) is 0.0158 m. The coefficient of friction between.

$$F_{\text{FrontMasterCylinder}} = 0.58 \times 914.63\text{N} = 530.4\text{N} \quad (2.46)$$

$$F_{\text{RearMasterCylinder}} = 0.42 \times 914.63\text{N} = 384.1\text{N} \quad (2.47)$$

The bore radius of the front master cylinder ($R_{\text{MasterCylinderFront}}$) is 5/16" (0.0079m) [4] and the bore radius of the rear master cylinder ($R_{\text{MasterCylinderRear}}$) is 7/16" (0.0111 m) [5]. The GP 320 caliper will be used for the vehicle which contains four pistons each with a radius of 0.015875 m ($R_{\text{Caliper Piston}}$) [6]. The force that is exerted onto the front and rear caliper pistons can be determined by using the following relationship:

$$F_{\text{FrontCaliper}} = \frac{F_{\text{FrontMasterCylinder}} \times \pi R_{\text{Caliper Piston}}^2}{\pi R_{\text{MasterCylinderFront}}^2} = \frac{527\text{N} \times 0.000791m^2}{0.000197m^2} = 2108\text{N} \quad (2.48)$$

The same relationship can be used to determine the force exerted on the rear caliper pistons:

$$F_{\text{RearCaliper}} = \frac{F_{\text{RearMasterCylinder}} \times \pi R_{\text{Caliper Piston}}^2}{\pi R_{\text{MasterCylinderRear}}^2} = \frac{398\text{N} \times 0.000791m^2}{0.000387m^2} = 813\text{N} \quad (2.49)$$

The total friction force applied onto the rotor (F_{rotor}) can be determined by multiplying the force on each caliper by the number of pistons (4) and the coefficient of friction between the brake pad and brake rotor. The coefficient of friction between the brake pads and the brake rotor was assumed to be 0.37 based from Shigley's Mechanical Engineering Design

Appendix [7].

$$F_{RotorFront} = F_{FrontCaliper} \times \mu_{PadRotor} \times \text{Number of Pistons} = 2310\text{N} \times 0.37 \times 4 = 3420\text{N} \quad (2.50)$$

$$F_{RotorRear} = F_{RearCaliper} \times \mu_{PadRotor} \times \text{Number of Pistons} = 889\text{N} \times 0.37 \times 4 = 1316\text{N} \quad (2.51)$$

The friction force on the front and rear tires ($F_{Wheel Friction}$) must be determined to ensure the wheels can lock at max speed. The friction wheel force can be determined in the following relationship. The coefficient of friction between the tire and the road is 0.9 assuming a dry road surface and slick tires [8].

$$F_{FrontWheelFriction} = F_{FrontWheelNormalForce} \times \mu_{TireRoad} = 1688.74\text{N} \times 0.9 = 1519.87\text{N} \quad (2.52)$$

$$F_{RearWheelFriction} = F_{RearWheelNormalForce} \times \mu_{TireRoad} = 637.15\text{N} \times 0.9 = 573.43\text{N} \quad (2.53)$$

The braking torque applied onto the rotor ($T_{PadRotor}$) and the wheel torque experienced at maximum speed (T_{Wheel}) can now be determined and compared. The distance between the center of the rotor to the brake pad is 0.125 m ($R_{Pad To Rotor}$) [6] and the radius of the wheel (R_{wheel}) is 0.25m.

$$T_{PadRotorFront} = F_{RotorFront} \times R_{PadToRotor} = 3420\text{N} \times 0.125\text{m} = 427.5\text{Nm} \quad (2.54)$$

$$T_{FrontWheel} = F_{FrontWheelFriction} \times R_{Wheel} = 1519.87\text{N} \times 0.25\text{m} = 379.96\text{Nm} \quad (2.55)$$

$$T_{PadRotorRear} = F_{RotorRear} \times R_{PadToRotor} = 1316\text{N} \times 0.125\text{m} = 164.5\text{Nm} \quad (2.56)$$

$$T_{RearWheel} = F_{RearWheelFriction} \times R_{Wheel} = 573.43\text{N} \times 0.25\text{m} = 143.35\text{Nm} \quad (2.57)$$

For both front and rear tires, $T_{PadRotor}$ is larger than the T_{Wheel} by a factor of 1.12 and 1.14 respectively. Therefore, the wheels will lock when a force of 300 N is applied to the brake pedal.

2.1.8 Powertrain

Sprocket ratio modeling

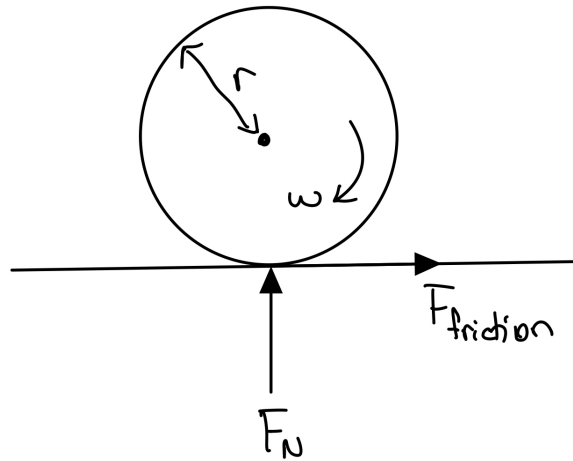


Figure 2.12: Tire Free Body Diagram

The normal force F_N on the rear wheel depends on the mass of the vehicle and the position of the center of mass from the middle of the wheel. By, using the horizontal distance of the center of mass, a rear bias of 0.507 is calculated. The normal force can now be calculated.

$$F_N = Mg (\text{bias}_{\text{rear}}) \quad (2.58)$$

$$F_N = 303.465 \text{ kg} (9.81 \text{ m/s}^2) (0.507) = 1510.1 \text{ N} \quad (2.59)$$

The friction force on the tire can now be calculated assuming that the coefficient of friction on the tire is 0.9.

$$F_{\text{friction}} = \mu (F_N) \quad (2.60)$$

$$F_{\text{friction}} = (0.9(1510.1N)) = 1359N \quad (2.61)$$

This force is the maximum force needed to be produced from the torque to move the car while avoiding slippage of the tires. As a result, it is used to find the torque that needs to be exerted from the shaft and motor. The motor chosen for the FSAE vehicle is an Emraxx 228 that produces a torque of 140.03 Nm, assuming that the motor uses all the 70kW that the accumulator can produce.

A tire with a radius of 255.27 mm is being used. As a result, to produce a friction force of 1359 N, a torque can be calculated using $T = F_{\text{friction}}(r_{\text{tire}})$.

$$T = 1359N(0.25527m) = 346.93Nm \quad (2.62)$$

The ratio of the torque on the wheel and the motor can be used to select a sprocket ratio.

$$\frac{T_{\text{tire}}}{T_{\text{motor}}} = \frac{346.93\text{Nm}}{140.03\text{Nm}} \approx 2.5 \quad (2.63)$$

A gear ratio of 35:14 is selected. The pitch of the sprocket will be designed for a 428 Chain with a pitch of 12.7 mm. A relationship between the pitch and the sprocket diameter can determine the size of the sprockets that need to be used.

$$PD = \frac{P}{\sin\left(\frac{180^\circ}{N}\right)} \quad (2.64)$$

Where PD is the pitch diameter, P is the chain pitch and N is the number of teeth on the sprocket.

For the small sprocket, the following pitch diameter is calculated.

$$PD = \frac{12.7}{\sin\left(\frac{180^\circ}{14}\right)} = 28.54mm \quad (2.65)$$

For the small sprocket, the following pitch diameter is calculated.

$$PD = \frac{12.7}{\sin\left(\frac{180^\circ}{35}\right)} = 70.84mm \quad (2.66)$$

Chapter 3

Analysis

3.1 Chassis

3.1.1 Description of Inputs and Outputs

A stress analysis will be conducted on the chassis by applying the concept of Finite Element Analysis (FEA). The points where the tubes intersect are the nodes and the tubes will be modeled as 3-D frame elements. The inputs in this case would be forces that are applied to the nodes of the structure which would define the type of analysis being performed. The following are the inputs being applied to this analysis: torsion couples and front, rear, and side collisions. The outputs are wall thickness of the tubes that are being subjected to the respective force or torque.

3.1.2 Assumptions and Materials

It is assumed that frame elements do not experience any shear stress, impacted elements are in static, elements will only deform elastically, and parameterization of the chassis aims for a minimum safety factor 2.0 for all kinds of loads. The material selected for the space-frame is 4130 steel which has a low carbon content and is more suitable for welding.

3.1.3 Stress Analysis

To demonstrate the theory of FEA, sample calculations will be performed on element 4 shown in figure 3.1. The rest of the calculations will be performed using MATLAB.

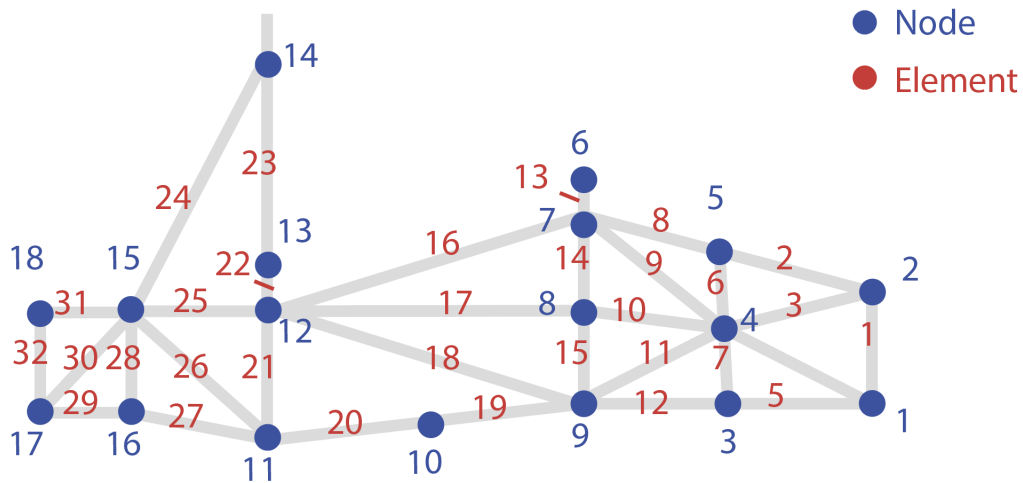


Figure 3.1: Nodes and Elements on the Chassis

Modelling element 4 as a 2-D frame elements permits the calculations of axial stresses, shear stresses, bending stresses, and torsional stresses.

Element 4 Sample Calculation

Node 1 of element 4 is subjected to a front impact force which was calculated to be 18245 N in the modeling section. The total force acting on node 1 is 4561.4 N. Calculations are done using the MATLAB code in B.12

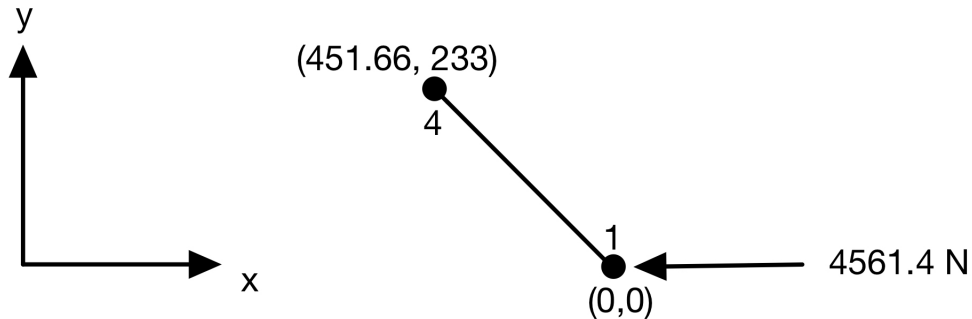


Figure 3.2: Element 4 free body diagram

The minimum required geometric characteristics for front bulkhead tubing must be size B. Therefore, the cross-sectional area (A) is 119.6 mm^2 , the modulus of elasticity (E) is 205 GPa , the moment of inertia (I) is 8508.8 mm^4 , and the polar moment of inertia (J) is 17017.6 mm^4 .

The length of element 4 can be determined using the nodal coordinates in figure 3.2.

$$L = \sqrt{(x_j - x_i)^2 + (y_j - y_i)^2} \quad (3.1)$$

$$L = \sqrt{(451.66 - 0)^2 + (233 - 0)^2} = 506.8 \text{ mm} \quad (3.2)$$

After collecting the parameters above, the element stiffness matrix B.19 derived in Appendix B can be used to characterize element 4.

$$[K^{4'}] = 10^7 \begin{bmatrix} 0.00484 & 0 & 0 & -0.00484 & 0 & 0 \\ 0 & 0.000016 & 0.00407 & 0 & -0.000016 & 0.00407 \\ 0 & 0.00407 & 1.377 & 0 & -0.00407 & 0.688 \\ -0.00484 & 0 & 0 & 0.00484 & 0 & 0 \\ 0 & -0.000016 & -0.00407 & 0 & 0 & 0 \\ 0 & 0.00407 & 0.688 & 0 & -0.00407 & 2.75 \end{bmatrix} \quad (3.3)$$

As shown in Appendix B, this matrix needs to be rotated onto the global coordinates using a rotation matrix $[R]$.

$$[R] = \begin{bmatrix} 0.891 & 0.454 & 0 & 0 & 0 & 0 \\ -0.454 & 0.891 & 0 & 0 & 0 & 0 \\ 0 & 0 & 0.002 & 0 & 0 & 0 \\ 0 & 0 & 0 & 0.891 & 0.454 & 0 \\ 0 & 0 & 0 & -0.454 & 0.891 & 0 \\ 0 & 0 & 0 & 0 & 0 & 0.002 \end{bmatrix} \quad (3.4)$$

Using the equation below, the global matrix $[K^4]$ is computed.

$$[K^4] = 10^4 \begin{bmatrix} 3.85 & 1.95 & -0.00365 & -3.85 & -1.95 & -0.00365 \\ 1.95 & 1.01 & 0.00716 & -1.95 & -1.01 & 0.00416 \\ -0.00365 & 0.00716 & 0.00536 & 0.00365 & -0.00716 & 0.00267 \\ -3.85 & -1.95 & 0.00365 & 3.84 & 1.957 & 0 \\ -1.95 & -1.009 & -0.00716 & 1.95 & 0.996 & 0 \\ -0.00365 & 0.00716 & 0.00268 & 0.00365 & -0.00716 & 0.0107 \end{bmatrix} \quad (3.5)$$

Using $[U^4] = [K^4]^{-1}[F^4]$, where $[F^4]$ is the external force applied on element 4, we can calculate the global displacement $[U^4]$.

$$[U^4]^\top = \begin{bmatrix} 0.574 & -0.273 & -0.0184 & 0.0209 & -0.203 & 0.0283 \end{bmatrix} \quad (3.6)$$

Rotating the displacement vector on the local coordinates using $[U^{e'}] = [R][U^e]$ enables the computation of the local external force vector using $[F^{e'}] = [K^{e'}][U^{e'}]$.

$$[U^4]^\top = \begin{bmatrix} -0.0725 & -0.269 & -0.0000364 & 0.00935 & -0.028 & -0.000056 \end{bmatrix} \quad (3.7)$$

The local external force vector is represented as follows.

$$[F^{4'}]^\top = \begin{bmatrix} F_{x_1} & F_{y_1} & M_{z1} & F_{x_4} & F_{y_4} & M_{z4} \end{bmatrix} \quad (3.8)$$

Where F_x is the axial force, F_y is the transverse force, and M_z is the bending moment in the z-axis.

$$\left[F^{4'} \right]^T = \begin{bmatrix} -3960N & -42.5N & -10720Nm & 3960N & 44.7N & 11625Nm \end{bmatrix} \quad (3.9)$$

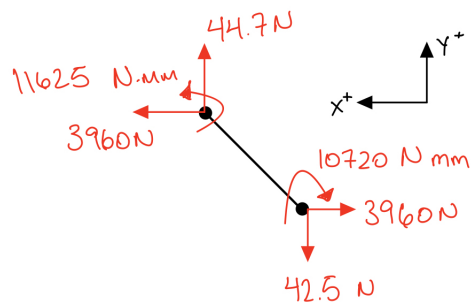


Figure 3.3: Reaction forces on Element 4 FBD

These forces are used to calculate the axial stress (σ_{axial}), bending stress (σ_{bending}) and shear stress (τ_{shear}) that element 4 experiences.

$$\sigma_{\text{axial}} = \frac{F_X}{A} = \frac{3960N}{119.6mm^2} = 33.11MPa \quad (3.10)$$

$$\sigma_{\text{bending}} = \frac{(M_z)(c)}{I} = \frac{(11625Nm)(12.69mm)}{8508.8mm^4} = 17.33MPa \quad (3.11)$$

Where c is the outer radius of the tube.

$$\tau_{\text{shear}} = \frac{(44.7N)}{119.6mm^4} = 0.37MPa \quad (3.12)$$

These stresses are used in the collision cases to calculate a safety factor.

Front Impact Analysis

The same steps as the sample calculation section are taken to find the stresses due to a front impact force. In this case, the rear bulkhead is fixed and forces of 4561.5 N are applied to nodes 1 and 2.

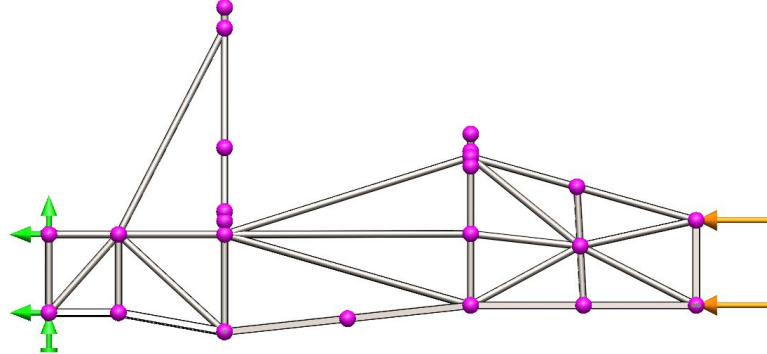


Figure 3.4: Front Impact FBD

The highest axial forces, transverse forces, and moments are extracted from the MATLAB code in the appendix to calculate their respective stresses.

$$\sigma_{\text{axial}} = 17.11 \text{ MPa} \quad (3.13)$$

$$\sigma_{\text{bending}} = 54.94 \text{ MPa} \quad (3.14)$$

$$\tau_{\text{shear}} = 2.65 \text{ MPa} \quad (3.15)$$

The safety factor can be calculated by dividing the stresses computed above by the material yield strength. For 4130 steel, the yield strength is 435 MPa.

$$n = \frac{\sigma_{\text{yield}}}{\sigma} \quad (3.16)$$

$$n = \frac{435 MPa}{68.47 MPa} = 25 \quad (3.17)$$

$$n = \frac{435 MPa}{311.96 MPa} = 7.9 \quad (3.18)$$

$$n = \frac{435 MPa}{2.65 MPa} = 164 \quad (3.19)$$

The lowest safety factor calculated is 7.9 which can be lowered by decreasing the thickness of the tube. Refer to figure B.5 and figure B.6 in Appendix B for a Solidworks simulation that outputs a safety factor of 2.5 which will aid the parametrization goals of the chassis.

Rear Impact Analysis

The same steps as the sample calculation section are taken to find the stresses due to a rear impact force. In this case, the front bulkhead is fixed and forces of 4561.5 N are applied to nodes 17 and 18.

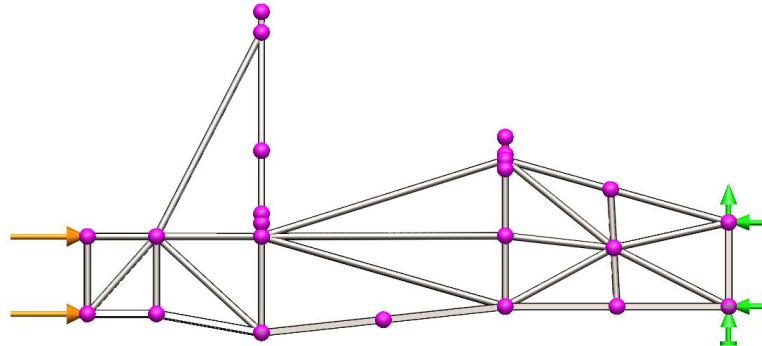


Figure 3.5: Rear Impact FBD

The highest axial forces, transverse forces, and moments are extracted from the Matlab code in B.12 to calculate their respective stresses.

$$\sigma_{\text{axial}} = 9.7 \text{ MPa} \quad (3.20)$$

$$\sigma_{\text{bending}} = 301.3 \text{ MPa} \quad (3.21)$$

$$\tau_{\text{shear}} = 10 \text{ MPa} \quad (3.22)$$

$$n = \frac{\sigma_{\text{yield}}}{\sigma} \quad (3.23)$$

$$n = \frac{435 \text{ MPa}}{2.65 \text{ MPa}} = 45 \quad (3.24)$$

$$n = \frac{435 \text{ MPa}}{1.06 \text{ MPa}} = 1.44 \quad (3.25)$$

$$n = \frac{435 \text{ MPa}}{2.65 \text{ MPa}} = 43.5 \quad (3.26)$$

The lowest safety factor is 1.44 which is lower than 2.0. This can be increased by increasing the diameter of the tubes. Refer to figure figure B.7 and figure B.8 in Appendix B for a Solidoworks simulation which outputs a safety factor of 2.7 which will aid the parametrization goals of the chassis.

Side Impact Analysis

The same steps as the sample calculation section are taken to find the stresses due to a side impact force. In this case, the front and rear bulkheads are fixed and forces of -3935 N are applied to nodes 7, 8, 9, 11, and 12.

The highest axial forces, transverse forces, and moments are extracted from the Matlab code in Appendix B to calculated their respective stresses.

$$\sigma_{\text{axial}} = 55.4 \text{ MPa} \quad (3.27)$$

$$\sigma_{\text{bending}} = 14.36 \text{ MPa} \quad (3.28)$$

$$\tau_{\text{shear}} = 73.9 \text{ MPa} \quad (3.29)$$

$$n = \frac{\sigma_{\text{yield}}}{\sigma} \quad (3.30)$$

$$n = \frac{435 \text{ MPa}}{2.65 \text{ MPa}} = 8.1 \quad (3.31)$$

$$n = \frac{435 \text{ MPa}}{1.06 \text{ MPa}} = 31 \quad (3.32)$$

$$n = \frac{435 \text{ MPa}}{2.65 \text{ MPa}} = 5.9 \quad (3.33)$$

The lowest safety factor is 5.9. This can be lowered by reducing the wall thickness of the tubes of the chassis. Refer to figure B.9 and figure B.10 in Appendix B for a Solidworks simulation that outputs a safety factor of 2.7 that will help the parametrization of the chassis.

3.2 Suspension

3.2.1 Forces acting on Suspension Components

The components are made out of 4130 steel with an elastic modulus (E) of 205 GPa, a tensile strength of 670 MPa, and a yield strength of 435 MPa.

It is assumed that the suspension structure is a rigid body connected to rigid truss members that are pinned at both ends. Except for springs, it is assumed that all components in the system are rigid bodies without deformation. Lastly, the influence of gravity of each component and friction at the hinge points of each ball are ignored.

To determine the forces experienced by the suspension members, the largest forces on the tire patch under the combined conditions of braking, cornering, and acceleration were considered. These forces are transferred to the wheel center, providing three forces and three moments along the three axes.

For the front, the lateral force (F_x) is 1438.79 N, the vertical force (F_y) is 1661 N, and the longitudinal force (F_z) is 1495.49 N. For the rear, the lateral force (F_x) is 1388.5 N, the vertical force (F_y) is 1710.56 N, and the longitudinal force (F_z) is 1539.5 N. The x, y, and z coordinates of the control arms, push rods, and tie rod are tabulated in the appendix.

INSERT FBD OF FRONT CONTROL ARMS AND TIRE HERE: 3D force analysis diagram

First, unit vectors for the suspension members are created. Member AB, one of the lower control arm members, will be used as an example. Let A and B represent the corresponding suspension points such that

$$A = (A_x, A_y, A_z) = (596.9 \text{ mm}, 7.94 \text{ mm}, 658.16 \text{ mm}) \quad (3.34)$$

$$B = (B_x, B_y, B_z) = (294.72 \text{ mm}, 0 \text{ mm}, 877.99 \text{ mm})$$

where A_x and B_x are the X-coordinates, A_y and B_y are the Y-coordinates, and A_z and B_z are the Z-coordinates of points A and B.

The vector from point A to point B and its magnitude are calculated such that

$$\begin{aligned}\overrightarrow{AB} &= (A_x - B_x, A_y - B_y, A_z - B_z) \\ &= (596.9 \text{ mm} - 294.72 \text{ mm}, 7.94 \text{ mm} - 0 \text{ mm}, 658.16 \text{ mm} - 877.99 \text{ mm}) \quad (3.35) \\ &= (302.18 \text{ mm}, 7.94 \text{ mm}, -219.83 \text{ mm})\end{aligned}$$

$$\begin{aligned}|AB| &= [(A_x - B_x)^2 + (A_y - B_y)^2 + (A_z - B_z)^2]^{1/2} \\ &= [(302.18 \text{ mm})^2 + (7.94 \text{ mm})^2 + (-219.83 \text{ mm})^2]^{1/2} \quad (3.36) \\ &= 373.77 \text{ mm}^2\end{aligned}$$

The unit vector can then be found using

$$\begin{aligned}\widehat{\overrightarrow{AB}} &= \frac{\overrightarrow{AB}}{|AB|} = \left(\frac{302.18}{373.77}, \frac{7.94}{373.77}, \frac{-219.83}{373.77} \right) \\ &= (0.8085, 0.0212, -0.5882) \quad (3.37)\end{aligned}$$

The same procedure is used to calculate a unit vector for each of the six suspension members resulting in unit vectors $\widehat{\overrightarrow{AC}}$, $\widehat{\overrightarrow{DE}}$, $\widehat{\overrightarrow{DF}}$, $\widehat{\overrightarrow{GH}}$, and $\widehat{\overrightarrow{IJ}}$ as shown in APPENDIX. Since this is a static structure, the sum of the forces must equal 0. The three equations below express the summation of forces in the x, y, and z coordinates.

$$\sum F_x = 0 = F_{AB} \widehat{\overrightarrow{AB}_x} + F_{AC} \widehat{\overrightarrow{AC}_x} + F_{DE} \widehat{\overrightarrow{DE}_x} + F_{DF} \widehat{\overrightarrow{DF}_x} + F_{GH} \widehat{\overrightarrow{GH}_x} + F_{IJ} \widehat{\overrightarrow{IJ}_x} + F_x \quad (3.38)$$

$$\sum F_y = 0 = F_{AB} \widehat{\overrightarrow{AB}_y} + F_{AC} \widehat{\overrightarrow{AC}_y} + F_{DE} \widehat{\overrightarrow{DE}_y} + F_{DF} \widehat{\overrightarrow{DF}_y} + F_{GH} \widehat{\overrightarrow{GH}_y} + F_{IJ} \widehat{\overrightarrow{IJ}_y} + F_y \quad (3.39)$$

$$\sum F_z = 0 = F_{AB} \widehat{\overrightarrow{AB}_z} + F_{AC} \widehat{\overrightarrow{AC}_z} + F_{DE} \widehat{\overrightarrow{DE}_z} + F_{DF} \widehat{\overrightarrow{DF}_z} + F_{GH} \widehat{\overrightarrow{GH}_z} + F_{IJ} \widehat{\overrightarrow{IJ}_z} + F_z \quad (3.40)$$

where F_{AB} is the axial load in member AB and F_x is the X-component of the force at the wheel center for the specific loading scenario. All five other forces follow the same

nomenclature.

The front wheel center point will be called WC and will have an x, y, and z coordinate. Using it as the starting point, vectors connecting the wheel center to each of the outboard suspension points (A,D,G,I) are created. In this example, r_A is calculated using

$$\begin{aligned}
 r_A &= A - WC \\
 &= (r_{AX}, r_{AY}, r_{AZ}) \\
 &= (596.9 \text{ mm} - 626.9 \text{ mm}, 7.94 \text{ mm} - 122.24 \text{ mm}, 658.16 \text{ mm} - 658.16 \text{ mm}) \\
 &= (-30.00 \text{ mm}, -114.30 \text{ mm}, 0 \text{ mm})
 \end{aligned} \tag{3.41}$$

The same process is repeated for each of the four outboard suspension points (A,D,G,I). These vectors will become the r vectors. To sum the moments about the wheel center, the cross product of the specified r and F vectors are used to determine the moments about the wheel center in the x, y, and z directions.

$$\sum M_X = O = F_{AC} (\widehat{AC}_Z r_{AY} - \widehat{AC}_Y r_{AZ}) + F_{AB} (\widehat{AB}_Z r_{AY} - \widehat{AB}_Y r_{AZ}) + F_{DF} (\widehat{DF}_Z r_{DY} - \widehat{DF}_Y r_{DZ}) + F_{DE} (\widehat{DE}_Z r_{DY} - \widehat{DE}_Y r_{DZ}) + F_{IJ} (\widehat{IJ}_Z r_{IY} - \widehat{IJ}_Y r_{IZ}) + F_{GH} (\widehat{GH}_Z r_{GY} - \widehat{GH}_Y r_{GZ}) + M_X \tag{3.42}$$

$$\sum M_Y = O = F_{AC} (\widehat{AC}_Z r_{AX} - \widehat{AC}_X r_{AZ}) + F_{AB} (\widehat{AB}_Z r_{AX} - \widehat{AB}_X r_{AZ}) + F_{DF} (\widehat{DF}_Z r_{DX} - \widehat{DF}_X r_{DZ}) + F_{DE} (\widehat{DE}_Z r_{DX} - \widehat{DE}_X r_{DZ}) + F_{IJ} (\widehat{IJ}_Z r_{IX} - \widehat{IJ}_X r_{IZ}) + F_{GH} (\widehat{GH}_Z r_{GX} - \widehat{GH}_X r_{GZ}) + M_Y \tag{3.43}$$

$$\sum M_Z = O = F_{AC} (\widehat{AC}_Y r_{AX} - \widehat{AC}_X r_{AY}) + F_{AB} (\widehat{AB}_Y r_{AX} - \widehat{AB}_X r_{AY}) + F_{DF} (\widehat{DF}_Y r_{DX} - \widehat{DF}_X r_{DY}) + F_{DE} (\widehat{DE}_Y r_{DX} - \widehat{DE}_X r_{DY}) + F_{IJ} (\widehat{IJ}_Y r_{IX} - \widehat{IJ}_X r_{IY}) + F_{GH} (\widehat{GH}_Y r_{GX} - \widehat{GH}_X r_{GY}) + M_Z \tag{3.44}$$

With the six equations (three force equations and three moment equations) the forces in each of the six members can be calculated. The resulting overall equation for member loads is given as

$$[A]\{x\} = \{b\} \tag{3.45}$$

where

$$[A] = \begin{bmatrix} \widehat{AC}_X & \widehat{AB}_X & \widehat{DF}_X & \widehat{DE}_X & \widehat{IJ}_X & \widehat{GH}_X \\ \widehat{AC}_Y & \widehat{AB}_Y & \widehat{DF}_Y & \widehat{DE}_Y & \widehat{IJ}_Y & \widehat{GH}_Y \\ \widehat{AC}_Z & \widehat{AB}_Z & \widehat{DF}_Z & \widehat{DE}_Z & \widehat{IJ}_Z & \widehat{GH}_Z \\ \left(\widehat{AC}_Z r_{AY} - \widehat{AC}_Y r_{AZ} \right) & \left(\widehat{AB}_Z r_{AY} - \widehat{AB}_Y r_{AZ} \right) & \left(\widehat{DF}_Z r_{DY} - \widehat{DF}_Y r_{DZ} \right) & \left(\widehat{DE}_Z r_{DY} - \widehat{DE}_Y r_{DZ} \right) & \left(\widehat{IJ}_Z r_{IY} - \widehat{IJ}_Y r_{IZ} \right) & \left(\widehat{GH}_Z r_{GY} - \widehat{GH}_Y r_{GZ} \right) \\ \left(\widehat{AC}_Z r_{AX} - \widehat{AC}_X r_{AZ} \right) & \left(\widehat{AB}_Z r_{AX} - \widehat{AB}_X r_{AZ} \right) & \left(\widehat{DF}_Z r_{DX} - \widehat{DF}_X r_{DZ} \right) & \left(\widehat{DE}_Z r_{DX} - \widehat{DE}_X r_{DZ} \right) & \left(\widehat{IJ}_Z r_{IX} - \widehat{IJ}_X r_{IZ} \right) & \left(\widehat{GH}_Z r_{GX} - \widehat{GH}_X r_{GZ} \right) \\ \left(\widehat{AC}_Y r_{AX} - \widehat{AC}_X r_{AY} \right) & \left(\widehat{AB}_Y r_{AX} - \widehat{AB}_X r_{AY} \right) & \left(\widehat{DF}_Y r_{DX} - \widehat{DF}_X r_{DY} \right) & \left(\widehat{DE}_Y r_{DX} - \widehat{DE}_X r_{DY} \right) & \left(\widehat{IJ}_Y r_{IX} - \widehat{IJ}_X r_{IY} \right) & \left(\widehat{GH}_Y r_{GX} - \widehat{GH}_X r_{GY} \right) \end{bmatrix} \quad (3.46)$$

$$\{x\} = \begin{Bmatrix} F_{AC} \\ F_{AB} \\ F_{DF} \\ F_{DE} \\ F_{IJ} \\ F_{GH} \end{Bmatrix} \quad (3.47)$$

$$\{b\} = \begin{Bmatrix} F_X \\ F_Y \\ F_Z \\ M_X \\ M_Y \\ M_Z \end{Bmatrix} \quad (3.48)$$

A MATLAB program has been designed to solve these equations in a 6x6 matrix in B.10.3 for the front suspension. A similar MATLAB program has been designed to solve the rear suspension equations in a 5x5 matrix in B.10.4. The program solves for the six unknowns using matrix algebra by isolating for x such that

$$\{x\} = [B][A]^{-1} \quad (3.49)$$

For the front suspension, F_{AC} is -5957.44 N, F_{AB} is -1554.85 N, F_{DF} is 4025.03 N, F_{DE} is 2106.43 N, F_{IJ} is 64.16 N, and F_{GH} is -967.17 N. For the rear suspension, F_{KM} is -6111.31 N, F_{KL} is -708.25 N, F_{NP} is 3914.52 N, F_{NO} is 1869.32 N, and F_{QR} is -1012.58 N. The positive forces are tensile loads and the negative forces are compressive loads.

The worst affected member for buckling is member AC which has a length of 393.05 mm. The outer diameter is 20 mm and the internal diameter is 16 mm. The cross-sectional area is calculated using

$$A = \frac{\pi}{4} (d_o^2 - d_i^2) = \frac{\pi}{4} (20^2 - 16^2) = 113.10 \text{ mm}^2 \quad (3.50)$$

where d_o is the outer diameter in mm and d_i is the inner diameter in mm. The second moment of inertia of a hollow, circular cross section is calculated using

$$I_x = \frac{\pi}{4} (r_o^4 - r_i^4) = \frac{\pi}{4} (10^4 - 8^4) = 4637 \text{ mm}^4 \quad (3.51)$$

where r_o is the outer radius in mm and r_i is the inner radius in mm. Using the elastic modulus (E), column effective length factor (k), and unsupported length of the column (l), the critical load (P_{cr}) is calculated using

$$P_{cr} = \frac{\pi^2 EI}{(kl)^2} = \frac{\pi^2 (205,000 \text{ MPa}) (4637 \text{ mm}^4)}{(393.05 \text{ mm})^2} = 60729.57 \text{ N} \quad (3.52)$$

The column effective length factor of 1 is due to the end conditions of the members that are pinned on each end. With the calculated critical load of 60729.57 N for member AC, the factor of safety can be calculated using

$$FoS = \frac{P_{cr}}{|F_{AC}|} = \frac{60729.57 \text{ N}}{5957.44 \text{ N}} = 10.2 \quad (3.53)$$

The worst affected member for yielding is member DF which has a length of 393.71 mm. Member DF has the same area and second moment of inertia as member AC. The axial stress is calculated using

$$\sigma_{axial} = \frac{F_{DF}}{A} = \frac{4025.03 \text{ N}}{113.10 \text{ mm}^2} = 35.59 \text{ MPa} \quad (3.54)$$

where F_{DF} is the axial load on member DF in newtons and P_{cr} is the critical load in newtons. The factor of safety for axial stress is calculated using

$$FoS = \frac{\sigma_y}{\sigma_{axial}} = \frac{435 \text{ MPa}}{35.59 \text{ MPa}} = 12.22 \quad (3.55)$$

The two factors of safety calculated ensure that the suspension members do not fail under buckling or yielding during the competition. The factors of safety can be further optimized to reduce the overall weight of the vehicle.

Bolt Analysis: To obtain a safety factor, the critical shear stress and actual shear stress must be determined. The maximum shear stress can be determined by the equation below.

$$\tau_{max} = \frac{4 * V}{3 * A} \quad (3.56)$$

V is the shear force exerted on the cross-sectional area A . The type of bolt being used is an M8 bolt, which has a major diameter of 8mm. In the figure below, the cross-sectional area and shear can be found.

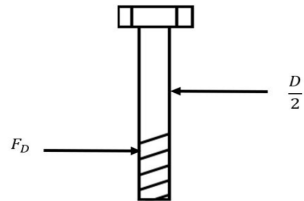


Figure 3.6: FBD of suspension member bolts for mounting

$$A = \pi * d^2 / 4 = \pi * (8 \text{ mm})^2 / 4 = 50.2 \text{ mm}^2 \quad (3.57)$$

By selecting the bolt and nut material as class SAE grade 8.8

$$S_y = 660 \text{ MPa}$$

, the safety factor can be found [9]. From the distortion energy theory we get the following for the safety factor:

$$S_{sy} = (0.58)(660\text{MPa}) = 382.3\text{MPa} \quad (3.58)$$

$$\eta = \frac{S_{sy}}{\tau_{\max}} = \frac{382.3\text{MPa}}{22.07} = 12.9 \quad (3.59)$$

3.3 Steering Knuckle

The Heim Joint bolt is used to fasten the heim joint to the steering arm. The Heim Joint bolt must be able to withstand the force needed to rotate the steering knuckle.

3.3.1 Description of Inputs and Outputs

The input force is the force applied from the tie rod and the output is the force that is applied onto the Heim Joint Bolt that will turn the steering knuckle.

3.3.2 Constants and Safety Factors

The tire width (T_{width}) is 0.23876 m and the tire radius (T_{radius}) is 0.25527 m. The coefficient of friction between the tire and the road ($\mu_{tireRoad}$) is 0.9 because it is assumed that the tires are slick and the track is dry. The minimum acceptable safety factor for the Heim Joint bolt is 1.3. As shown in section B.34 (TODO: add section), the maximum turning angle for the inner wheel (α_{Inner}) is 27.59 ° or 0.481 rad. The Angle between the steering arm and the knuckle (β) will be 15.31 ° or 0.267 rad. The distance between the kingpin axis and steering arm heim joint is 0.08m, and the diameter of the heim joint bolt ($D_{HeimJoint}$) will be assumed to be 0.008m.

3.3.3 Assumptions and Materials

There are a few assumptions with the steering model. These assumptions are that the contact patch is a circle, the bolt will only fail due to shearing, and the mass of the bolt is negligible.

3.3.4 Sketch of component and FBD

F_K represents the force on kingpin axis, F_{SA} represents the lateral force,

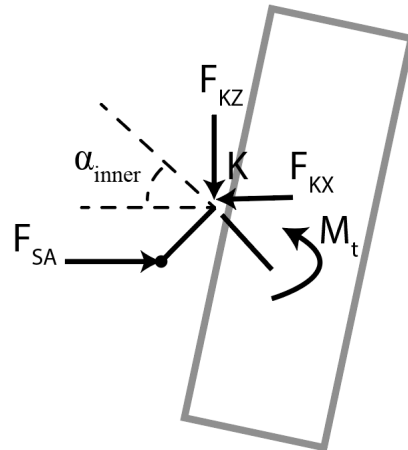


Figure 3.7: FBD of steering knuckle and wheel

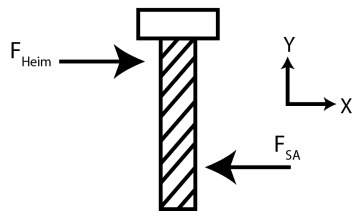


Figure 3.8: FBD of the bolt connecting the steering arm to the heim joint

3.3.5 Stress Analysis

The small element area (dA) of the contact patch of the tire can be modeled with the following equation, where r represents the element radius, the angle difference is represented by $d\theta$, and dr represents the radius difference as the rotation of the tire changes.

$$dA = rd\theta dr \quad (3.60)$$

The friction force in one area element (dF_f) can be determined by multiplying the friction coefficient by the normal force and substituting in equation 3.60. P represents the pressure caused by the normal force on the contact patch area.

$$dF_f = \mu \times dF_n = \mu \times P \times dA = \mu P r d\theta dr \quad (3.61)$$

The equation for the moment of friction (M_f) can be determined by integrating the result from equation 3.61 where R_t represents the total radius of the contact patch and F_N represents the total normal force.

$$M_f = \int_0^{2\pi} \int_0^{R_t} \mu P r^2 d\theta dr = \mu P \int_0^{2\pi} \int_0^{R_t} r^2 d\theta dr = \frac{\mu F_N}{\pi R_t^2} \int_0^{2\pi} \int_0^{R_t} r^2 d\theta dr \quad (3.62)$$

$$M_f = \frac{2}{3} \mu F_N R_t = \frac{2}{3} \times 0.9 \times 733.45 \text{ N} \times 0.1 \text{ m} = 44 \text{ Nm} \quad (3.63)$$

M_f and the analysis of the lateral forces applied on the steering arm is modelled in figure 3.7. The maximum angle of the tire (α_i) is 27.59° (0.481 rad). The lateral force (F_{SA}) can be determined by calculating the sum of moments around the kingpin axis (point K) and the angle of the steering arm (β):

$$F_{SA} = \frac{M_t}{d_{Heim} \cos(90^\circ - \alpha_i - \beta)} = \frac{44 \text{ Nm}}{0.08 \text{ m} \cos(90^\circ - 27.59^\circ - 15.31^\circ)} = 807.6 \text{ N} \quad (3.64)$$

The relationship between F_{SA} and F_{HEIM} is shown in figure 3.8. F_{HEIM} can be determined by analysing the forces in the x direction.

$$\sum F_z = 0 = F_{HEIM} - F_{SA} \quad (3.65)$$

$$F_{HEIM} = F_{SA} = 807.6\text{N} \quad (3.66)$$

The cross sectional area of the heim bolt is determined to calculate the maximum shear stress of the heim joint bolt. V represents the shear force and A represents the cross sectional area (8 mm since an M8 bolt is used).

$$A = \frac{\pi \times d^2}{4} = \frac{\pi \times 0.008m^2}{4} = 0.00005024m^2 \quad (3.67)$$

$$\tau_{MAX} = \frac{4V}{3A} = \frac{4}{3} \frac{807.6\text{N}}{0.00005024m^2} = 21.433143\text{MPa} \quad (3.68)$$

The shear yield strength (S_{Sy}) of the heim joint bolt can be determined using the material properties. The material of the heim joint bolt and nut is SAE grade 4.6 ($S_y = 240 \text{ MPa}$)

$$S_{Sy} = 0.58(S_y) = 0.58(240\text{MPa}) = 139.2\text{MPa} \quad (3.69)$$

The safety factor of the heim joint bolt can now be determined:

$$n = \frac{S_{Sy}}{\tau_{AMax}} = \frac{139.2 \text{ MPa}}{21.43 \text{ MPa}} = 6.49 \quad (3.70)$$

3.3.6 Critical Review

The safety factor for the heim joint bolt was high. The safety factor can be reduced by using a bolt with a smaller cross sectional area or a weaker material.

3.3.7 Flowchart for parameterization

3.4 Steering Arm Heim Joint

The steering arm heim joint is used to transfer force to the steering arm bolt while providing two rotational degrees of freedom to enable the tie rod to follow the movement of the suspension arms and rotation of the steering knuckle. The same analysis can also be applied to the heim joint connecting the rack pin to the tie rod.

3.4.1 Description of Inputs and Outputs

The input force applied to the steering arm heim joint is the force applied from the tie rod. The output is the reaction force onto the steering arm bolt.

3.4.2 Constants and safety factors

The angle between the tie rod and the heim joint will be $2.81^\circ(0.0491 \text{ rad})$ from the horizontal plane. The ideal safety factor for the heim joint is 1.5.

3.4.3 Assumptions, simplifications and materials

It will be assumed that the heim joints will only fail due to tensile, bending and shear stress at the threaded area. It is also assumed that the threading in the heim joint contains the same material properties as the M6 bolt. AISI 1018 will be used as the material for the heim joint.

3.4.4 Sketch of component and FBD

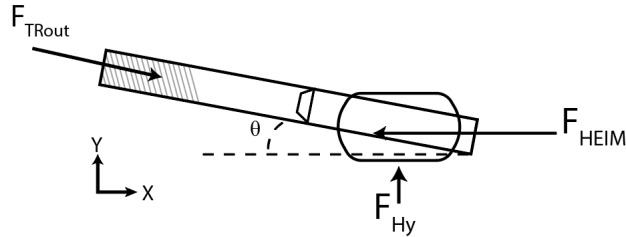


Figure 3.9: FBD of the steering arm heim joint

The input force (F_{TRout}) causes the output force F_{HEIM} at the ball of the heim joint and F_{HY} onto the steering arm.

3.4.5 Stress Analysis

Since F_{HEIM} and ϑ are known, the axial load F_{TRout} can be determined with the following equation.

$$\sum F_x = 0 = F_{TRout} \cos(\theta) - F_{HEIM} F_{TRout} = \frac{807.6\text{N}}{\cos(0.049\text{rad})} = 808.57\text{N} \quad (3.71)$$

The axial load on the threads of the heim joint can be determined with the following equation.

$$\sigma_{axial} = \frac{F_{axial}}{A_{thread}} = \frac{808.57\text{N}}{20.1\text{mm}^2} = 40.22\text{MPa} \quad (3.72)$$

The safety factor of the heim joint can be now calculated.

$$n = \frac{S_y}{\sigma_{axial}} = \frac{220\text{MPa}}{40.22\text{MPa}} = 5.46 \quad (3.73)$$

3.4.6 Critical Review

The safety factor of this heim joint is high. One way to reduce the safety factor of the heim joint is to use a lighter material or use a ball joint instead of a heim joint.

3.4.7 Flowchart for parameterization

3.5 Tie Rod

The tie rods are used to transfer the motion from the rack pin into the steering arm bolt.

3.5.1 Description of Inputs and Outputs

The input force of the tie rod is the pulling/pushing forces applied by the heim joint of the rack. The output force is applied onto the heim joint of the steering arm.

3.5.2 Constants and safety factors

The diameter of the tie rod (d_{TR}) is 0.0085 m. The diameter of the threaded hole (d_{TRhole}) is 0.006 m. The input force onto the tie rod (F_{TRin}) will be assumed to be the maximum of 808.57 N. The tie rod angle (ϑ) will be 2.81° (0.0491 rad). An acceptable safety factor for this component is 1.5.

3.5.3 Assumptions, simplifications and materials

The material used for the tie rod is steel alloy AISI 1018.

3.5.4 Sketch of component and FBD

The length of the tie rod (x_{TR}) will be 0.4072 m was found by determining the average length of the short and long arm of the suspension.

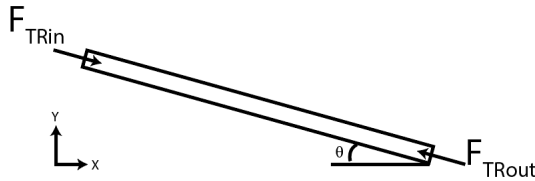


Figure 3.10: FBD of the Tie Rod

3.5.5 Stress Analysis

The cross sectional area of the tie rod (A_{TR}) must first be determined to calculate the axial stress. The cross sectional area can then be used to determine the axial stress and safety factor. A yield strength of 220 MPa was used.

$$A_{TR} = \frac{\pi}{4}(d_0^2 - d_i^2) = \frac{\pi}{4}[(0.0085m)^2 - (0.006m)^2] = 2.84 \times 10^{-5} \quad (3.74)$$

$$\sigma_{axial} = \frac{F_{TR}}{A_{TR}} = \frac{808.57N}{2.84 \times 10^{-5}} = 28.41 \text{ MPa} \quad (3.75)$$

$$n = \frac{S_y}{\sigma_{axial}} = \frac{220 \text{ MPa}}{28.41 \text{ MPa}} = 7.74 \quad (3.76)$$

Tie rods are also subjected to compressive loading, or buckling. To determine the critical buckling, the moment of inertia must first be calculated. The moment of inertia can then be used to determine the critical buckling force.

$$I = \frac{\pi}{2}[(\frac{D_{TR}}{2})^4 - (\frac{D_{TRhole}}{2})^4] = \frac{\pi}{2}[(\frac{0.0085m}{2})^4 - (\frac{0.006m}{2})^4] = 3.85 \times 10^{-10}m^4 \quad (3.77)$$

$$P_{cr} = \frac{\pi^2 \times E \times I}{L^2} = \frac{\pi^2 \times (2.05 \times 10^{11} \text{Pa}) \times (3.85 \times 10^{-10} m^4)}{0.4072m} = 1911.26 \text{ N} \quad (3.78)$$

$$n = \frac{\frac{P_{CR}}{A_{TR}}}{\frac{F_{TR}}{A_{TR}}} = \frac{P_{CR}}{F_{TR}} = \frac{1911.26 \text{N}}{808.57 \text{N}} = 2.36 \quad (3.79)$$

3.5.6 Critical Review

Various materials can be used to lower the safety factor calculated during tensile and compressive loading.

3.5.7 Flowchart for parameterization

3.6 Rack Pin

The rack heim joint is used to transfer forces from the rack pin to the tie rod.

3.6.1 Description of Inputs and Outputs

The input force onto the rack pin is the force from the rack. The output force is the reaction force onto the rack heim joint.

3.6.2 Constants and safety factors

The diameter of the rack pin (d_{Pin}) will be assumed to be 0.006 m. The yield stress (S_y) of the rack pin is 2.20×10^8 Pa. An acceptable safety factor for this pin is 1.5.

3.6.3 Assumptions, simplifications and materials

It is assumed that the rack pin will fail in double shear. The mass of the rack pin will also be neglected.

3.6.4 Sketch of component and FBD

TODO: add illustration

3.6.5 Stress Analysis

The sum of the forces from the free body diagram can be analysed to determine force applied onto the rack. F_{HEIM2} represents the force from the rack heim joint.

$$\sum F_x = 0 = F_{HEIM2} - \frac{F_P}{2} - \frac{F_P}{2} = 808.57\text{N} - F_P \quad (3.80)$$

$$F_P = 808.576\text{N} \quad (3.81)$$

The shear yield strength can be determined using distortion energy theory as shown in the following equation:

$$S_{Sy} = 0.58(S_y) = 0.58(240 \text{ MPa}) = 1.28 \times 10^8 \text{ Pa} \quad (3.82)$$

The cross sectional area must be determined to find the critical load. The critical load can then be used to find maximum shear stress (τ_{max}), actual shear stress (τ_{actual}), and the safety factor.

$$A = \frac{\pi \times d^2}{4} = \frac{\pi(0.006m)^2}{4} = 0.00002826 \text{ m}^2 \quad (3.83)$$

$$F_{cr} = 2S_{Sy}A = 2(1.28 \times 10^8 \text{ Pa})(0.00002826m^2) = 7.21 \times 10^3 \text{ N} \quad (3.84)$$

$$\tau_{max} = \frac{4V}{3A} = \frac{4}{3} \frac{7.21 \times 10^3\text{N}}{0.00002826m^2} = 1361.06 \text{ MPa} \quad (3.85)$$

$$\tau_{actual} = \frac{4V}{3A} = \frac{4}{3} \frac{808.576\text{N}}{0.00002826m^2} = 144.66 \text{ MPa} \quad (3.86)$$

$$n = \frac{\tau_{max}}{\tau_{actual}} = \frac{1361.06 \text{ MPa}}{144.66 \text{ MPa}} = 9.408 \quad (3.87)$$

3.6.6 Critical Review

The safety factor of the rack pin is much larger than the desired 1.5. The resultant safety factor can be reduced by lowering the diameter of the rack pin

3.6.7 Flowchart for parameterization

3.7 Rack

The rack is used to convert the rotational motion of the pinion into a linear motion to turn the wheels.

3.7.1 Description of Inputs and Outputs

The input force of the rack is the force applied from the teeth of the pinion. The output force is the reaction force applied to the rack pins connecting the heim joints.

3.7.2 Constants and safety factors

The height of the rack from the chassis (H_R) is 0.02 m. The length of the rack (L_R) was determined to be 0.4572 m from section B.34 (TODO: add reference). The width of the rack (W_R) is 0.0381 m (TODO: add rack reference), and the pin hole diameter is 0.006 m. The angle at which the pins are connected to the tie rods is 30° (0.523 rad). A suitable safety factor of 1.7 is desired for this component. It is assumed that the stress concentration factor caused by the pin hole (k_t) is 2.8 [10].

3.7.3 Assumptions, simplifications and materials

The main assumption is that the failure point will occur at the ends of the rack. The chosen material is AISI 1018 steel. The mass of the rack will be neglected.

3.7.4 Sketch of component and FBD

The pinion provides an input tangential force (F_{Pt}) and a radial force (F_{Pr}). F_{R1x} and F_{R1y} are the forces responsible for turning the right wheel, and F_{F2z} and F_{F2y} are responsible for rotating the left wheel. F_{C1y} and F_{C1x} are the vertical reactions onto the casing of the rack and pinion. The stress concentration of the rack is assumed to be

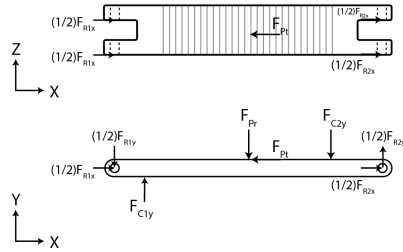


Figure 3.11: FBD of steering rack

3.7.5 Stress Analysis

It can be assumed that $F_{R1x} = F_{R2x}$, thus:

$$F_{R1x} = F_{R2x} = F_{Pin}\phi = F808.57 \text{ N} \times 0.52 \text{ rad} = 700.35 \text{ N} \quad (3.88)$$

F_{Pt} can be determined by applying the sum of forces of the figure B.12. F_{Pt} will be used to analyse the forces on the pinion.

$$\sum F_x = 0 = \frac{F_{R1x}}{2} + \frac{F_{R1x}}{2} - F_{Pt} + \frac{F_{R2x}}{2} + \frac{F_{R2x}}{2} = F_{R1x} - F_{Pt} + F_{R2x} \quad (3.89)$$

$$F_{Pt} = F_{R1x} + F_{R2x} = 700.35 \text{ N} + 700.35 \text{ N} = 1400.71 \text{ N} \quad (3.90)$$

The stress on one prong of the rack end can now be calculated to determine the safety factor.

$$\sigma_{prong} = k_t \frac{P}{A} = k_t \frac{F_{R1x}}{2A} = 2.8 \frac{700.35 \text{ N}}{2(0.02 \text{ m} - 0.006 \text{ m})(\frac{0.0381 \text{ m}}{3})} = 5.51 \text{ MPa} \quad (3.91)$$

$$n = \frac{S_y}{\sigma_{prong}} = \frac{220 \text{ MPa}}{5.51 \text{ MPa}} = 39.89 \quad (3.92)$$

3.7.6 Critical Review

Although the safety factor of the rack was high, no changes will be implemented to the rack since a sufficient clearance is required by the heim joint between the rack ends.

3.7.7 Flowchart for parameterization

3.8 Pinion

The pinion is the component of the steering that rotates from the shafts and transfers the force onto the rack.

3.8.1 Description of Inputs and Outputs

The input force onto the pinion is the force transferred from the pinion key. The output force is the tangential and radial forces applied onto the rack.

3.8.2 Constants and safety factors

Several parameters of the gear will be assumed. The overload factor (k_o) will be the maximum value of 2.25 as it is assumed the pinion will encounter medium shock and the mounting correction factor (k_m) will be 1.6. The pinion diameter (d_p) will initially be set to 88.9 mm.

3.8.3 Assumptions, simplifications and materials

It is assumed that the maximum pitch line velocities the pinion will endure will be negligible. [10]. It is also assumed that the gear will fail at the teeth, and the force applied on the key only contributes to torque, not forces. The mass of the pinion will also be neglected. The material of the pinion will be AISI 1018 steel.

3.8.4 Sketch of component and FBD

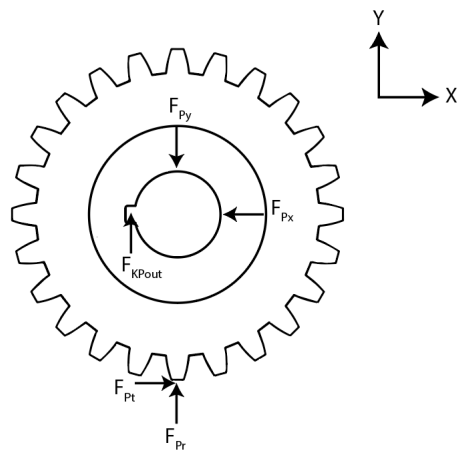


Figure 3.12: FBD of the pinion

3.8.5 Stress Analysis

The transmitted load (F_t) created from the teeth meshing between the rack and pinion can be calculated in the following equation using the torque transmitted (T) and the pinion diameter.

$$T = \frac{F_t d_p}{2} = \frac{1327.86 \text{ N} \times 0.0889 \text{ m}}{2} = 59.023 \text{ Nm} \quad (3.93)$$

The reactions of the forces on the secondary steering shaft F_{px} and F_{Py} can be determined by calculating the sum of forces.

$$\sum F_x = 0 = F_{pt} - F_{px} = 1327.86 \text{ N} - F_{px} \quad (3.94)$$

$$F_{px} = 1327.86 \text{ N} \quad (3.95)$$

The radial force (F_r) and ϕ can be determined using the gear's pressure angle of 20°.

$$F_r = (1327.86 \text{ N}) \tan(20^\circ) = 483.03 \text{ N} \quad (3.96)$$

To calculate the gear bending stress during normal operation, the following equation be used, where σ is the bending stress, P is the diametrical pitch, b is the pinion width, J is the geometry factor, K_v is the dynamic factor, K_O is the overload factor and K_m is the mounting correction factor [10]

$$\sigma = \frac{F_T P K_V K_O K_M}{b J} = \frac{(298.51 \text{ lbf})(8 \frac{\text{teeth}}{\text{inch}})(1.5 \text{ in})(1)(2.25)(1.5)}{(1.5 \text{ in})(0.33)} = 16282.71 \text{ Psi} = 112.26 \text{ MPa} \quad (3.97)$$

The bending fatigue strength must also be calculated to determine the bending stress and safety factor.

$$S_n = (S'_n)(C_L)(C_G)(C_S)(K_r)(K_t)(K_{ms}) = (220 \text{ MPa})(1)(1)(0.79)(0.897)(1)(1.4) = 218.25 \text{ MPa} \quad (3.98)$$

$$n = \frac{S_n}{\sigma} = \frac{218.26 \text{ MPa}}{112.29 \text{ MPa}} = 1.94 \quad (3.99)$$

3.8.6 Critical Review

The safety factor of the pinion is acceptable for this chosen rack.

3.8.7 Flowchart for parameterization

3.9 Pinion Key

3.9.1 Description of Inputs and Outputs

The input force on the pinion key is the force applied from the secondary steering shaft. The output force is the reaction on the pinion gear.

3.9.2 Constants and safety factors

A key width (w_{key}) of 0.004 was used. The height of the key (h_{key}) will also be 0.004 m. The pinion key length (l_{key}) was 0.03 m. The secondary shaft diameter (d_{sshaft}) is 0.022 m

3.9.3 Assumptions, simplifications and materials

It is assumed that the pinion key will only fail due to shear. The chosen material is AISI 1018. The mass of the pinion key will be neglected.

3.9.4 Sketch of component and FBD

The input force on the pinion key is F_{KPin} and the output force is F_{KPOut}

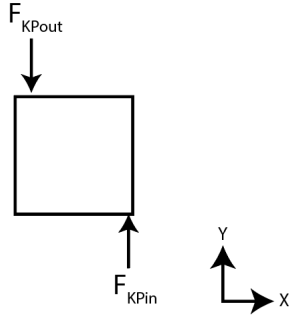


Figure 3.13: FBD of the Pinion Key

3.9.5 Stress Analysis

The torque applied on the pinion key can be determined using the output force and the radius. The torque transmitted (T) was previously calculated to be 59.02 Nm.

$$F_{KPout} = \frac{T}{r} = \frac{59.02 \text{ Nm}}{\frac{0.022\text{m}}{2} + \frac{0.004\text{m}}{2}} = 4501.32 \text{ N} \quad (3.100)$$

The sum of forces can now be applied to determine F_{KPin}

$$\sum F_y = 0 = F_{KPout} - F_{KPin} = 4501.32 \text{ N} - F_{KPin} \quad (3.101)$$

$$F_{KPin} = 4501.32 \text{ N} \quad (3.102)$$

The maximum shear stress for a rectangular cross section can be determined with the following equation, where τ_{max} is the maximum shear stress, V is the shear force, and A is the area of the shear plane. The safety factor can then be determined.

$$\tau_{max} = \frac{3V}{2A} = \frac{3 \cdot 4501.32 \text{ N}}{2 \cdot 0.004 \text{ m}} = 56.26 \text{ MPa} \quad (3.103)$$

$$n = \frac{S_{Sy}}{\tau_{max}} = \frac{128 \text{ MPa}}{56.26 \text{ MPa}} = 2.26 \quad (3.104)$$

3.9.6 Critical Review

The calculated safety factor is within the acceptable range, meaning the parameters such as the pinion key width, length, and height are acceptable.

3.9.7 Flowchart for parameterization

3.10 Universal Joint

The u-joint is the component that transfers the torque from the primary steering shaft to the secondary steering shaft.

3.10.1 Description of Inputs and Outputs

The input force is the torque applied onto the primary yoke. The output force is on the other end of the yoke arm.

3.10.2 Constants and safety factors

The joint diameter for pins on universal joint ($d_{PinJoint}$) 0.01327 mm.

3.10.3 Assumptions, simplifications and materials

It is assumed that the pin will only fail due to shear stress. The material used for the U-joint is AISI 1018. It is assumed that value of F_{UB} is the force applied from the yoke arms.

3.10.4 Sketch of component and FBD

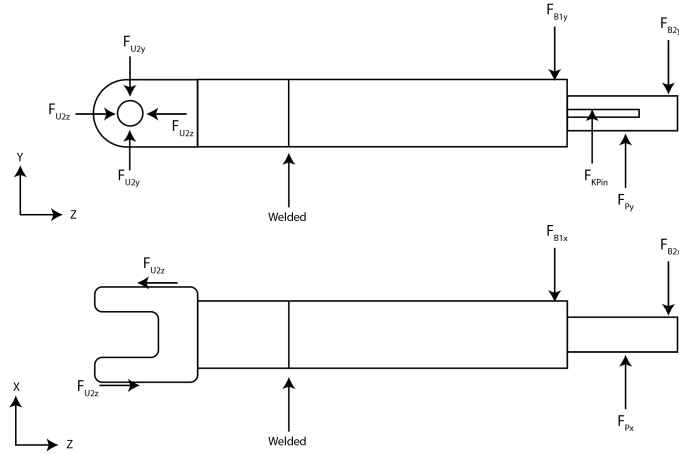


Figure 3.14: FBD of the shaft of the U-Joint

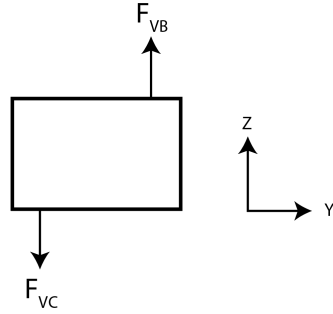


Figure 3.15: FBD of the U-joint pin

3.10.5 Stress Analysis

To determine the forces acting on the U-joint from the shaft, the forces on figure 3.14 are examined. The distance between the U-Joint arms ($d_{\text{betweenArms}}$) is 0.0635 m. The

thickness of the U-Joint (t_{UJoint}) is 0.00476 m. The diameter of the smaller steering shaft ($d_{smallerShaft}$) is 0.022 m. The width of the key (w_{key}) of the U-Joint is 4 mm wide. The diameter of the joint pins on the universal joint ($d_{JointPin}$) is 0.013 mm. F_{UB} is the input force applied from the bushing, and F_{UC} is the reaction on the cross. To determine the shear stress and safety factor, the following equation is used.

$$\sum M_z = 0 = 2F_{U2y}(d_{betweenArms} + \frac{t_{UJoint}}{2}) - F_{PKin}(d_{smallerShaft} - \frac{w_{key}}{2}) \quad (3.105)$$

$$F_{U2y} = \frac{F_{PKin}(d_{smallerShaft} - \frac{w_{key}}{2})}{2(d_{betweenArms} + \frac{t_{UJoint}}{2})} = \frac{4501.32N(0.022\text{ m} - \frac{0.004\text{ m}}{2})}{2(0.0635\text{ m} + \frac{0.00476\text{ m}}{2})} = 690.94\text{ N} \quad (3.106)$$

$$\tau_{max} = \frac{2V}{3\pi(\frac{d_{JointPin}}{2})^2} = \frac{2 \cdot 690.94\text{ N}}{3\pi(\frac{0.013\text{ mm}}{2})^2} = 3.33\text{ MPa} \quad (3.107)$$

$$n = \frac{S_{Sy}}{\tau_{max}} = \frac{0.58S_y}{\tau_{max}} = \frac{0.58(220\text{ MPa})}{3.33\text{ MPa}} = 38.29 \quad (3.108)$$

3.10.6 Critical Review

A very large safety factor was calculated for the U-Joint. Thus, the thicknesses of the U-Joint, the diameter of the steering shafts, and the material chosen can be altered to reduce the safety factor and lower the weight of the vehicle.

3.10.7 Flowchart for parameterization

3.11 Brake Rotors

This section will analyse the rotor to ensure it can withstand the braking force from the brake pad. This section will also analyse the steering knuckle to prove that it can withstand the braking moment from the caliper experienced when pressing the brake pads against the rotor.

3.11.1 Safety Factors

A safety factor of at least 20 should be achieved at the brake rotors since the rotors are heavily under stress throughout a race.

3.11.2 Assumptions, simplifications, and materials

For this analysis, we will assume that the rotor does not have drilled slots, the braking force from the pad onto the rotor is constant and distributed evenly, the vehicle is running at max speed, and the yield stress for stainless steel is constant at 276 MPa.

3.11.3 Sketch of component and FBD

3.11.4 Stress analysis

Using the pad area of the caliper (0.00235 m^2) and the highest force applied onto the rotors (2108 N from equation 2.48), we can determine the stress experienced from the brake pad.

$$\sigma_{Rotor} = \frac{F \times \text{Number of Pistons}}{A} = \frac{2108\text{N} \times 4}{0.00235\text{m}^2} = 3.925\text{MPa} \quad (3.109)$$

Using the yield strength of stainless steel, we can determine safety factor of the rotor.

$$n = \frac{\sigma}{S_y} = \frac{276\text{MPa}}{3.925\text{MPa}} = 70.31 \quad (3.110)$$

3.11.5 Critical review

In conclusion, the rotor can withstand the force of the brake pad from the caliper.

3.12 Powertrain

3.12.1 Analysis Outline

The components to be analyzed in this section are the sprockets, chain, and half axle shaft.

3.12.2 Inputs and Outputs

The torque produced from the motor is considered an input. The sprockets reduce the torque and a traction force is outputted to the tire.

3.12.3 Assumptions and Materials

To perform the analysis, the following assumptions are to be made:

- The CV remain horizontal during the analysis
- No torsional stress in the CV joint
- No torque lost from the sprocket and the tire
- No friction between links on the chain

7075 tempered steel alloy with a yield strength of 503 MPa is chosen for the sprockets, AISI 1045 Carbon Steel with a yield strength of 310 MPa is chosen for the chain, and 4130 Steel with a yield strength of 435 MPa is chosen for the half axle shafts.

3.12.4 Stress Analysis

Half Shaft

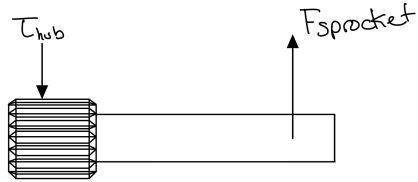


Figure 3.16: Half Axle Shaft Free Body Diagram

As noted in figure 3.21, there is a torsional stress on the splines of the shaft that connect to the wheel hub. This stress can be calculated using the following equation.

$$\tau = \frac{Tr}{J} \quad (3.111)$$

Where r is the radius of the splines and J is the polar moment of inertia.

$$\tau = \frac{346930Nmm12.75mm}{41510.75mm^4} = 106.56MPa \quad (3.112)$$

$$n = \frac{\sigma_y}{\tau_{shear}} = \frac{435MPa}{106.56MPa} = 4.08 \quad (3.113)$$

As shown in figure 3.21, the tangential force from the sprocket exerted on the half axle shaft can cause bending stress in the shaft.

$$\sigma_{bending} = \frac{Mc}{I} = \frac{346930Nmm12.75mm}{20755.3mm^4} = 213.12MPa \quad (3.114)$$

$$n = \frac{\sigma_y}{\sigma_{bending}} = \frac{435MPa}{213.12MPa} = 2.04 \quad (3.115)$$

The lowest safety factor is 2.04 which reasonable. The safety factor can be slightly increased by increasing the radius of the diameter.

Sprockets

Figure 3.17: Sprocket Free Body Diagram

As shown in figure 3.22, the tangential force the chain exerts on the sprockets cause bending stresses in the sprockets. The moment exerted on the big sprocket is 340.93 Nm and small sprocket is 140.03 Nm.

$$\sigma_{bending} = \frac{Mc}{I} = \frac{346930Nmm70.84mm}{19757694.34mm^4} = 1.24MPa \quad (3.116)$$

$$\sigma_{bending} = \frac{Mc}{I} = \frac{140030Nmm28.5367mm}{500082.7mm^4} = 7.99MPa \quad (3.117)$$

$$n = \frac{\sigma_y}{\sigma_{bending}} = \frac{503MPa}{1.24MPa} = 404.38 \quad (3.118)$$

$$n = \frac{\sigma_y}{\sigma_{bending}} = \frac{503MPa}{7.99MPa} = 62.94 \quad (3.119)$$

The safety factors are very high in this case. However, sprocket safety factor are usually decreased by removing material form the sprocket. This is hard to model especially when trying to calculate the moment of inertia as the sprocket has non-linear patterns of removed materials.

Chain Links

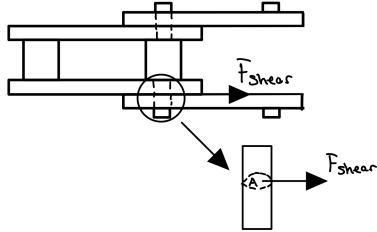


Figure 3.18: Chain Shaft Free Body Diagram

The two links exert a shear force which act on the link pin. The link pin diameter is considered 4.7625 mm produced an circular cross-sectional area A of 17.81 mm^2 .

$$\tau_{shear} = \frac{F_y}{A} = \frac{4897.42 \text{ N}}{17.8139 \text{ mm}^2} = 274.92 \text{ MPa} \quad (3.120)$$

$$n = \frac{\sigma_y}{\tau_{shear}} = \frac{310 \text{ MPa}}{274.92 \text{ MPa}} = 1.1276 \quad (3.121)$$

This safety factor is considered low. A safety factor of 2.5 would be appropriate. This can be achieved by increasing the diameter of the link pin.

3.13 Battery Mount Analysis

3.13.1 Description of Inputs/Outputs

The inputs to the battery mounts are:

Thickness of Top Mount $t_{topmount}$ 0.02 m, thickness of Bottom Mount $t_{botmount}$ 0.01 m, Max Force Applied Top Mount F_{TMmax} 117.72 N, Distance between Force and Bolt d_f 0.08 m, Bolt Diameter D_{bolt} 0.02 m, and a Bolt Length L_{bolt} 0.038 m. Yield Strength $S_y = 220 \text{ MPa}$

3.13.2 Justification of Inputs, Parameters

The battery mounts will need to withstand the weight of the battery and must be able to withstand any extra loads which may be experienced. Therefore, the total force that the mounts need to withstand will be assumed to be $3 \times \text{the weight of the battery}$.

The mounts are to made of Steel Alloy A36 Hot rolled.

3.13.3 Bolt Analysis

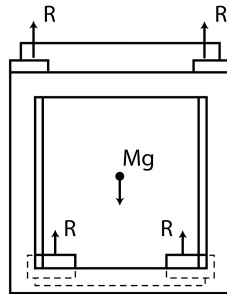


Figure 3.19: FBD of Forces acting on Battery Mounts

The analysis for the bolt is straight forward, taking the moment created from the force which can be found by taking the sum forces:

$$\Sigma(F_y) = 0 \quad (3.122)$$

$$(m * g) + 8 * R_{bm} = 0 \quad (3.123)$$

$$R_{bm} = 39.28N \quad (3.124)$$

Assuming the force which the mound needs to account for is 3 times R_{bm}

$$R_{bm} = 117.72N \quad (3.125)$$

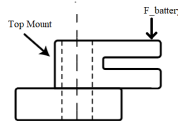


Figure 3.20: FBD of Forces acting on Battery Mount

Thus, the bending stress acting on the bolt can be defined as the following:

$$\sigma = \frac{R_{bm} * d_f * d_f}{I_{bolt}} = \frac{117.72N * 0.08m * 0.08m}{\frac{\pi}{32} * (0.02m)^4} = 47987770.7Pa \quad (3.126)$$

Thus, the safety factor for the bolt can be determined as follows

$$n = \frac{S_y}{\sigma} = \frac{220000000Pa}{47987770.7Pa} = 4.584 \quad (3.127)$$

Hence, since a safety factor greater than 1.5 is achieved the bolt is safe and can withstand the loads induced from the weight of the battery.

3.14 Springs and Dampers

3.14.1 Description of Inputs/Outputs

The inputs for the vibration analysis will be the sprung and unsprung masses based on the weight distribution for front and rear suspension.

3.14.2 Justification of Inputs, constants and Parameters

Where the inputs will be: Total Mass of the Car $m_T = 303.465kg$, Front Sprung Mass per Corner $m_{fsprung} = 55.0051kg$ Rear Sprung Mass per Corner $m_{rsprung} = 56.624kg$ Front Unsprung Mass per Corner $m_{funsprung} = 19.7608kg$ Rear Unsprung Mass per Corner $m_{runsprung} = 20.342kg$ Rear Unsprung Mass per Corner $m_{runsprung} = 20.342kg$ Motion Ratio $MR = 0.641$, and finally the Tire Stiffness $K_t = 147281.66N/m$.

3.14.3 Assumption, Simplifications and Materials

It is assumed that the suspension is initially at rest.

A 1 DOF vibrations model is used to determine the Spring Stiffness through the car's natural frequency.

The analysis will focus on the front suspension as the analysis method will be identical to the rear suspension.

3.14.4 Spring and Damper Modelling

The spring rate K_s can be calculated provided the motion ratio is known and the ride frequencies of the car is known. Various studies show that a typical ride frequency for a race car with moderate down force would have a ride frequency between 2.0 - 4.0 Hz. Thus, by assuming that the vehicle being designed has a ride frequency of 3.5 Hz.

$$K_s = 4 * (\pi)^2 * (\omega_r)^2 * (m_{unsprung}) * \left(\frac{1}{MR}\right) \quad (3.128)$$

where ω_r is the ride frequency. Thus, the Spring Rate for the front suspension can be found to be:

$$K_s = 4 * (\pi)^2 * (3.5Hz)^2 * (19.706) * \left(\frac{1}{0.461}\right) = 14885.62N/m \quad (3.129)$$

Thus, the wheel rate can then be determined using the following relationship:

$$K_w = K_s * (MR)^2 \quad (3.130)$$

$$K_w = (14885.62N/m) * (0.641)^2 = 9546.86N/m \quad (3.131)$$

This further allows us to determine the desired damping ratio, and the critical damping coefficient. Where the critical damping ratio can be defined as:

$$b_{critical} = 2 * \sqrt{m_{total} * \frac{K_w * K_t}{K_w + K_t}} \quad (3.132)$$

$$b_{critical} = 2 * \sqrt{(303.5) * \frac{9546.86(N/m) * 147281.67(N/m)}{9546.86(N/m) + 147281.67(N/m)}} = 3298.98Ns/m \quad (3.133)$$

Since, the critical damping coefficient is responsible for returning the system to its equilibrium state as quickly as possible, and determines the point at which the system becomes critically damped. The damping coefficient can be determined using the critical damping ratio and the damping ratio ζ .

$$b_{front} = \zeta * b_{critical} = 0.65 * 3298.98Ns/m = 2144.32Ns/m \quad (3.134)$$

Thus, the damping coefficient for the front is 2144.32 Ns/m

3.14.5 Fatigue and Safety Analysis

The endurance strength amplitude component was defined by Zimmerli in Shigley's to be $S_{sa} = 398MPa$ for peened springs.

$$n_f = \frac{S_{sa}}{\tau_a} = \frac{398}{208.5} = 1.91 \quad (3.135)$$

Thus, the spring can be considered fatigue safe as it is greater than 1.5.

The safety factor when the spring is at its solid length can also be determined.

$$n_f = \frac{S_{sy}}{\tau_s} = \frac{624.66}{479.4} = 1.3 \quad (3.136)$$

This is greater than the recommended safety factor of 1.2 and thus, the spring safety factor at its solid length is safe.

Damper Analysis

Justification of Inputs, constants and Parameters

Based on the FOX shock absorber aforementioned a rebound length of 416.5 mm is determined, for our model however we will assume a rebound length of 350 mm based off our geometry set up. The compression length of the shock absorber can be found by taking the solid deflection found from the spring section and subtracting it from the rebound length.

$$L_{comp} = L_{rebound} - \delta_s = 350\text{mm} - 105\text{mm} = 245\text{mm} \quad (3.137)$$

The diameter of the piston can also be determined by taking the inner diameter of the spring multiplying it by a clearance factor (0.85) and then subtracting the thickness of the damper wall assumed to be 1.5 mm.

$$D_{Housing} = ID * 0.85 - 2 * t_{damper} = 42\text{mm} * 0.85 - 2 * 1.5 = 32.7\text{mm}. \quad (3.138)$$

Assumptions and Simplifications

To conduct a damper analysis simplifications must be made to model the flow of the fluid going into the valve. These include assuming that the flow is fully developed, negligible gravitational forces, no pressure drop across damper, the fluid will be assumed to be incompressible, and finally a steady state flow is assumed.

Damper Analysis

It is necessary to analyze the flow rate of the fluid, as it will be responsible for the forces applied on the piston. Using the general flow rate equation and further specifying that the damper is circular on can solve for the velocity of the fluid and its flow rate. Refer to appendix B.9

$$V_z = \frac{dP}{dz} \frac{r^2}{4\mu} - \frac{dP}{dz} \frac{R^2}{4\mu} = \frac{dP}{dz} \frac{1}{4\mu} [r^2 - R^2] \quad (3.139)$$

$$Q_{\text{comp}} = -\frac{D_{\text{housing}}^4 F_{\text{piston}}}{32\mu L_{\text{comp}} (D_{\text{Housing}}^2 - 3D_{\text{orifice}}^2)} \quad (3.140)$$

$$D_{\text{orifice}}^2 = \frac{D_{\text{housing}}^2 - \sqrt{\frac{CD_{\text{housing}}^4}{8\pi\mu L_{\text{comp}}}}}{N} \quad (3.141)$$

Therefore, provided the piston diameter which was found to be 32.7 mm and the compression length of 245 mm calculated earlier, and assuming that there are 3 orifices ($N=3$) and given that the viscosity for SAE 30 oil is $146.7 \frac{\text{mm}^2}{\text{s}}$ at 40 degrees Celsius then, the orifice diameter can be calculated :

$$D_{\text{orifice}}^2 = \frac{(37\text{mm})^2 - \sqrt{\frac{2.144 \frac{\text{Ns}}{\text{mm}} * (37\text{mm})^4}{8*\pi*146.7 \frac{\text{mm}^2}{\text{s}} * 245(\text{mm})}}}{3} = 21.4\text{mm} \quad (3.142)$$

3.15 Powertrain

3.15.1 Analysis Outline

The components to be analyzed in this section are the sprockets, chain, and half axle shaft.

3.15.2 Inputs and Outputs

The torque produced from the motor is considered an input. The sprockets reduce the torque and a traction force is outputted to the tire.

3.15.3 Assumptions and Materials

To perform the analysis, the following assumptions are to be made:

- The CV remain horizontal during the analysis
- No torsional stress in the CV joint
- No torque lost from the sprocket and the tire
- No friction between links on the chain

7075 tempered steel alloy with a yield strength of 503 MPa is chosen for the sprockets, AISI 1045 Carbon Steel with a yield strength of 310 MPa is chosen for the chain, and 4130 Steel with a yield strength of 435 MPa is chosen for the half axle shafts.

3.15.4 Stress Analysis

Half Shaft

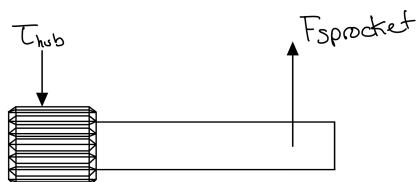


Figure 3.21: Half Axle Shaft Free Body Diagram

As noted in figure 3.21, there is a torsional stress on the splines of the shaft that connect to the wheel hub. This stress can be calculated using the following equation.

$$\tau = \frac{Tr}{J} \quad (3.143)$$

Where r is the radius of the splines and J is the polar moment of inertia.

$$\tau = \frac{346930Nmm12.75mm}{41510.75mm^4} = 106.56MPa \quad (3.144)$$

$$n = \frac{\sigma_y}{\tau_{shear}} = \frac{435MPa}{106.56MPa} = 4.08 \quad (3.145)$$

As shown in figure 3.21, the tangential force from the sprocket exerted on the half axle shaft can cause bending stress in the shaft.

$$\sigma_{bending} = \frac{Mc}{I} = \frac{346930Nmm12.75mm}{20755.3mm^4} = 213.12MPa \quad (3.146)$$

$$n = \frac{\sigma_y}{\sigma_{bending}} = \frac{435MPa}{213.12MPa} = 2.04 \quad (3.147)$$

The lowest safety factor is 2.04 which is reasonable. The safety factor can be slightly increased by increasing the radius of the diameter.

Sprockets

Figure 3.22: Sprocket Free Body Diagram

As shown in figure 3.22, the tangential force the chain exerts on the sprockets cause bending stresses in the sprockets. The moment exerted on the big sprocket is 340.93 Nm and small sprocket is 140.03 Nm.

$$\sigma_{bending} = \frac{Mc}{I} = \frac{346930Nmm70.84mm}{19757694.34mm^4} = 1.24MPa \quad (3.148)$$

$$\sigma_{bending} = \frac{Mc}{I} = \frac{140030Nmm28.5367mm}{500082.7mm^4} = 7.99MPa \quad (3.149)$$

$$n = \frac{\sigma_y}{\sigma_{bending}} = \frac{503MPa}{1.24MPa} = 404.38 \quad (3.150)$$

$$n = \frac{\sigma_y}{\sigma_{bending}} = \frac{503MPa}{7.99MPa} = 62.94 \quad (3.151)$$

The safety factors are very high in this case. However, sprocket safety factor are usually decreased by removing material form the sprocket. This is hard to model especially when trying to calculate the moment of inertia as the sprocket as non-linear patterns of removed materials.

Chain Links

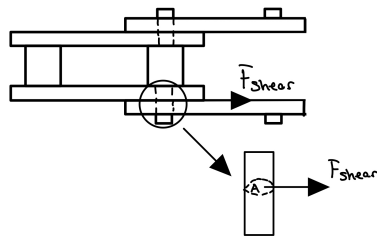


Figure 3.23: Chain Shaft Free Body Diagram

The two links exert a shear force which act on the link pin. The link pin diameter is considered 4.7625 mm produced an circular cross-sectional area A of 17.81 mm².

$$\tau_{shear} = \frac{F_y}{A} = \frac{4897.42N}{17.8139mm^2} = 274.92MPa \quad (3.152)$$

$$n = \frac{\sigma_y}{\tau_{\text{shear}}} = \frac{310 \text{ MPa}}{274.92 \text{ MPa}} = 1.1276 \quad (3.153)$$

This safety factor is considered low. A safety factor of 2.5 would be appropriate. This can be achieved by increasing the diameter of the link pin.

Chapter 4

Discussion and Future Work

The analysis for certain portions of this report were not illustrated in full this includes but is not limited to, the primary and secondary steering shafts which the calculations for have been determined and can be found in appendix ???. The suspension mounts will also need to be further analyzed to ensure that they can satisfy the safety factors required.

Bibliography

- [1] *Forward Vehicle Dynamics*, pages 39–94. Springer International Publishing AG, 3 edition.
- [2] Formula SAE rules 2022.
- [3] Ioannis Oxyzoglou. Design & development of an aerodynamic package for a fsae race car. *University of Thessaly*, 2017.
- [4] Wilwood disc brakes - 5/8" master cylinders. <https://www.wilwood.com/MasterCylinders/MasterCylinderProd?itemno=260-10371>.
- [5] Wilwood disc brakes - 7/8" master cylinders description. <https://www.wilwood.com/MasterCylinders/MasterCylinderProd?itemno=260-10374>.
- [6] Wilwood disc brakes - calipers description. <https://www.wilwood.com/MasterCylinders/MasterCylinderProd?itemno=260-10374>.
- [7] J. Keith Nisbeth and Richard G. Budynas. *Shigley's Mechanical Engineering Design*. McGraw-Hill Education, 2011.
- [8] Friction and automobile tires. <http://hyperphysics.phy-astr.gsu.edu/hbase/Mechanics/frictire.html>.
- [9] Robert C. Juvinall and Kurt M. Marshek. *Fundamentals of machine component design*. John Wiley & Sons, 5th ed edition.
- [10] R. C. Juvinall and M. M. Marshek. *Fundamentals of Machine Component Design (Fifth edition)*. 2012.
- [11] Henrik Dahlberg. Aerodynamic development of formula student race car, 2014.

- [12] Richard G. Budynas and J. Keith Nisbett. *Shigley's mechanical engineering design.* McGraw-Hill series in mechanical engineering. McGraw-Hill, 9th ed edition.
- [13] Ashish Avinash Vadhe. Design and optimization of formula SAE suspension system. 8(3).
- [14] Jahee Campbell-Brennan. Rising rate suspension: A design guide.

APPENDICES

Appendix A

Design Solution

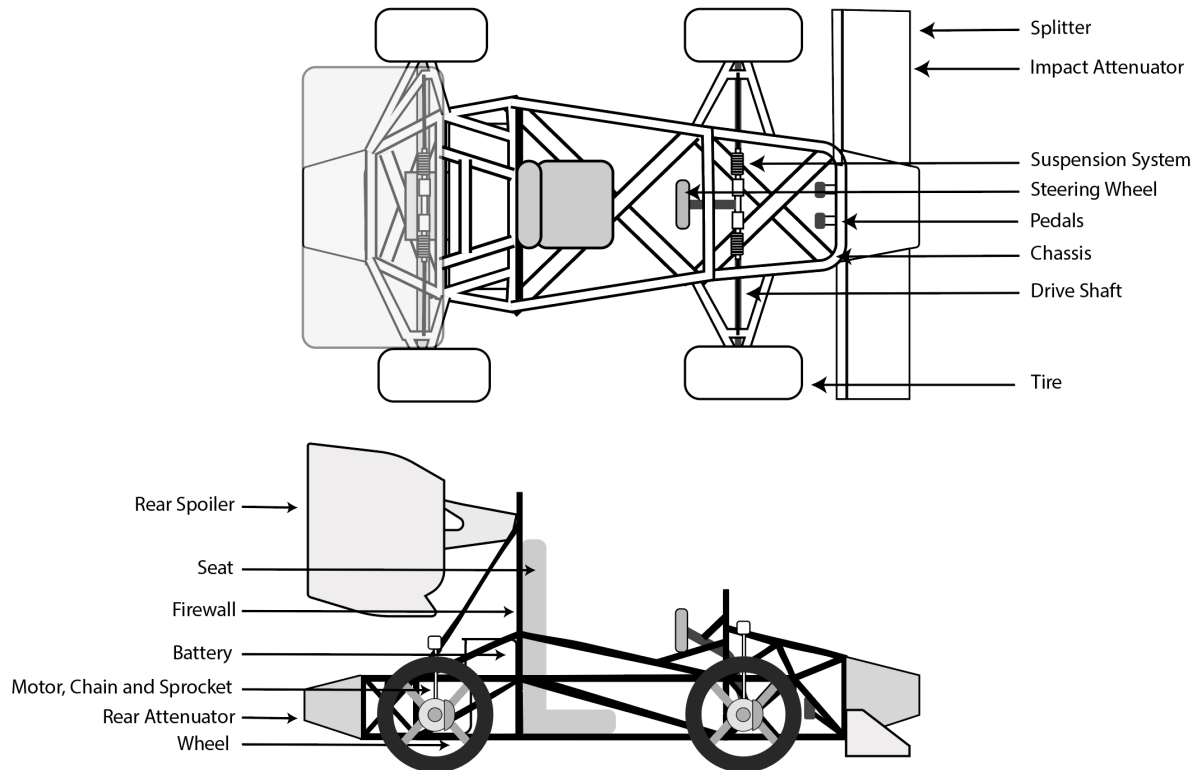


Figure A.1: Updated Solution of the vehicle with labeled components

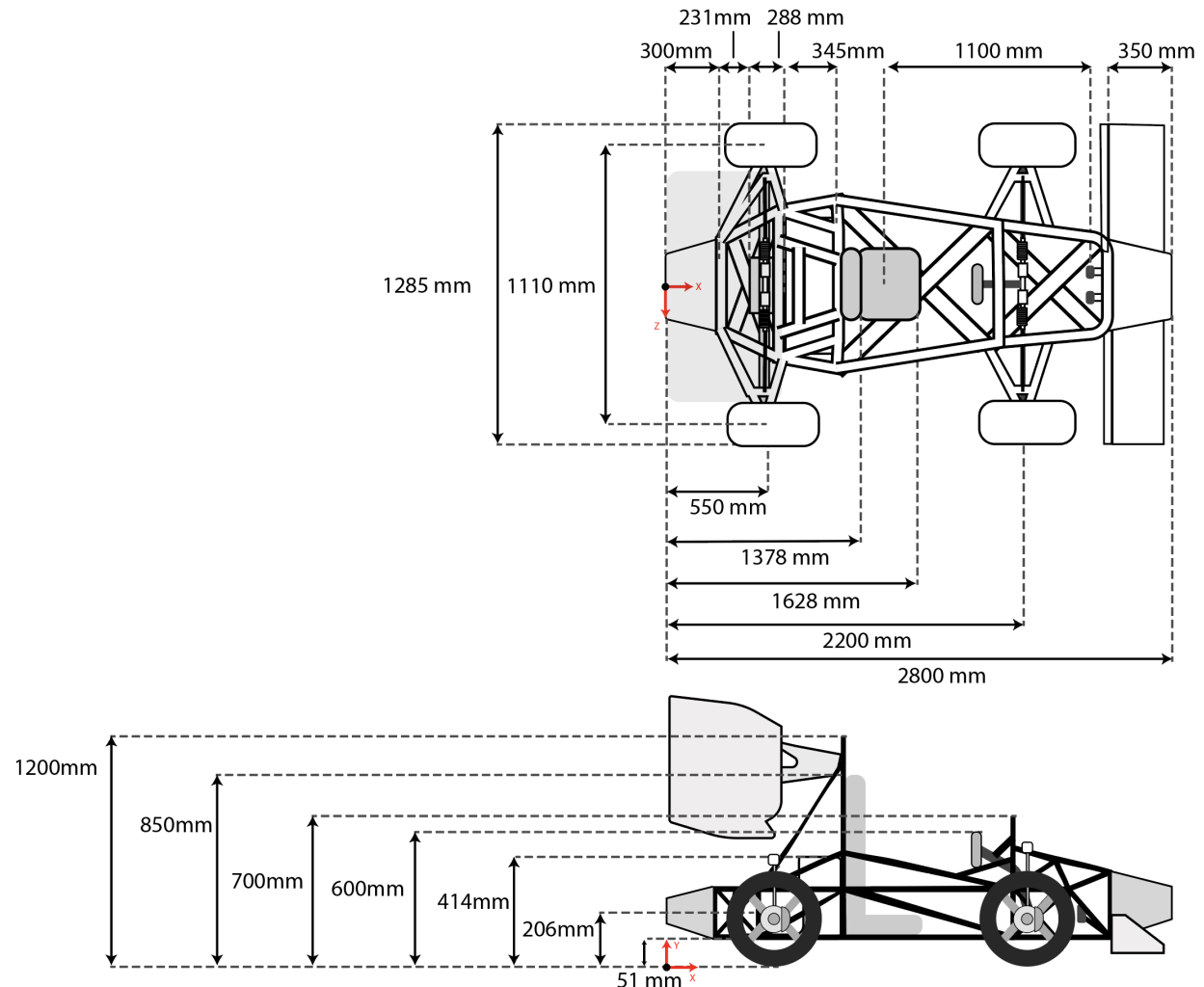


Figure A.2: Updated Solution of the vehicle with dimensions

Appendix B

Chassis

To model the stiffness matrix of a frame element ([Ke]), bar ([Kbar]) and beam ([Kbeam]) element stiffness matrices are linearly superimposed because displacements, strains and rotations are assumed to be negligible. The resulting frame element stiffness matrix models 3 degrees of freedom in a 2D plane which are the axial deformation in the x direction, u ; deflection in the y direction, v ; and the rotation in the x-y plane.

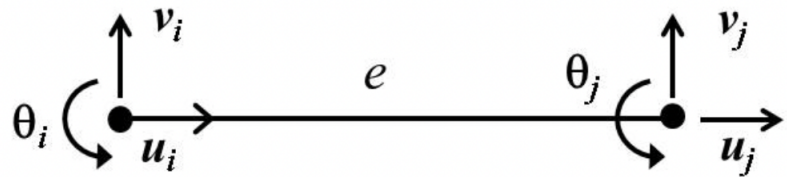


Figure B.1: Frame element FBD

Consider the following bar element with nodes i and j.

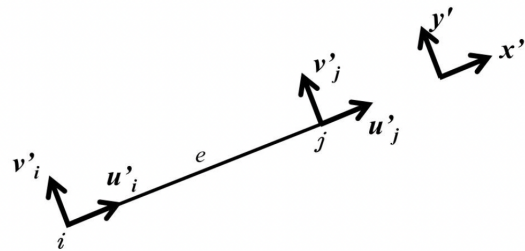


Figure B.2: Bar element FBD

The axial elongation is mathematically modeled as the following.

$$\delta = \frac{PL}{AE} \quad (\text{B.1})$$

Where P is the axial load, L is the length of the element, A is the cross-sectional area of the element, and E is the elastic modulus of the element.

The axial elongation can be rewritten in the following form as it is assumed that the elastic range is not exceeded, therefore A treated as a constant.

$$\delta = u'_j - u'_i \quad (\text{B.2})$$

The load P is split into the x and y directions and equation C.1 can be rewritten as the following.

$$F'_{xi} = \frac{AE}{L} (u'_i - u'_j) \quad (\text{B.3})$$

$$F'_{xj} = \frac{AE}{L} (u'_j - u'_i) \quad (\text{B.4})$$

Bar elements do not withstand transverse loads, so forces on the y axis are considered 0

$$F'_{yj} = F'_{xj} = 0 \quad (\text{B.5})$$

The equations above can be written in matrix form as the following that represent $[K_{bar}]\{U\} = \{F\}$, where $[K_{bar}]$ is the bar element stiffness matrix, $\{U\}$ is the displacement vector, and $\{F\}$ is the external forces vector.

$$\frac{AE}{L} \begin{bmatrix} 1 & 0 & -1 & 0 \\ 0 & 0 & 0 & 0 \\ -1 & 0 & 1 & 0 \\ 0 & 0 & 0 & 0 \end{bmatrix} \begin{Bmatrix} u'_i \\ v'_i \\ u'_j \\ v'_j \end{Bmatrix} = \begin{Bmatrix} F'_{xi} \\ F'_{yi} \\ F'_{xj} \\ F'_{yj} \end{Bmatrix} \quad (\text{B.6})$$

This matrix allows us to model the elements axial deformation in the x direction, u; deflection in the y direction, v.

If the same bar element is now modeled as a beam element, the bending in the x-y plane can be modeled.

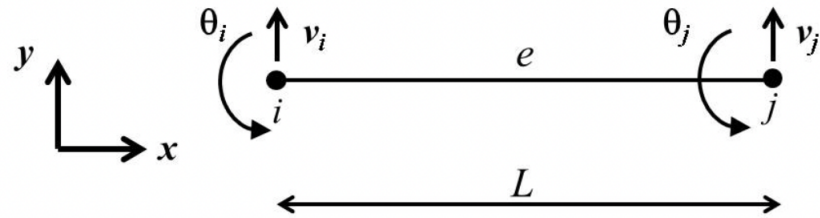


Figure B.3: Beam element FBD

In the absence of distributed loads, the equilibrium equation for the element is the following.

$$\frac{d^4v}{dx^4} = 0 \quad (\text{B.7})$$

The boundary conditions of the element can be expressed in terms of nodal values.

For node i:

$$\begin{aligned}
v(0) &= v_i \\
&= c_1 \\
\frac{dv(0)}{dx} &= \theta_i \\
&= c_2
\end{aligned} \tag{B.8}$$

For node j:

$$\begin{aligned}
v(L) &= v_j \\
&= c_1 + c_2 L + c_3 L^2 + c_4 L^3 \\
\frac{dv(L)}{dx} &= \theta_j \\
&= c_2 + 2c_3 L + 3c_4 L^2
\end{aligned} \tag{B.9}$$

In matrix format, the above relationships can be expressed as the following, where $\{A\}$ is called the coefficient matrix.

$$\left\{ \begin{array}{l} v_i \\ \theta_i \\ v_j \\ \theta_j \end{array} \right\} = \left[\begin{array}{cccc} 1 & 0 & 0 & 0 \\ 0 & 1 & 0 & 0 \\ 1 & L & L^2 & L^3 \\ 0 & 1 & 2L & 3L^2 \end{array} \right] \left\{ \begin{array}{l} c_1 \\ c_2 \\ c_3 \\ c_4 \end{array} \right\} \text{ or } \{U^e\} = [A]\{Q\} \tag{B.10}$$

By inverting $[A]$, we can solve for $\{Q\}$ in terms of $\{U^e\}$.

$$[A]^{-1} = \left[\begin{array}{cccc} 1 & 0 & 0 & 0 \\ 0 & 1 & 0 & 0 \\ -\frac{3}{L^2} & -\frac{2}{L} & \frac{3}{L^2} & -\frac{1}{L} \\ \frac{2}{L^3} & \frac{1}{L^2} & -\frac{2}{L^3} & \frac{1}{L^2} \end{array} \right] \tag{B.11}$$

Finally, $v(x)$ can be written in matrix form as:

$$v(x) = \left[\begin{array}{cccc} 1 & x & x^2 & x^3 \end{array} \right] \{Q\} = \left[\begin{array}{cccc} 1 & x & x^2 & x^3 \end{array} \right] [A]^{-1} \{U^e\} \tag{B.12}$$

$$v(x) = [N] \{U^e\} \quad (\text{B.13})$$

$$[N] = \begin{bmatrix} 1 & x & x^2 & x^3 \end{bmatrix} [A]^{-1} \quad (\text{B.14})$$

$$[N] = \begin{bmatrix} N_1(x) & N_2(x) & N_3(x) & N_4(x) \end{bmatrix} \quad (\text{B.15})$$

$$[N] = \begin{bmatrix} 1 - \frac{3x^2}{L^2} + \frac{2x^3}{L^3} & x - \frac{2x^2}{L} + \frac{x^3}{L^2} & \frac{3x^2}{L^2} - \frac{2x^3}{L^3} & -\frac{x^2}{L} + \frac{x^3}{L^2} \end{bmatrix} \quad (\text{B.16})$$

By applying the principle of virtual work, the stiffness matrix [Kbeam] can be modeled as the following.

$$[K^e] = \frac{EI}{L^3} \begin{bmatrix} 12 & 6L & -12 & 6L \\ 6L & 4L^2 & -6L & 2L^2 \\ -12 & -6L & 12 & -6L \\ 6L & 2L^2 & -6L & 4L^2 \end{bmatrix} \quad (\text{B.17})$$

Now, we can construct the frame element stiffness matrix which will be used in the analysis of the chassis.

$$[K^e] = \begin{bmatrix} [k_{\text{Bar}}^e] & [0] \\ [0] & [k_{\text{Beam}}^e] \end{bmatrix} \quad (\text{B.18})$$

Constructing the bar and beam stiffness matrices results in the following 6x6 stiffness matrix.

$$[K^e] = \begin{bmatrix} \frac{AE}{L} & 0 & 0 & -\frac{AE}{L} & 0 & 0 \\ 0 & \frac{12EI_z}{L^3} & \frac{6EI_z}{L^2} & 0 & -\frac{12EI_z}{L^3} & \frac{6EI_z}{L^2} \\ 0 & \frac{6E_z}{L^2} & \frac{4EI_z}{L} & 0 & -\frac{6EI_z}{L^2} & \frac{2EI_z}{L} \\ -\frac{AE}{L} & 0 & 0 & \frac{AE}{L} & 0 & 0 \\ 0 & -\frac{12EI_z}{L^3} & -\frac{6EI_z}{L^2} & 0 & \frac{12EI_z}{L^3} & -\frac{6EI_z}{rL^2} \\ 0 & \frac{6EI_z}{L^2} & \frac{2EI_z}{L} & 0 & -\frac{6EI_z}{L^2} & \frac{4x_z}{L} \end{bmatrix} \quad (\text{B.19})$$

As mentioned, each frame has three degrees of freedom, which can be expressed in a displacement vector

$$\{U^e\}^T = [u_i \ u_j \ v_i \ \theta_i \ v_j \ \theta_j] \quad (\text{B.20})$$

It is important to note that the above matrix is suitable for elements that are perfectly aligned in the xy-plane. Some elements in the chassis are not oriented in the xy-plane, therefore, the respective stiffness matrices have to be rotated from the local axis to the global axis. Anything on the local matrix is represented by a prime notation. For example, the local stiffness matrix is represented as $[K']$.

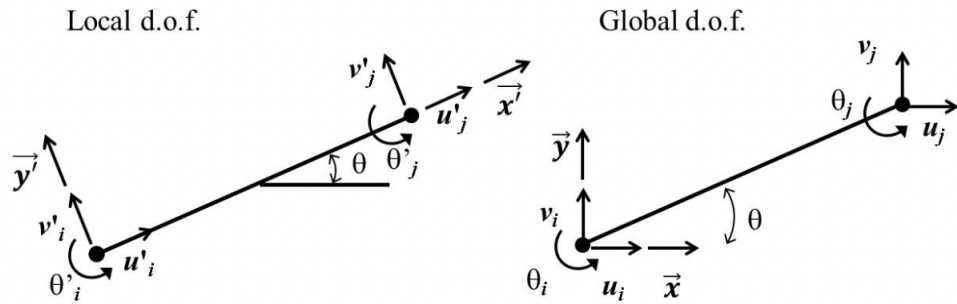


Figure B.4: Rotation of element to the global coordinates

The following geometric relationships are developed from the figure above.

$$\begin{aligned}
u'_i &= lu_i + mv_i \\
v'_i &= -mu_i + lv_i \\
\theta'_i &= \theta_i \\
u'_j &= lu_j + mv_j \\
v'_j &= -mu_j + lv_j \\
\theta'_j &= \theta_j
\end{aligned} \tag{B.21}$$

These relationships can be represented in matrix format.

$$\left\{ \begin{array}{l} u'_i \\ v'_i \\ \theta'_i \\ u'_j \\ v'_j \\ \theta'_j \end{array} \right\} = \left[\begin{array}{cccccc} l & m & 0 & 0 & 0 & 0 \\ -m & l & 0 & 0 & 0 & 0 \\ 0 & 0 & 1 & 0 & 0 & 0 \\ 0 & 0 & 0 & l & m & 0 \\ 0 & 0 & 0 & -m & l & 0 \\ 0 & 0 & 0 & 0 & 0 & 1 \end{array} \right] \left\{ \begin{array}{l} u_i \\ v_i \\ \theta_i \\ u_j \\ v_j \\ \theta_j \end{array} \right\} \tag{B.22}$$

Such that, $\{U^{e'}\} = [R]\{U^e\}$, where $[R]$ is the rotation matrix. This rotation matrix is used to rotate elements of the chassis to the global plane and is done by $[K^e] = [R]^T [K^{e'}] [R]$.

B.0.1 Chassis Simulations

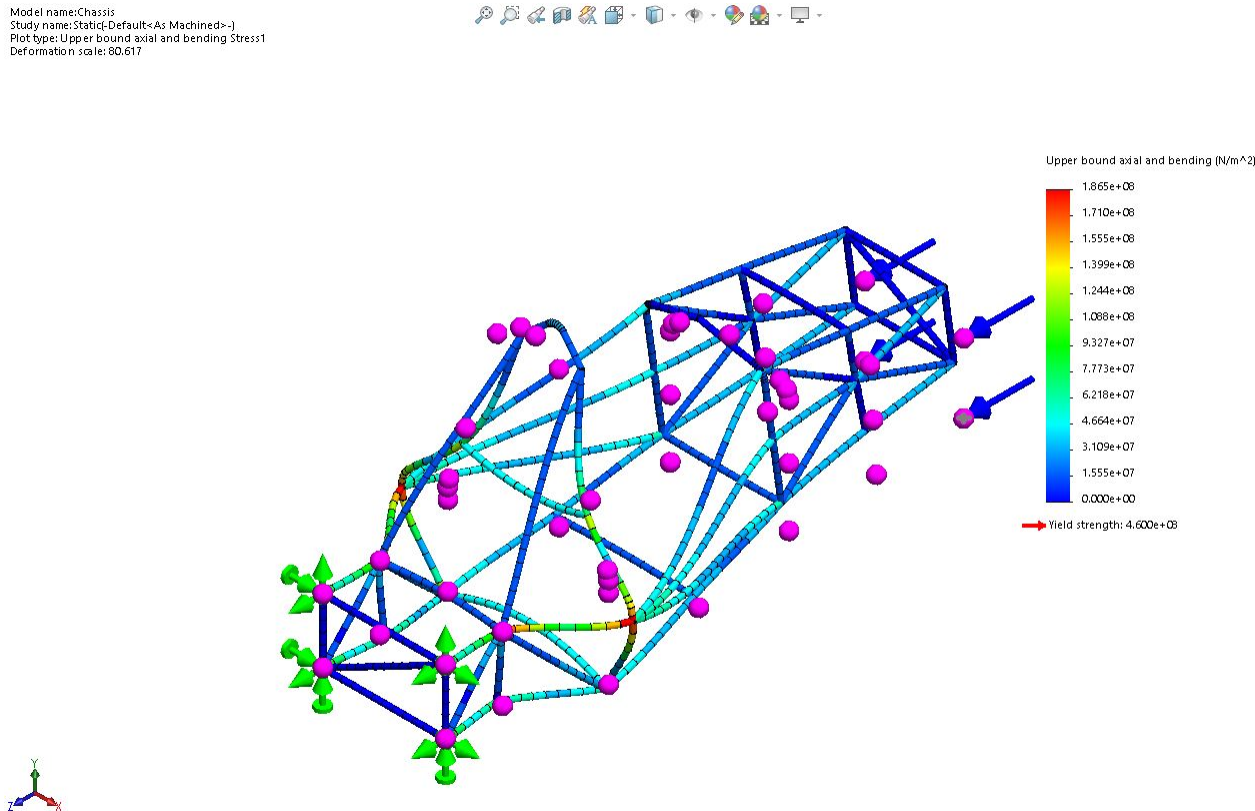


Figure B.5: Front Impact Simulation Stress Plot

Model name:Chassis
Study name:Static-Default-As Machined->
Plot type: Factor of Safety Factor of Safety1
Criterion : Automatic
Factor of safety distribution: Min FOS = 2.5



Model name:Chassis
Study name:Static-Default<As Machined>-
Plot type:Upper bound axial and bending Stress1
Deformation scale: 70.8471

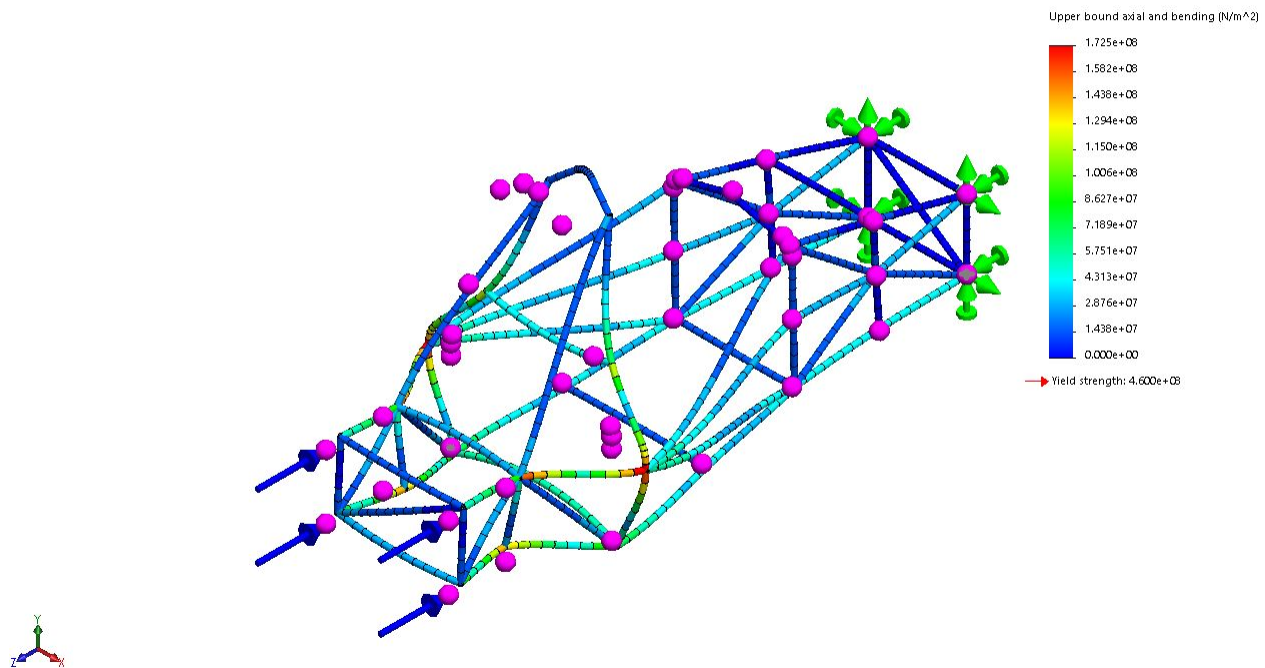


Figure B.7: Rear Impact Simulation Stress Plot

Model name:Chassis
Study name:Static-Default<As Machined>-
Plot type:Factor of Safety Factor of Safety1
Criterion:Automatic
Factor of safety distribution: Min FOS = 2.7

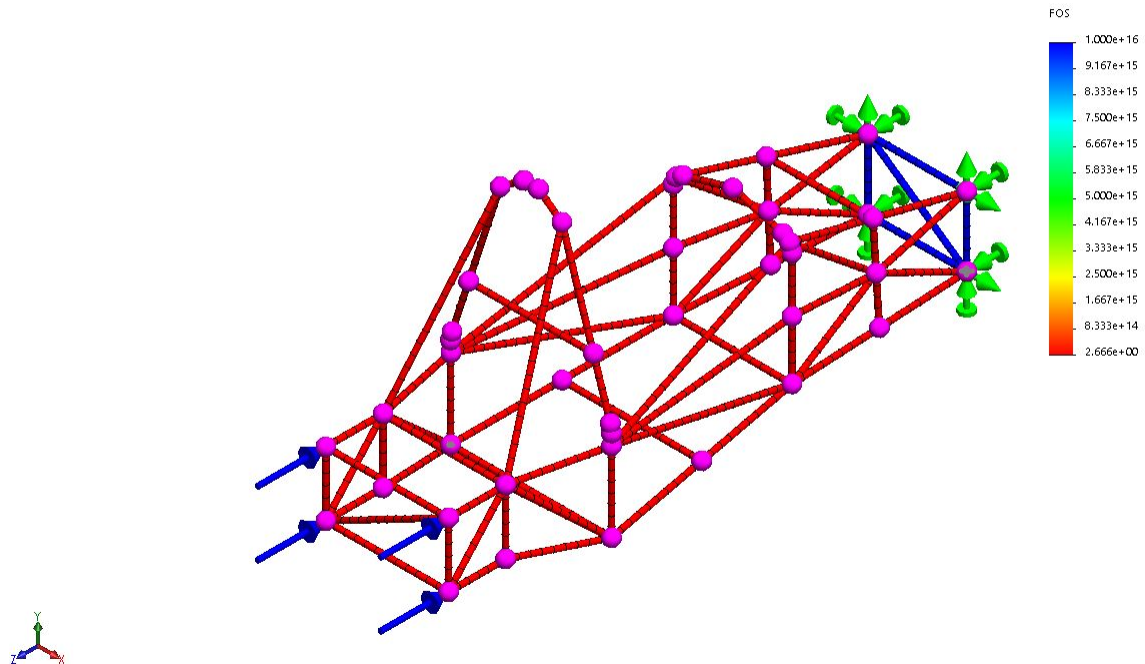


Figure B.8: Rear Impact Simulation Safety Factor Plot

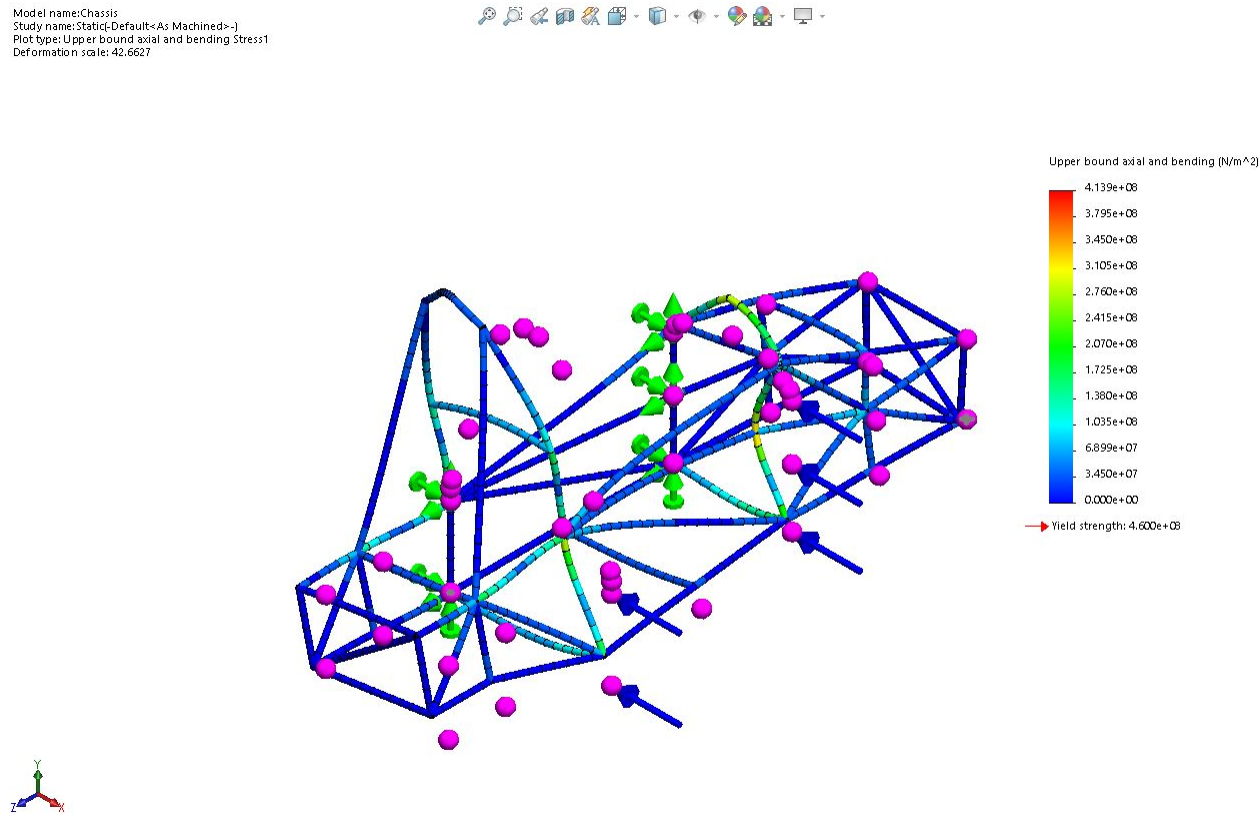


Figure B.9: Side Impact Simulation Stress Plot

Model name:Chassis
Study name:Static-Default->As Machined->
Plot type:Factor of Safety Factor of Safety1
Criterion :Automatic
Factor of safety distribution: Min FOS = 1.1

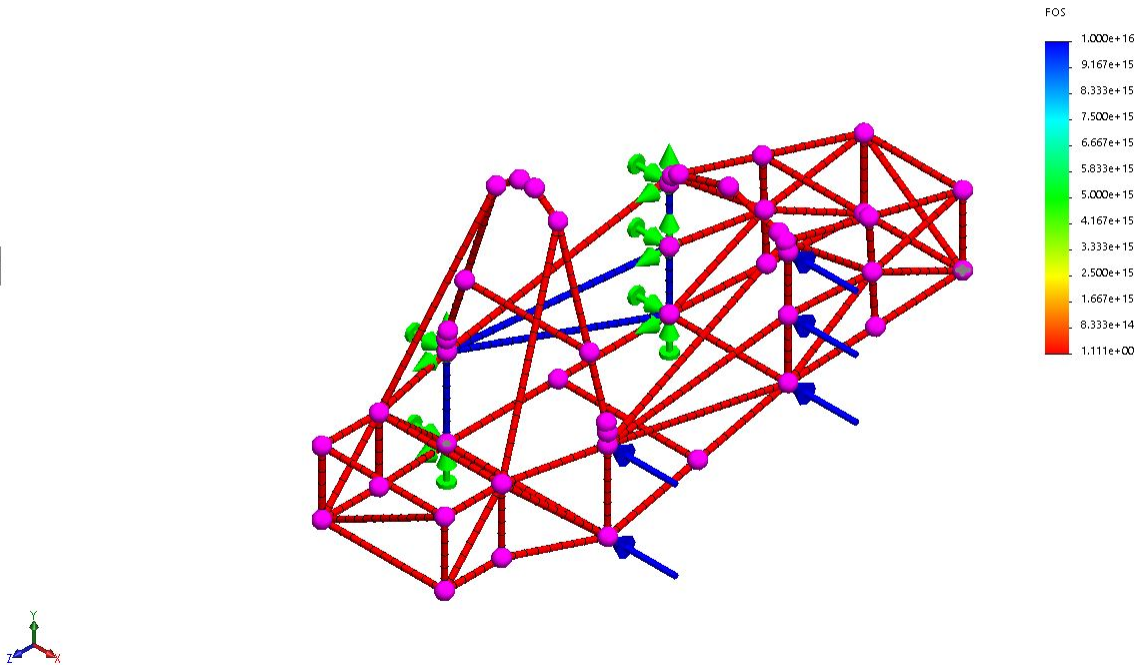


Figure B.10: Side Impact Simulation Safety Factor Plot

B.1 Brake Flow

B.1.1 Flowchart

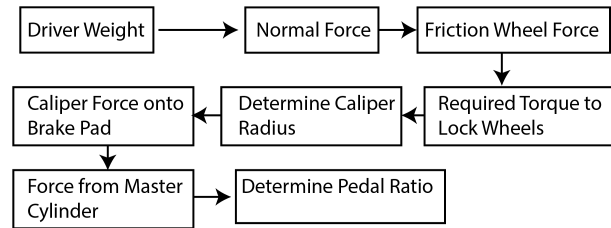


Figure B.11: Flowchart of the Brake Flow

B.2 Chassis Flowchart

B.2.1 Flowchart

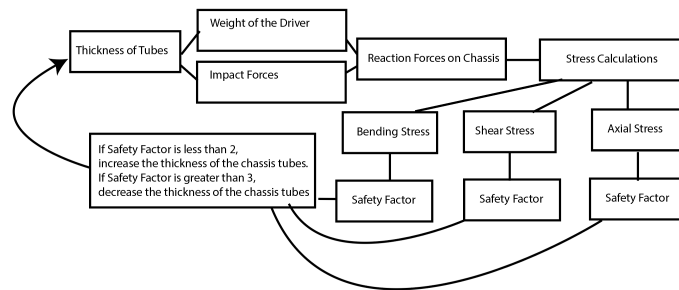


Figure B.12: Flowchart of the Chassis Flow

B.3 Acceleration Equation Derivations

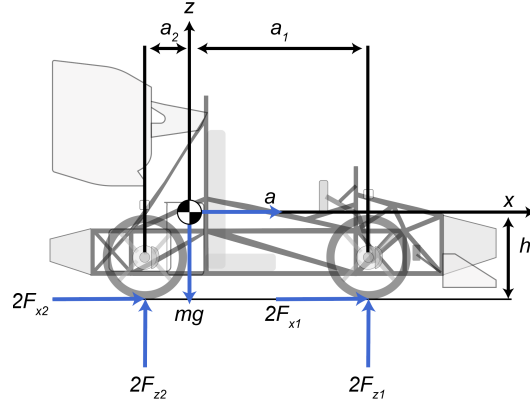


Figure B.13: FBD of an Accelerating Car on a Level Road

Defining the sum of forces from the FBD above:

$$\Sigma (F_x) = ma \quad (\text{B.23})$$

$$\Sigma (F_z) = 0 \quad (\text{B.24})$$

$$\Sigma (M_y) = 0 \quad (\text{B.25})$$

$$F_{xf} + F_{xr} = \frac{ma}{2} \quad (\text{B.26})$$

$$- gm + 2F_{zf} + 2F_{zr} = 0 \quad (\text{B.27})$$

Isolating for F_{zf}

$$F_{zf} = \frac{gm}{2} - F_{zr} \quad (\text{B.28})$$

Substituting it into the equation B.27

$$- 2F_{zf}a_1 + 2F_{zr}a_2 - 2(F_{xf} + F_{xr})h = 0 \quad (\text{B.29})$$

Substituting equations B.26 into B.27

$$- mah - 2F_{zf}a_1 + 2F_{zr}a_2 = 0 \quad (\text{B.30})$$

Simplifying and solving for F_{zr}

$$F_{zr} = \frac{mah + 2F_{zf}a_1}{2a_2} \quad (\text{B.31})$$

$$F_{zr} = \frac{mah + 2\left(\frac{gm}{2} - F_{gr}\right)a_1}{2a_2} \quad (\text{B.32})$$

$$F_{zr} = \frac{mah + gma_1}{2a_1 + 2a_2} \quad (\text{B.33})$$

Substituting F_{zr} into F_{zf} to find:

$$F_{zf} = \frac{gm}{2} - \frac{mah + gma_1}{2a_1 + 2a_2} \quad (\text{B.34})$$

B.4 Maximum Achievable Acceleration

To find the max acceleration our vehicle can achieve we first must assess the maximum tractive forces our car can achieve from a stand still. These forces can simply be calculated as they are the normal forces acting on the rear wheels multiplied by the coefficient of friction of the car. We are considering the normal forces on the rear wheels as they are

they are the only wheels which will be able to propel the car forward since the vehicle is rear wheel drive.

Therefore, the following normal forces can be determined:

$$F_{x_r} = \frac{1}{2}((303.5kg \times 9.81\frac{m}{s^2})(\frac{0.813}{0.813m + 0.789m})) * 0.9 = 1359.74N \quad (B.35)$$

Then the theoretical max acceleration that can be achieved at the wheels without slip is:

$$a_{max} = \frac{1359.74N}{303.5} = 4.48\frac{m}{s^2} \quad (B.36)$$

Having determined the maximum tractive force the vehicle can achieve from a stand still, then it can be concluded that should the driving force from the motor exceed the tractive force the vehicle will be slipping and won't be able to accelerate efficiently. The torque would be needed to achieve this acceleration can be found simply by multiply the tractive force by the wheel radius.

$$a_{max} = \frac{1359.74N}{0.25527m} = 346.93N.m \quad (B.37)$$

Therefore, having selected the EMRAX 228 motor, and knowing the maximum power the battery can output is 70.66 kW, then the peak torque which the motor can output is 140 N.m. Provided the gear reduction selected has a 1:2.5 gear reduction, then the torque transmitted to the wheels would be and thus the force transmitted from the wheels is:

$$T_{wheels} = 140Nm * 2.5 = 350Nm \quad (B.38)$$

$$F_{wheels} = \frac{350Nm}{0.25527m} = 1371.09N \quad (B.39)$$

Thus the max acceleration produced from the motor is:

$$a_{acc,max} = 1371.09N * 303.5 = 4.517 \frac{m}{s^2} \quad (\text{B.40})$$

B.5 Deceleration Equation Derivations

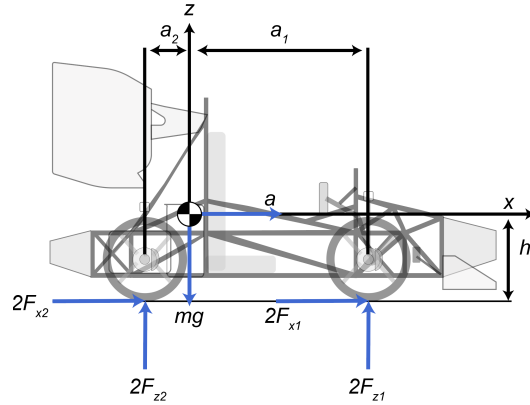


Figure B.14: FBD of an Accelerating Car on a Level Road

Sum of Forces and Sum of Moments from FBD.

$$\Sigma(F_x) = ma \quad (\text{B.41})$$

$$\Sigma(F_z) = 0 \quad (\text{B.42})$$

$$\Sigma(M_y) = 0 \quad (\text{B.43})$$

$$2F_{xf} + 2F_{xr} = -ma \quad (\text{B.44})$$

$$-mg + F_{Lcar} - F_{Lf} - F_{Lr} + 2F_{zf} + 2F_{zr} = 0 \quad (\text{B.45})$$

Isolating for F_{zf} from equation B.45

$$\left[\left[F_{zf} = \frac{mg}{2} - \frac{F_{Lcax'}}{2} - F_{zr} + \frac{F_{Lr}}{2} + \frac{F_{Lf}}{2} \right] \right] \quad (\text{B.46})$$

$$-2F_{ff}a_1 + 2F_{zr}a_2 - 2(F_{xf} + F_{xr})h + F_{Lr}l_r - F_{Lf}l_f = 0 \quad (\text{B.47})$$

$$mah - F_{Lf}l_f + F_{Lr}l_r - 2F_{zf}a_1 + 2F_{zr}a_2 = 0 \quad (\text{B.48})$$

Substituting equation B.44 into equation B.47 and substituting F_{zf} into equation B.47 then simplifying and isolating for F_{zr}

$$F_{zr} = \frac{-mah + F_{Lf}l_f - F_{Lr}l_r + 2F_{zf}a_1}{2a_2} \quad (\text{B.49})$$

$$F_{zr} = \frac{-mah + F_{Lf}l_f - F_{Lr}l_r + 2\left(\frac{mg}{2} - \frac{F_{Lcar}}{2} - F_{gr} + \frac{F_{Lr}}{2} + \frac{F_{Lf}}{2}\right)a_1}{2a_2} \quad (\text{B.50})$$

$$\left[\left[F_{zr} = -\frac{mah - a_1mg + a_1F_{Lcar} - a_1F_{Lf} - F_{Lf}l_f - a_1F_{Lr} + F_{Lr}l_r}{2(a_2 + a_1)} \right] \right] \quad (\text{B.51})$$

Substituting into B.46 and simplifying to find:

$$F_{zf} = \frac{mg}{2} - \frac{F_{Lcar}}{2} + \frac{mah - a_1mg + a_1F_{Lcar} - a_1F_{Lf} - F_{Lf}l_f - a_1F_{Lr} + F_{Lr}l_r}{2a_2 + 2a_1} + \frac{F_{Lr}}{2} + \frac{F_{Lf}}{2} \quad (\text{B.52})$$

$$F_{zf} = \frac{(mg - F_{Lcar} + F_{Lf} + F_{Lr}) a_2 + mah + F_{Lr}l_r - F_{Lf}l_f}{2a_2 + 2a_1} \quad (\text{B.53})$$

The maximum deceleration of the car can be found by using sum of forces on z and x from the figure above. Assuming that the vehicle is at its maximum velocity of 105 km/hr and it is to decelerate to a stop. Then the forces that will be acting on the car in the z direction would be the lift force, the down-forces, and the weight of the vehicle, and knowing that the car will slip if the acceleration is too high as it can not exceed the tractive force. The following can be determined:

$$F_f = -ma \quad (\text{B.54})$$

$$F_z = mg - F_{Lcar} + F_{Lf} + F_{Lr} \quad (\text{B.55})$$

$$F_z = \text{Weight of the Car} + \text{Total Forces Lift} \quad (\text{B.56})$$

$$F_f = F_z\mu \quad (\text{B.57})$$

$$a = -\frac{(mg - F_{Lcar} + F_{Lf} + F_{Lr}) \mu}{m} \quad (\text{B.58})$$

$$a = -((1647.21 \text{ N}) + (2977.34 \text{ N})) * (0.9) \frac{\text{m}}{303.5 \text{ kg} = -13.714 \frac{\text{m}}{\text{s}^2}}$$

Thus, the car will decelerate at a maximum deceleration of 1.39 g's or 13.174 m/s⁻²

B.6 Cornering Calculations and Equation Derivations

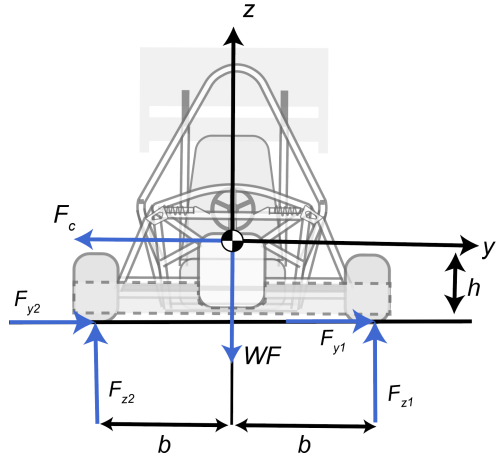


Figure B.15: Reaction at Wheels Due to Applied Centripetal Force

Sum of Forces and Sum of Moments

$$\Sigma(F_y) = 0 \quad (\text{B.59})$$

$$\Sigma(F_z) = 0 \quad (\text{B.60})$$

$$\Sigma(M_y) = 0 \quad (\text{B.61})$$

$$-F_C R_{\text{Bias}} + F_{yl} + F_{yr} = 0 \quad (\text{B.62})$$

Isolating for F_{yr} and isolating for F_{zfl} and solving for F_{zfr}

$$F_{yr} = F_C R_{\text{Bias}} - F_{yl} \quad (\text{B.63})$$

$$-WfR_{\text{Bias}} - F_{Lf}R_{\text{Bias}} + F_{zfl} + F_{zfr} = 0 \quad (\text{B.64})$$

$$[[F_{zfl} = WfR_{\text{Bias}} + F_{Lf}R_{\text{Bias}} - F_{zfr}]] \quad (\text{B.65})$$

$$h(F_{yr} + F_{yl}) + bF_{zfr} - bF_{zfl} = 0 \quad (\text{B.66})$$

$$F_{zfl} = -\frac{-h(F_{yr} + F_{yl}) - bF_{zfr}}{b} \quad (\text{B.67})$$

$$hF_C R_{\text{Bias}} + bF_{zfr} - b(WfR_{\text{Bias}} + F_{Lf}R_{\text{Bias}} - F_{zfr}) = 0 \quad (\text{B.68})$$

$$F_{zfr} = \frac{R_{\text{Bias}} (bWf + bF_{Lf} - hF_C)}{2b} \quad (\text{B.69})$$

Substituting F_{zfr} into F_{zfl} to find:

$$F_{zfl} = WfR_{\text{Bias}} + F_{Lf}R_{\text{Bias}} - \frac{R_{\text{Bias}} (bWf + bF_{Lf} - hF_C)}{2b} \quad (\text{B.70})$$

$$F_{zfl} = \frac{R_{\text{Bias}} ((Wf + F_{Lf}) b + hF_C)}{2b} \quad (\text{B.71})$$

Where the bias for the front half of the car is:

$$R_{\text{Bias}} = \frac{a_2}{a_2 + a_1} \quad (\text{B.72})$$

or for the rear

$$R_{\text{Bias}} = \frac{a_1}{a_2 + a_1} \quad (\text{B.73})$$

B.7 Maximum Cornering Speed at different Radii

The maximum cornering speed around a corner can be modeled simply as the following:

$$v_{max} = \sqrt{\mu * g * R} \quad (\text{B.74})$$

Where R is the corner radius, μ is the coefficient of friction and g is the gravitational acceleration.

Cornering Radius (m)	Max Velocity (m/s)	F_c	F_friction
1	2.971363323	2679.292485	2696.844823
2	4.229944508	2714.863217	2714.863217
3	5.197883559	2733.005132	2733.005132
4	6.022154018	2751.391142	2751.391142
5	6.755735483	2770.026208	2770.026208
6	7.42572724	2788.915425	2788.915425
7	8.048189961	2808.064027	2808.064027
8	8.633566921	2827.477395	2827.477395
9	9.189099784	2847.161057	2847.161057
10	9.720054129	2867.120698	2867.120698
11	10.23040127	2887.362164	2887.362164
12	10.72322491	2907.891466	2907.891466
13	11.20097716	2928.714787	2928.714787
14	11.66564704	2949.83849	2949.83849
15	12.11887538	2971.26912	2971.26912
16	12.56203557	2993.013418	2993.013418
17	12.99629184	3015.078319	3015.078319
18	13.42264227	3037.470967	3037.470967
19	13.84195109	3060.19872	3060.19872
20	14.25497344	3083.269155	3083.269155
21	14.66237452	3106.690083	3106.690083
22	15.06474476	3130.469551	3130.469551
23	15.46261186	3154.615857	3154.615857
24	15.85645049	3179.137554	3179.137554
25	16.2466002	3204.043466	3204.043466
26	16.63372191	3229.342693	3229.342693
27	17.01790328	3255.044627	3255.044627
28	17.39956323	3281.15896	3281.15896

Speeds with the relative Centripetal and Friction Forces

3175.157554 3175.157555 Page 108

B.8 Aerodynamic Load Distribution Model

This section serves the purpose of illustrating how different forces and moments act on the vehicle. It will also introduce how the reaction forces for the rear wheels can be calculated. The sum of forces and moments for the diagram illustrated in figure B.16 are illustrated below [11]:

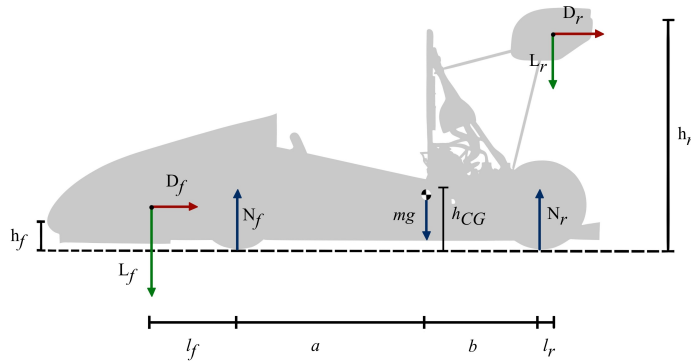


Figure B.16: FBD for forces acting on the vehicle

$$\Sigma F = 0 \Rightarrow N_f + N_r - mg - L_f - L_r + L_F \quad (B.75)$$

$$\Sigma M_{CG} = 0 \Rightarrow bN_r + (a + l_f)L_F - (a)N_f - (b + l_r)L_r - (h_{CG} - h_r)D_r + (h_{CG} - h_f)D_f \quad (B.76)$$

The following can be determined after simplifying the equations of motion above:

$$N_r = \frac{(l_r + b)L_r - (l_f + a)L_f + (h_{CG} - h_r)D_r - (h_{CG} - h_f)D_f + amg + aL_f + aL_r}{a + b} \quad (B.77)$$

This equation gives the force on the rear tyres, which can be used to determine the load distribution of aerodynamic forces. The forces experienced on the rear tyres of the vehicle

are therefore:

$$N_r = -0.363L_f + 1.1303L_r + 1493.825 + 229.455D_r - 230.051D_f \quad (\text{B.78})$$

B.8.0.1 Aerodynamic Effects on Cornering Performance

This section will analyse the aerodynamic effects induced on the tyres whilst cornering. This can be demonstrated by analysing the maximum allowed velocity a vehicle can corner at without losing its grip. Which is the velocity at which the fictional force is equal to the centripetal force [11].

$$\mu F_z = \mu(mg + \frac{1}{2}\rho C_L A v^2) = \frac{mv^2}{R} \quad (\text{B.79})$$

$$v = \sqrt{\frac{\mu mg}{\frac{m}{R} - \frac{1}{2}\rho C_L A \mu}} \quad (\text{B.80})$$

Where, g is the gravitational acceleration, μ is the coefficient of friction, ρ is the air density, C_L is the coefficient of lift, A is the frontal area, and R is the radius of the corner. According to the FSAE rules the corners will vary in radii from 4.5 to 30 m for dynamic events. Thus, assuming a lift coefficient when no aerodynamic packages are installed is $C_L = 0.29$, and the lift coefficient when aerodynamic packages are installed is $C_L = 2.34$ [3], and the density of air to be $\rho = 1.225$, assuming a constant coefficient of friction of $\mu = 0.65$, and provided the mass of the car is 298 kg, the frontal area $A = 1.34m^2$, then the following can be calculated from a 9-30 m turn radius.

Table B.2 illustrates the different speeds which can be achieved as the vehicle is cornering with an aerodynamic package installed, and without one. Clearly, higher speeds can be achieved whilst cornering when an aerodynamic package is installed, as there is more down-force acting on the vehicle. [2]:

Table B.2: Cornering Speed differences with and without an Aerodynamic Package

Corner Radius R (m)	With Aerodynamic Package	W/O Aerodynamic Package
	Velocity (km/hr)	Velocity (km/hr)
4.5	19.42	19.30
8	26.04	25.75
12	32.10	31.56
16	37.31	36.48
20	41.99	40.81
24	46.31	44.74
28	50.36	48.37
30	52.30	50.08

B.9 Damper Equation Derivations

$$Q = \int_0^R (2)(\pi)(r)V_{\text{fluid}} dr \quad (\text{B.81})$$

Using Navier Stokes Equations and the conservation of mass:

$$\frac{d\rho}{dt} + \frac{1}{r} \frac{d}{dr} [(\rho)(r)(V_r)] + \frac{1}{r} \frac{d}{d\theta} [(\rho)(V_\theta)] + \frac{d}{dz} [(\rho)(V_z)] = 0 \quad (\text{B.82})$$

$$\rho \left(\frac{dV_z}{dt} + V_r \frac{dV_z}{dr} + \frac{V_\theta}{r} \frac{dV_z}{d\theta} + V_z \frac{dV_z}{dz} \right) = - \frac{dP}{dz} + \rho g_z + \mu \left(\frac{1}{r} \frac{d}{dr} \left(r \frac{dV_z}{dr} \right) \right) + \frac{1}{r^2} \frac{d^2 V_z}{d\theta^2} + \frac{d^2 V_z}{dz^2} \quad (\text{B.83})$$

Simplifying by assuming a fully developed flow:

$$\begin{aligned} \frac{1}{r} \frac{d}{dr} [(r)(V_r)] &= 0 \\ \frac{d}{dr} [(r)(V_r)] &= 0 \\ V_r &= 0 \end{aligned} \tag{B.84}$$

Having determined that the velocity in the direction at r is 0 everywhere the following can be determined:

$$\begin{aligned} -\frac{dP}{dz} + \mu \left(\frac{1}{r} \frac{d}{dr} \left(r \frac{dV_z}{dr} \right) \right) &= 0 \\ \int \mu \left(d \left(r \frac{dV_z}{dr} \right) \right) &= \int \frac{dP}{dz} r dr \\ \mu \left(r \frac{dV_z}{dr} \right) &= \frac{dP}{dz} \frac{r^2}{2} + c_1 \\ \int dV_z &= \int \frac{1}{\mu} \left(\frac{dP}{dz} \frac{r}{2} + \frac{C_1}{r} \right) dr = \\ V_z &= \frac{dP}{dz} \frac{r^2}{4\mu} + c_1 \ln(r) + C_2 \end{aligned} \tag{B.85}$$

Setting the boundary conditions of no slip, and velocity is constant at the free stream.

$$\begin{aligned} v_z &= 0 \text{ at } r = R \\ C_1 &= 0 \\ \frac{dv_z}{dr} &= 0 \text{ at } r = 0 \\ C_2 &= -\frac{dP}{dz} \frac{R^2}{4\mu} \end{aligned} \tag{B.86}$$

Thus, the flow rate can be now determined:

$$Q = \int_0^R V_{\text{fluid}} (2)(\pi)(r) dr = \int_0^R (2)(\pi)(r) \left[\frac{dP}{dz} \frac{1}{4\mu} [r^2 - R^2] \right] dr \tag{B.87}$$

$$\begin{aligned}
 Q &= (2)(\pi) \frac{dP}{dz} \frac{1}{4\mu} \int_0^R (r) [r^2 - R^2] dr = (2)(\pi) \frac{dP}{dz} \frac{1}{4\mu} \int_0^R r^3 - rR^2 dr \\
 Q &= (2)(\pi) \frac{dP}{dz} \frac{1}{4\mu} \left[\frac{r^4}{4} - \frac{r^2 R^2}{2} r R^2 \right]_0^R \\
 Q &= \frac{dP}{dz} \frac{\pi}{2\mu} \left[-\frac{R^4}{4} \right] = \frac{dP}{dz} \frac{\pi}{2\mu} \left[-\frac{D^4}{64} \right]
 \end{aligned} \tag{B.88}$$

Now determining area of flow compression, (Flow rate required to compress the plate attached to piston).

$$A_{\text{compression}} = \frac{\pi (D_{\text{Housing}}^2 - D_{\text{orifice}}^2 N)}{4} \tag{B.89}$$

Where N is the number of orifices.

Once the area is determined it can be further developed to find the following:

$$\frac{dP}{dZ} = \frac{F_{\text{piston}}}{AL_{\text{comp}}} \tag{B.90}$$

Simplifying the above equations

$$\frac{dP}{dZ}_{\text{comp}} = \frac{-4f_{\text{shock}}}{\pi L_{\text{comp}} (D_{\text{Housing}}^2 - 3D_{\text{orifice}}^2)} \tag{B.91}$$

$$Q_{\text{compression}} = -\frac{D_{\text{housing}}^4 F_{\text{piston}}}{32\mu L_{\text{comp}} (D_{\text{Housing}}^2 - 3D_{\text{orifice}}^2)} \tag{B.92}$$

$$F_{\text{Shock}} = -V_{\text{orifice}} \frac{8\pi\mu L_{\text{comp}} (D_{\text{housing}}^2 - 3D_{\text{orifice}}^2)}{D_h^4} \tag{B.93}$$

This equation can be further simplified as the force can be considered to be the Damping Coefficient multiplied by the velocity.

$$C = \frac{8\pi\mu L_{\text{comp}} (D_{\text{housing}}^2 - 3D_{\text{orifice}}^2)}{D_h^4} \quad (\text{B.94})$$

Thus, the orifice diameters can be determined by solving for D_{orifice}

$$D_{\text{orifice}}^2 = \frac{D_{\text{housing}}^2 - \sqrt{\frac{CD_{\text{housing}}^4}{8\pi\mu L_{\text{comp}}}}}{N} \quad (\text{B.95})$$

B.10 Suspension Force and Stress Analysis

B.10.1 Bolt Analysis

To obtain a safety factor, the critical shear stress and actual shear stress must be determined. The maximum shear stress can be determined by the equation below.

$$\tau_{\max} = \frac{4 * V}{3 * A} \quad (\text{B.96})$$

V is the shear force exerted on the cross-sectional area A . The type of bolt being used is an M8 bolt, which has a major diameter of 8mm. In the figure below, the cross-sectional area and shear can be found.

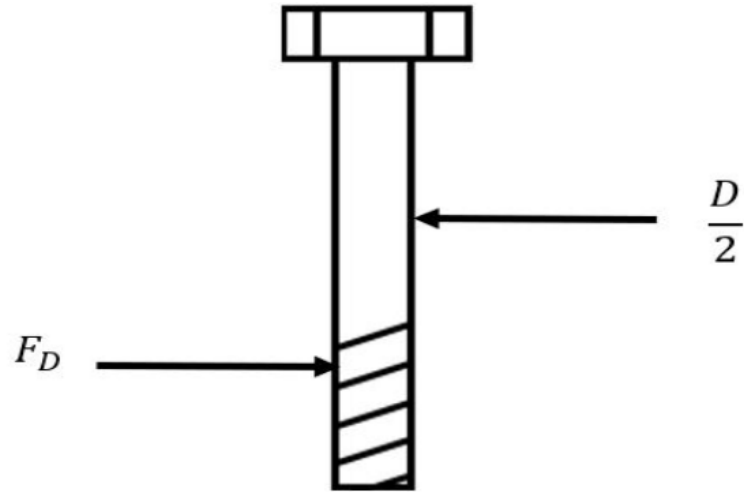


Figure B.17: FBD of Suspension Member Bolts for Mounting

$$A = \frac{\pi * d^2}{4} = \frac{\pi * (8 \text{ mm})^2}{4} = 50.2 \text{ mm}^2 \quad (\text{B.97})$$

By selecting the bolt and nut material as class SAE grade 8.8

$$S_y = 660 \text{ MPa}$$

, the safety factor can be found [9]. From the distortion energy theory we get the following for the safety factor:

$$S_{sy} = (0.58)(660 \text{ MPa}) = 382.3 \text{ MPa} \quad (\text{B.98})$$

$$\eta = \frac{S_{sy}}{\tau_{\max}} = \frac{382.3 \text{ MPa}}{22.07} = 12.9 \quad (\text{B.99})$$

B.10.2 Mount Weld Analysis

B.10.2.1 Description of Inputs and Outputs

B.10.2.2 Justification of Parameters and Safety Factors

The distance between the center of the mounting hole and the weld is 15 mm, the diameter of the tab is 37.5 mm and the thickness is 10 mm. These dimensions were chosen to fit the mounting points found from the suspension geometry.

The weld is a fillet weld with a leg size of $h = 6$ mm, selected in accordance with the Juvinall textbook. From this it is also determined that the minimum weld size should be 3 for sheets less than 6 mm [9]. Additional material is added due to the mounting tab being 10 mm.

The safety factor selected for the mounting tabs is 1.75 since a failure of this would result in catastrophic failure of the suspension and risk injury to the driver.

B.10.2.3 Assumptions, Simplifications and Material Selection

It is assumed that the weld will fail first in the mount leading to the weld being the concern of the analysis. It will also be assumed that the mount will be welded on 2 sides. The weld material selected is electrode E7010 due to its relatively high material strength (345 MPa yield strength), common availability and low cost.

B.10.2.4 Stress analysis

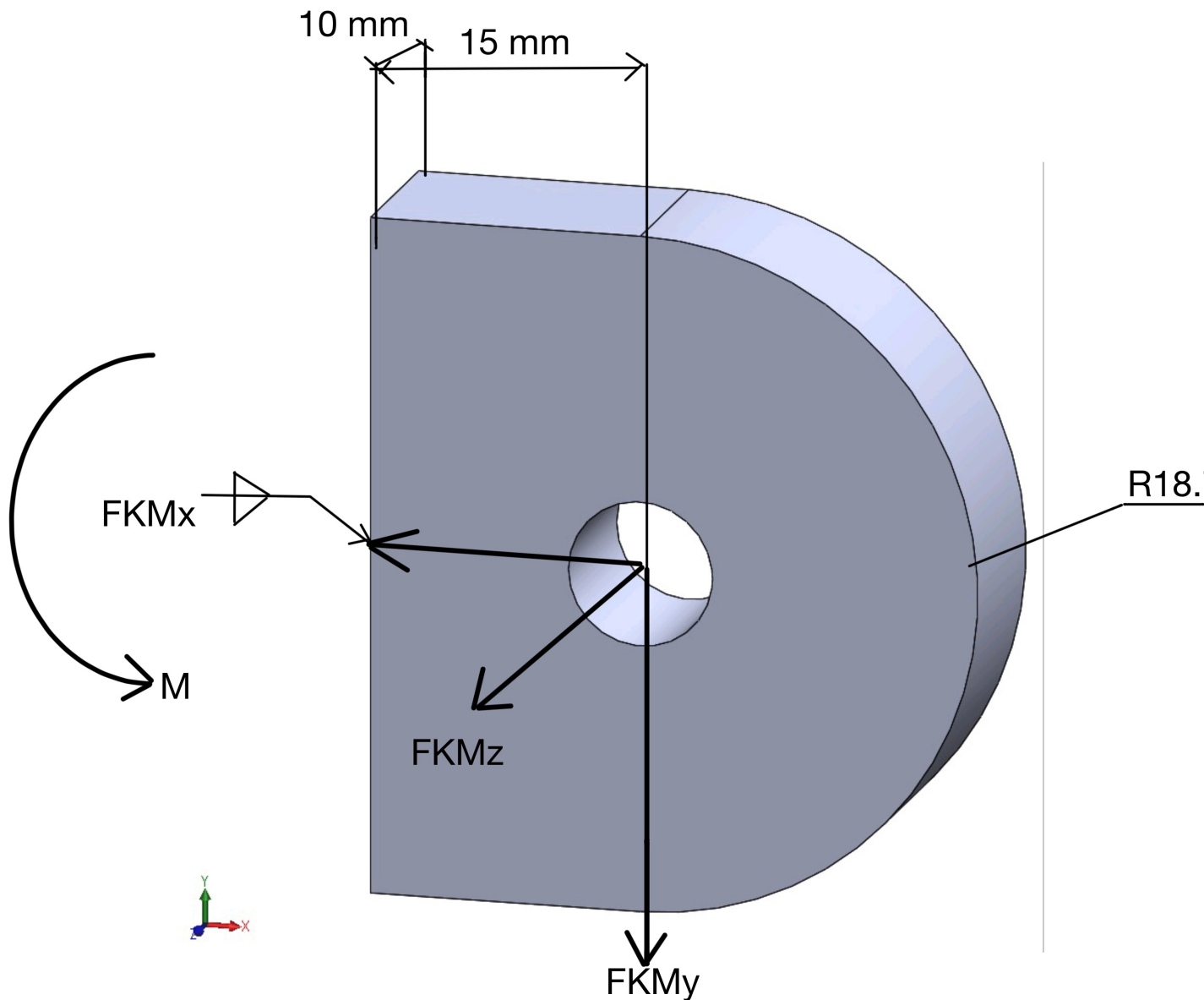


Figure B.18: FBD of Mount and Weld

From the FBD above, the forces at the mounting point can be translated to the weld point to get a transverse load of F_y of N at the weld.

Since the mounting tabs are considered cantilevers welded to the frame, the transverse load (F_y) produces a shear load and bending moment as reactions.

$$\tau' = \frac{V}{A} = \frac{F_y}{A} \quad (\text{B.100})$$

The welding profile is as seen in the figure below from the Shigley textbook [12]:

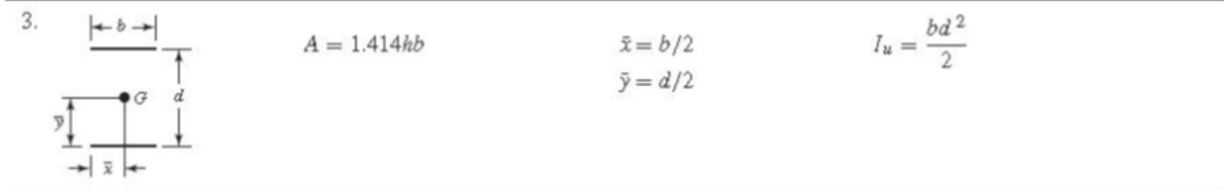


Figure B.19: Welding Profile

The shear load is a primary shear at the weld and can be calculated with Equation below [12].

$$\tau' = \frac{V}{A} = \frac{F_y}{A} = \frac{XXX \text{ N}}{318.5 \text{ mm}^2} = \text{MPa} \quad (\text{B.101})$$

The bending moment of the weld is analysed to get the secondary shear as follows [12]

$$\tau'' = \frac{Mc}{I} \quad (\text{B.102})$$

Since the transverse load and the distance between this force and the weld are known, one can calculate the bending moment.

$$M = (F_y)(15 \text{ mm}) = (\text{N})(15 \text{ mm}) = \text{N.mm} \quad (\text{B.103})$$

To determine the moment of inertia, first the unit moment of inertia of the weld profile determined as [X4]:

$$I_u = \frac{bd^2}{2} = \frac{(37.5 \text{ mm})(10 \text{ mm})^2}{2} = 1875 \text{ mm}^3 \quad (\text{B.104})$$

The moment of inertia can now be calculated as [12]:

$$I = 0.707(h) (I_u) = 0.707(6 \text{ mm}) (1875 \text{ mm}^3) = 7954 \text{ mm}^4 \quad (\text{B.105})$$

One can now calculate the secondary shear.

$$\tau'' = \frac{(\text{N.mm})(5 \text{ mm})}{7954 \text{ mm}^4} = \text{MPa} \quad (\text{B.106})$$

Finally, the total shear stress on the weld can now be calculated as [?].

$$\tau = \sqrt{\tau'^2 + \tau''^2} \quad (\text{B.107})$$

With the total shear stress, one can determine the safety factor.

$$n = \frac{S_{sy}}{\tau} = \frac{0.58 (S_y)}{\tau} \quad (\text{B.108})$$

B.10.2.5 Critical Review of Initial Results

Front Suspension Points

$$A = (A_X, A_Y, A_Z) = (596.9 \text{ mm}, 7.94 \text{ mm}, 658.16 \text{ mm}) \quad (\text{B.109})$$

$$B = (B_X, B_Y, B_Z) = (294.72 \text{ mm}, 0 \text{ mm}, 877.99 \text{ mm}) \quad (\text{B.110})$$

$$C = (C_X, C_Y, C_Z) = (271.18 \text{ mm}, 0 \text{ mm}, 438.32 \text{ mm}) \quad (\text{B.111})$$

$$D = (D_X, D_Y, D_Z) = (596.9 \text{ mm}, 236.54 \text{ mm}, 658.16 \text{ mm}) \quad (\text{B.112})$$

$$E = (E_X, E_Y, E_Z) = (294.5 \text{ mm}, 181.87 \text{ mm}, 878.01 \text{ mm}) \quad (\text{B.113})$$

$$F = (F_X, F_Y, F_Z) = (269.24 \text{ mm}, 177.3 \text{ mm}, 448.08 \text{ mm}) \quad (\text{B.114})$$

$$G = (G_X, G_Y, G_Z) = (514.26 \text{ mm}, 22.94 \text{ mm}, 658.16 \text{ mm}) \quad (\text{B.115})$$

$$H = (H_X, H_Y, H_Z) = (309.2 \text{ mm}, 560.73 \text{ mm}, 658.16 \text{ mm}) \quad (\text{B.116})$$

$$I = (I_X, I_Y, I_Z) = (586.91 \text{ mm}, 67.83 \text{ mm}, 580.77 \text{ mm}) \quad (\text{B.117})$$

$$J = (J_X, J_Y, J_Z) = (268.94 \text{ mm}, 66.52 \text{ mm}, 580.58 \text{ mm}) \quad (\text{B.118})$$

$$FWC = (FWC_X, FWC_Y, FWC_Z) = (626.9 \text{ mm}, 122.24 \text{ mm}, 658.16 \text{ mm}) \quad (\text{B.119})$$

Rear Suspension Points

$$K = (K_X, K_Y, K_Z) = (548.68 \text{ mm}, -20.33 \text{ mm}, 2384.37 \text{ mm}) \quad (\text{B.120})$$

$$L = (L_X, L_Y, L_Z) = (315 \text{ mm}, -26.48 \text{ mm}, 2519.95 \text{ mm}) \quad (\text{B.121})$$

$$M = (M_X, M_Y, M_Z) = (315 \text{ mm}, -26.48 \text{ mm}, 2250.12 \text{ mm}) \quad (\text{B.122})$$

$$N = (N_X, N_Y, N_Z) = (548.68 \text{ mm}, 208.27 \text{ mm}, 2384.37 \text{ mm}) \quad (\text{B.123})$$

$$O = (O_X, O_Y, O_Z) = (315 \text{ mm}, 163.13 \text{ mm}, 2519.95 \text{ mm}) \quad (\text{B.124})$$

$$P = (P_X, P_Y, P_Z) = (315 \text{ mm}, 163.13 \text{ mm}, 2249.29 \text{ mm}) \quad (\text{B.125})$$

$$Q = (Q_X, Q_Y, Q_Z) = (488 \text{ mm}, -6.93 \text{ mm}, 2400.88 \text{ mm}) \quad (\text{B.126})$$

$$R = (R_X, R_Y, R_Z) = (336.64 \text{ mm}, 325.22 \text{ mm}, 2452.49 \text{ mm}) \quad (\text{B.127})$$

$$RWC = (RWC_X, RWC_Y, RWC_Z) = (578.68 \text{ mm}, 93.97 \text{ mm}, 2384.37 \text{ mm}) \quad (\text{B.128})$$

(B.129)

(B.130)

(B.131)

$$\begin{aligned} r_D &= D - WC \\ &= (r_{D_X}, r_{D_Y}, r_{D_Z}) \\ &= (596.9 \text{ mm} - 626.9 \text{ mm}, 236.54 \text{ mm} - 122.24 \text{ mm}, 658.16 \text{ mm} - 658.16 \text{ mm}) \\ &= (-30.00 \text{ mm}, 114.3 \text{ mm}, 0 \text{ mm}) \end{aligned} \tag{B.132}$$

$$\begin{aligned} r_G &= G - WC \\ &= (r_{G_X}, r_{G_Y}, r_{G_Z}) \\ &= (514.26 \text{ mm} - 626.9 \text{ mm}, 22.94 \text{ mm} - 122.24 \text{ mm}, 658.16 \text{ mm} - 658.16 \text{ mm}) \\ &= (-112.64 \text{ mm}, -99.3 \text{ mm}, 0 \text{ mm}) \end{aligned} \tag{B.133}$$

$$\begin{aligned}
r_I &= I - WC \\
&= (r_{I_X}, r_{I_Y}, r_{I_Z}) \\
&= (586.91 \text{ mm} - 626.9 \text{ mm}, 67.83 \text{ mm} - 122.24 \text{ mm}, 580.77 \text{ mm} - 658.1 \text{ mm m}) \\
&= (-39.99 \text{ mm}, -54.41 \text{ mm}, -77.39 \text{ mm})
\end{aligned} \tag{B.134}$$

$$\begin{aligned}
\sum M_X = O &= F_{AC} (\widehat{AC}_Z r_{A_Y} - \widehat{AC}_Y r_{A_Z}) + F_{AB} (\widehat{AB}_Z r_{A_Y} - \widehat{AB}_Y r_{A_Z}) + \\
&\quad F_{DF} (\widehat{DF}_Z r_{D_Y} - \widehat{DF}_Y r_{D_Z}) + F_{DE} (\widehat{DE}_Z r_{D_Y} - \widehat{DE}_Y r_{D_Z}) + \\
&\quad F_{IJ} (\widehat{IJ}_Z r_{I_Y} - \widehat{IJ}_Y r_{I_Z}) + F_{GH} (\widehat{GH}_Z r_{G_Y} - \widehat{GH}_Y r_{G_Z}) + M_X
\end{aligned} \tag{B.135}$$

$$\begin{aligned}
\sum M_Y = O &= F_{AC} (\widehat{AC}_Z r_{A_X} - \widehat{AC}_X r_{A_Z}) + F_{AB} (\widehat{AB}_Z r_{A_X} - \widehat{AB}_X r_{A_Z}) + \\
&\quad F_{DF} (\widehat{DF}_Z r_{D_X} - \widehat{DF}_X r_{D_Z}) + F_{DE} (\widehat{DE}_Z r_{D_X} - \widehat{DE}_X r_{D_Z}) + \\
&\quad F_{IJ} (\widehat{IJ}_Z r_{I_X} - \widehat{IJ}_X r_{I_Z}) + F_{GH} (\widehat{GH}_Z r_{G_X} - \widehat{GH}_X r_{G_Z}) + M_Y
\end{aligned} \tag{B.136}$$

$$\begin{aligned}
\sum M_Z = O &= F_{AC} (\widehat{AC}_Y r_{A_X} - \widehat{AC}_X r_{A_Y}) + F_{AB} (\widehat{AB}_Y r_{A_X} - \widehat{AB}_X r_{A_Y}) + \\
&\quad F_{DF} (\widehat{DF}_Y r_{D_X} - \widehat{DF}_X r_{D_Y}) + F_{DE} (\widehat{DE}_Y r_{D_X} - \widehat{DE}_X r_{D_Y}) + \\
&\quad F_{IJ} (\widehat{IJ}_Y r_{I_X} - \widehat{IJ}_X r_{I_Y}) + F_{GH} (\widehat{GH}_Y r_{G_X} - \widehat{GH}_X r_{G_Y}) + M_Z
\end{aligned} \tag{B.137}$$

B.10.3 MATLAB program for front suspension

6x6 matrix developed for the front suspension (with tie rod)

```
clc; format long;
```

```

A = [0.828704311 0.808473745 0.832246334 0.800323279 0.999991335 0.356279976; 0.020201131
0.021243238 0.15046778 0.144688074 0.00411985 -0.934379248; 0.559321981 -0.58814873
0.533596746 -0.581848786 0.000597535 0; -63.93050247 67.22539987 60.99010806 -66.50531626
0.286323273 0; -16.77965944 17.64446191 -16.00790238 17.45546358 77.36543396 0; 94.11486886
91.7712519 -99.63978934 -95.81759304 54.24477574 140.6270801]; disp(A);

B = [-1438.79 ; 1661; -1495.49; 381753.7323; 49830; -1438790]; disp(B);

C = A; disp(C);

```

Output:

```

1.0e+03
-5.957444976974337
-1.554848703220399
4.025030625702482
2.106430362396803
0.064164956850315
-0.967166195703433

```

B.10.4 MATLAB program for rear suspension

5x5 matrix developed for the rear suspension (no tie rod)

```
clc; format long;
```

```

A = [0.866866558 0.864733903 0.853901901 0.853131429 0.410587839; 0.02281423 0.022758103
0.164948356 0.164799524 -0.901009187; 0.498017953 -0.501714407 0.493602657 -0.494982708
-0.140000253; -56.92345208 57.34595669 56.41878367 -56.57652352 29.00168725; 98.39842064
98.15634201 -102.549438 -102.4569081 123.131826]; disp(A);

B = [-1388.5; 1710.56; -1539.5; 392988.165; -1388500]; disp(B);

C = A; disp(C);

```

Output:

1.0e+03
-6.111308464288867
-0.708249849455443
3.914523457389819
1.869315591858076
-1.012583117385016

B.11 Suspension Geometry Derivation

B.11.1 Front Suspension

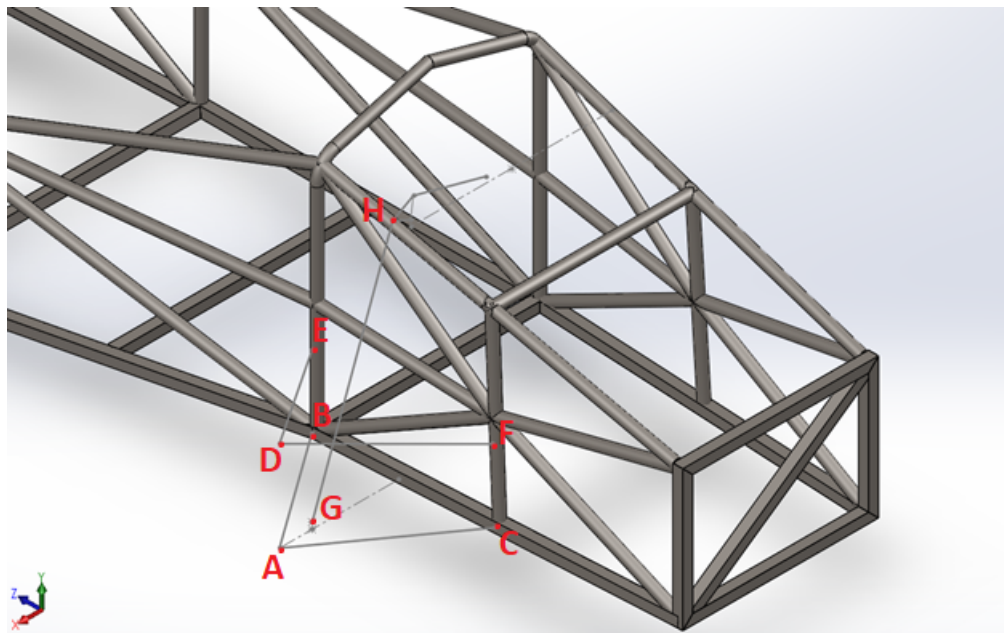


Figure B.20: Overall front suspension geometry with labeled points

Step 1:

Firstly, the track width is determined from the lower control arm spread angle, and its connection points to the chassis.

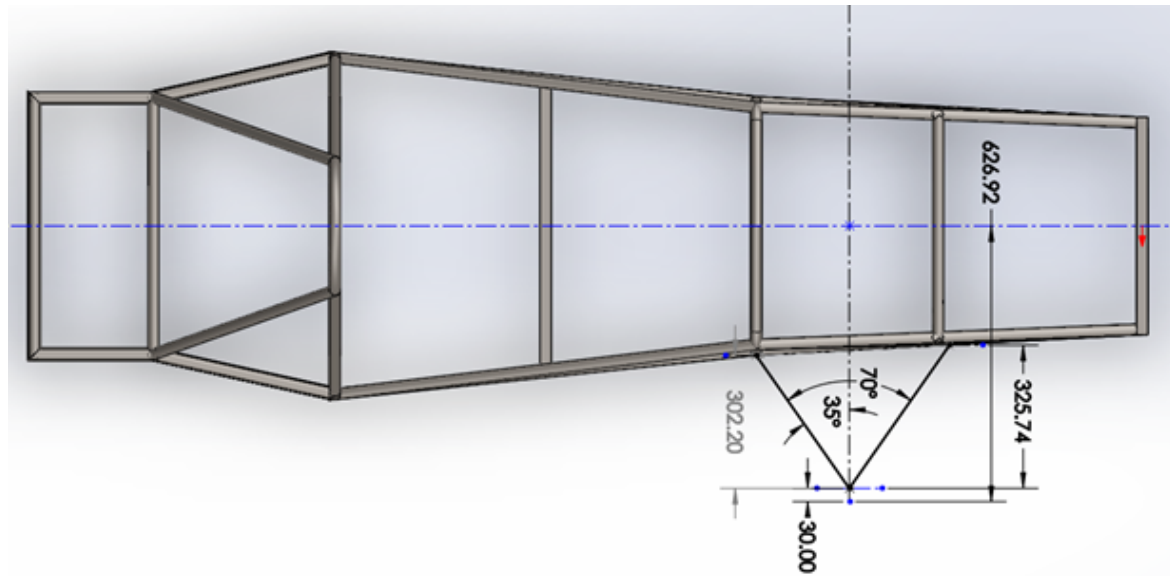


Figure B.21: Front suspension track width determination

It should be noted that X is in vertical direction, Z is horizontal direction for figure the figure above.

Firstly, the lower control arm should be mounted to the lower bar of the chassis coincident with the vertical front hoop and the subsequent vertical bar to its side. It should be noted that the actual mounting points are slightly offset from the chassis in the positive x direction by 15 mm.

Next, the wishbone angle is set as 70° with the tubes of the control arm at equal angles from the axis of symmetry. The scrub radius should be added at the end point of the wishbone where it connects to the steering knuckle. From this, the track width for the front is determined to be 1253.84 mm by getting the vertical distance from the center of the tire to the center-line of the chassis (in the figure above we get this as half the track

width which is 626.92 mm). We can see that the angle of the wishbone and the scrub radius in this case directly effect the length of the track width being that if the wishbone angle is increased, the track width decreases and similarly if the scrub radius increases, the track width also increases.

Step 2:

On a plane along the wishbone center-line, the following drawing is made, with a primary goal of finding the wishbone angles from the horizontal.

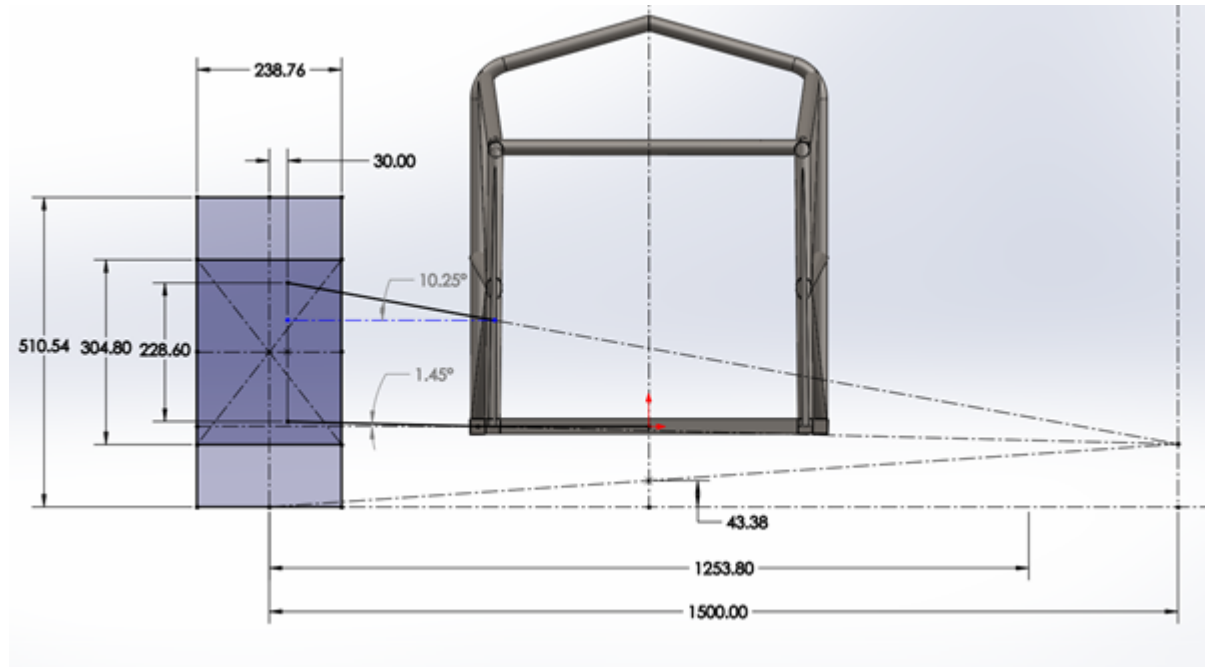


Figure B.22: Front suspension geometry front view

In this sketch the following parameters are considered and tuned to get the geometry:

- Camber: As described in the literature review, camber is usually tuned to be negative for an FSAE vehicle. For the sake of calculations, camber will be assumed to be 0°.
- Roll Center: Roll center is to be kept between the center of gravity and the ground. The roll center is best optimized when it is in the range between 15 and 30 percent of the

height of the center of gravity. In this case the roll center is the height of the center of mass multiplied by 0.15 which is found as $289.19 \text{ mm} * 0.15 = 43.38 \text{ mm}$.

- Swing Arm Length: For FSAE cars, swing arm length is best optimized when it is within the range of 1000 to 1800 mm. As such, a swing arm length (or instantaneous center) was assumed to be 1500 mm.
- King Pin Inclination (KPI): KPI was assumed to be zero for ease of calculations. Like the camber angle, KPI should be negative for a race car application.
- Scrub Radius: The distance of the wishbone mount point on the steering knuckle to the center of the tire, which is assumed to be 30 mm to avoid collisions within the tire.
- Wishbone Spread: Should be as large as possible so that the wishbones don't collide with the wheels at a maximum steering angle. This was assumed to be 70° in a previous step, in order to get a reasonable track width.

Step 3:

With angles found between the control arms and the horizontal in step 2, a 3D sketch can be made to determine the lower and upper control arm geometries by drawing in the connection points from the steering knuckle to the chassis mount points. This is shown in the figure below.

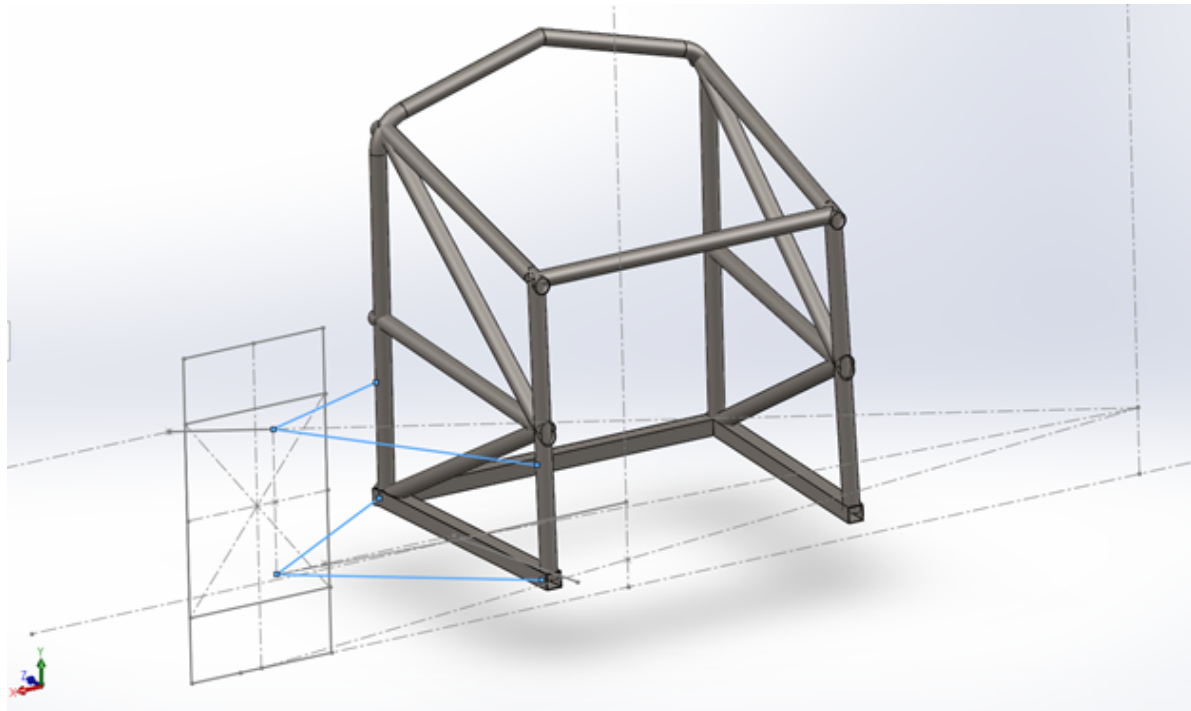


Figure B.23: Front control arms geometry determination

It should be noted that these points are used in the suspension analysis to locate the points of each node of the suspension components. Also, with the wishbone angles, angles between the control arms and the horizontal, and different component lengths, trigonometric relationships for each dimension can be set up for the future, which would help with parametrization. For now, since all the points have been plotted in 3D space, the lengths can be simply determined from within the measuring tool in SolidWorks.

Step 4:

The pushrod and rocker locations can now be made.

A sketch is made on the wishbone center-line from step 1 as the pushrod lies coincident on that plane. From here this, it is determined where the pushrod, rocker, and chassis mounts are in relation to the chassis itself.

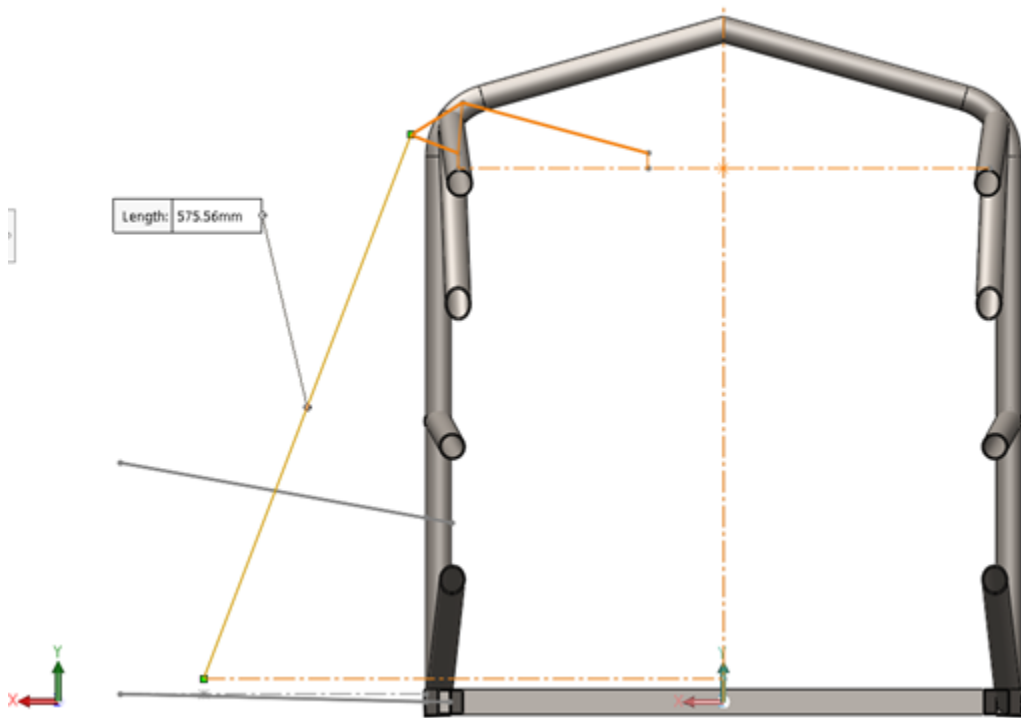


Figure B.24: Front view of front rocker and pushrod locations in relation to chassis

The rocker geometry is made in a way that the forces can be translated from the pushrod to the shock absorbers through rotation of the rocker about its pivot point (C). This is best optimized when the angle between the shock absorber and the pushrod is within the range of 80-120° [13]. This angle ensures that the system does not produce a regressive rate and can return to base ride height after the shock absorbers have been compressed [14].

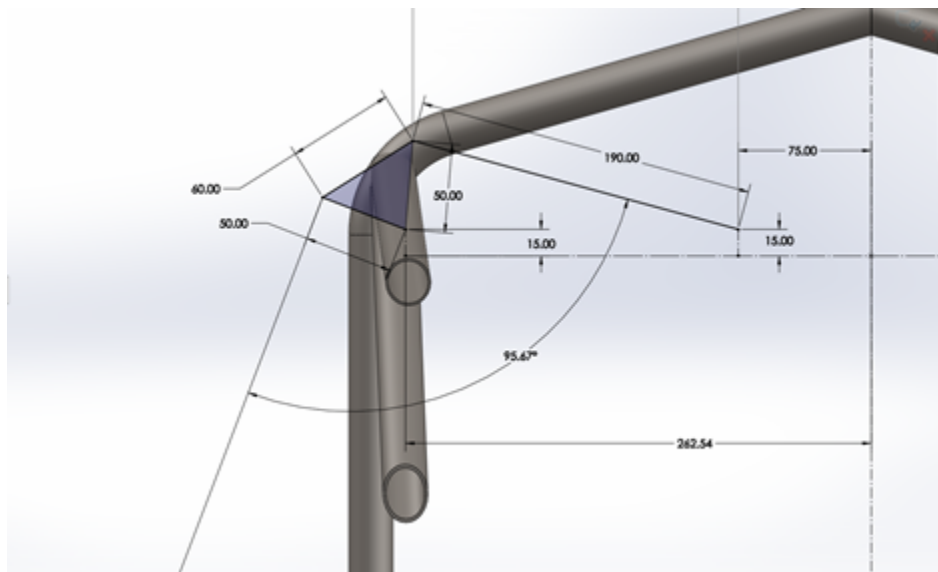


Figure B.25: Front rocker and shock absorber dimensions

From the figure above, the angles and values for each member are shown. The angle between the pushrod and shock absorber is seen to be 95.67° , which is within the optimized range ($80\text{-}120^\circ$). It should be noted that the mounting points are offset 15 mm from the connection points to the chassis as an approximation of where the mounts will be. The distance from the shock-chassis mount to the vertical center-line of the chassis is set to be 75 mm. The shock absorber length is set as 190 mm in an uncompressed state. From this, the rocker is dimensioned and a pushrod to shock angle is determined.

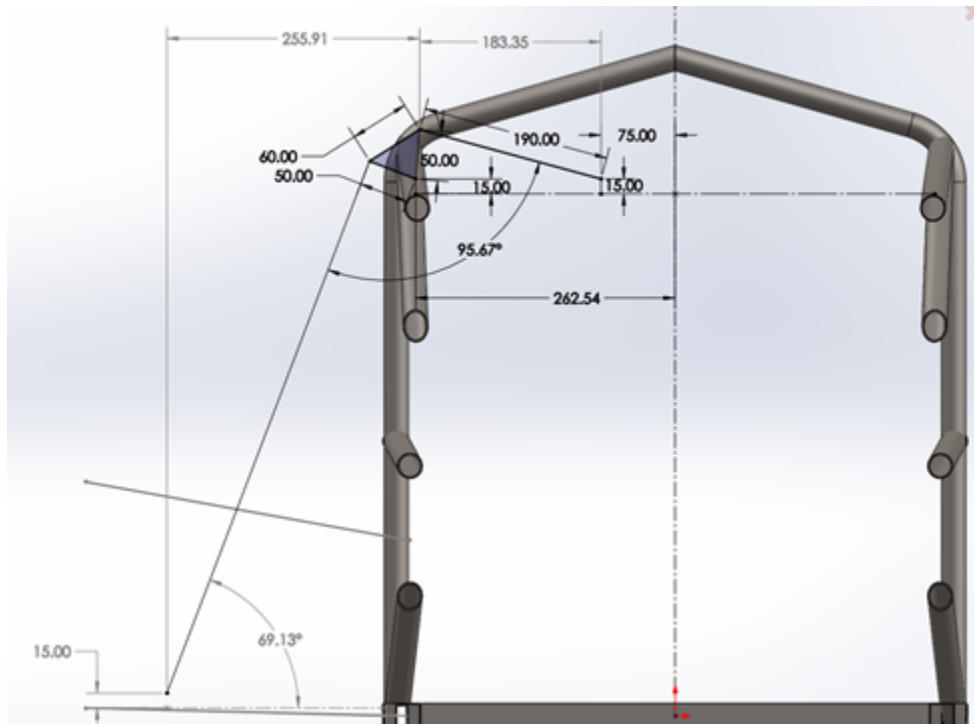


Figure B.26: Front pushrod location with respect to rocker

After setting the rocker dimensions and shock absorber location, a line can be made from the rocker-pushrod attachment point (point H), to the point where the pushrod connects to the lower control arm (point G). The pushrod angle with the horizontal θ is determined to be 69.13° .

B.11.2 Rear Suspension

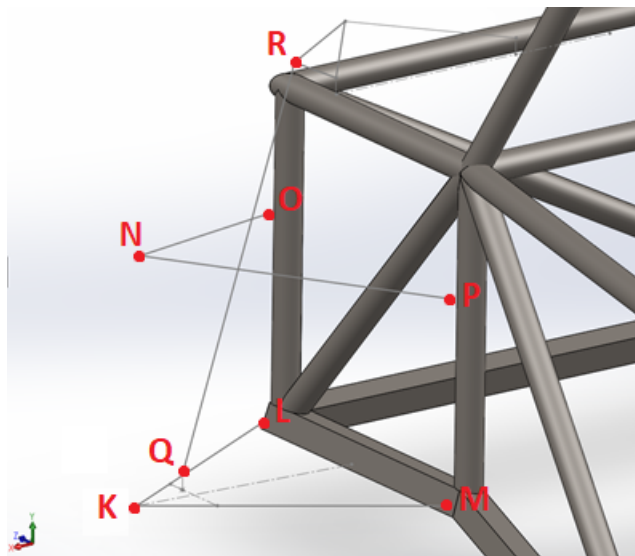


Figure B.27: Overall rear suspension geometry with labeled points

Step 1:

Firstly, the track width is determined from the lower control arm spread angle, and its connection points to the chassis.

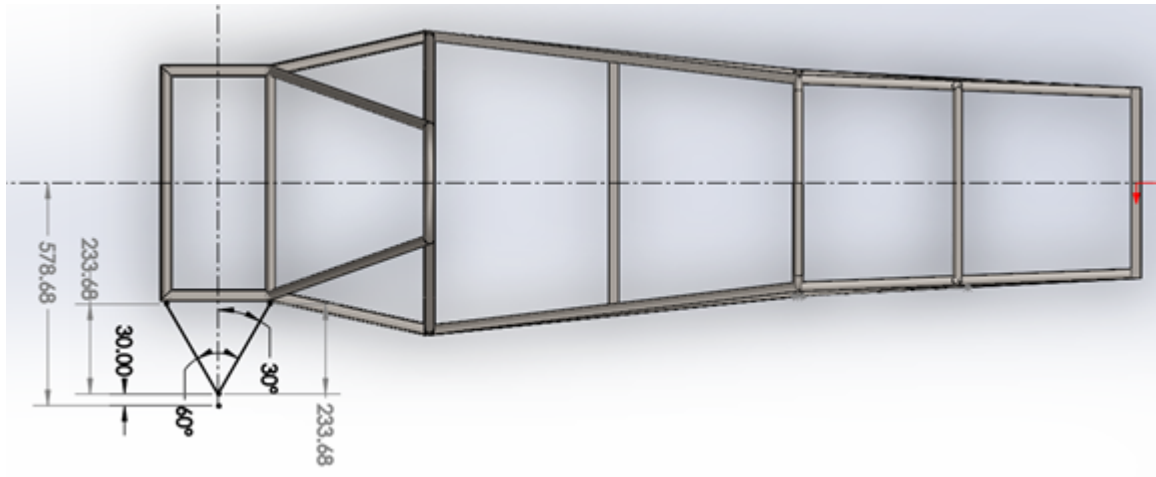


Figure B.28: Rear suspension track width determination

It should be noted that X is in vertical direction, Z is horizontal direction for figure the figure above.

Firstly, the lower control arm should be mounted to the lower bar of the chassis coincident with the vertical front hoop bar at the end of the car and the subsequent vertical bar to its side. It should be noted that the actual mounting points are slightly offset from the chassis in the positive x direction by 15 mm.

Next, the wishbone angle is set as 60° with the tubes of the control arm at equal angles from the axis of symmetry. The scrub radius should be added at the end point of the wishbone where it connects to the steering knuckle. From this, the track width for the front is determined to be 1157.36 mm by getting the vertical distance from the center of the tire to the center-line of the chassis (in the figure above we get this as half the track width which is 578.68 mm).

We can see that the angle of the wishbone and the scrub radius in this case directly affect the length of the track width being that if the wishbone angle is increased, the track width decreases and similarly if the scrub radius increases, the track width also increases. Also, this combination of wishbone angle and scrub radius was chosen so that the rear

track width was less than the front track width, which helps with the cornering of the vehicle [13].

Step 2:

On a plane along the wishbone center-line, the following drawing is made, with a primary goal of finding the wishbone angles from the horizontal.

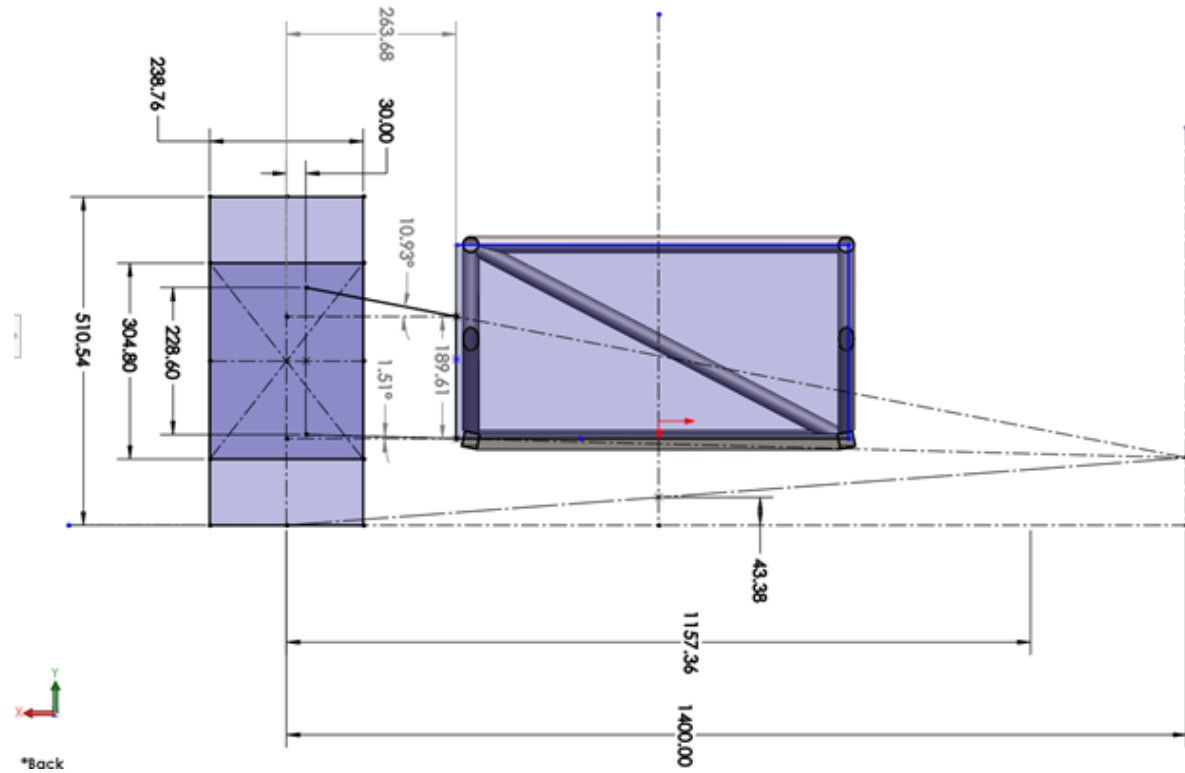


Figure B.29: Rear suspension geometry front view

In this sketch the following parameters are considered and tuned to get the geometry:

- Camber: As described in the literature review, camber is usually tuned to be negative for an FSAE vehicle. For the sake of calculations, camber will be assumed to be zero°.
- Roll Center: Roll center is to be kept between the center of gravity and the ground. The roll center is best optimized when it is in the range between 15 and 30 percent of the

height of the center of gravity. In this case the roll center is the height of the center of mass multiplied by 0.15 which is found as $289.19 \text{ mm} * 0.15 = 43.38 \text{ mm}$.

- Swing Arm Length: For FSAE cars, swing arm length is best optimized when it is within the range of 1000 to 1800 mm. As such, a swing arm length (or instantaneous center) was assumed to be 1400 mm.
- King Pin Inclination (KPI): KPI was assumed to be zero for ease of calculations. Like the camber angle, KPI should be negative for a race car application.
- Scrub Radius: The distance of the wishbone mount point on the steering knuckle to the center of the tire, which is assumed to be 30 mm to avoid collisions within the tire.
- Wishbone Spread: Should be as large as possible so that the wishbones don't collide with the wheels at a maximum steering angle. This was assumed to be 60° in a previous step, in order to get a reasonable track width.

Step 3:

With angles found between the control arms and the horizontal in step 2, a 3D sketch can be made to determine the lower and upper control arm geometries by drawing in the connection points from the steering knuckle to the chassis mount points. This is shown in the figure below.

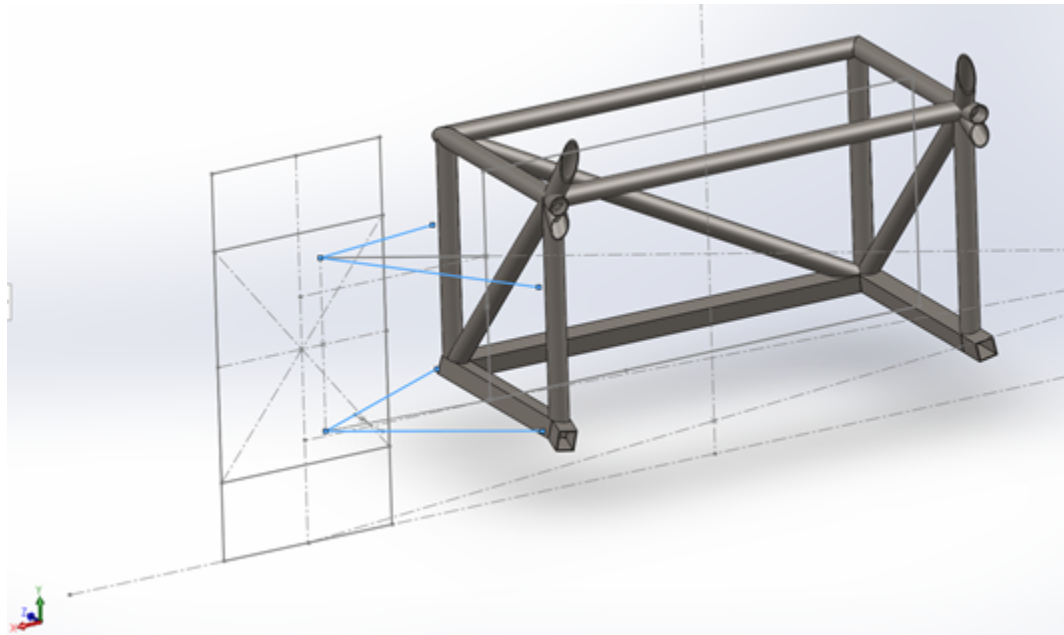


Figure B.30: Rear control arm geometry determination

It should be noted that these points are used in the suspension analysis to locate the points of each node of the suspension components. Also, with the wishbone angles, angles between the control arms and the horizontal, and different component lengths, trigonometric relationships for each dimension can be set up for the future, which would help with parametrization. For now, since all the points have been plotted in 3D space, the lengths can be simply determined from within the measuring tool in SolidWorks.

Step 4:

Pushrod and rocker locations are found in this step.

Firstly, a plane must be made on the determined location for where the rear shocks are mounted on the chassis. This location was set to be on a bar that will be made in front of the rear bar. From this, it is determined where the pushrod, rocker, and chassis mounts are in relation to the chassis itself. A depiction of this is shown in the figure below.

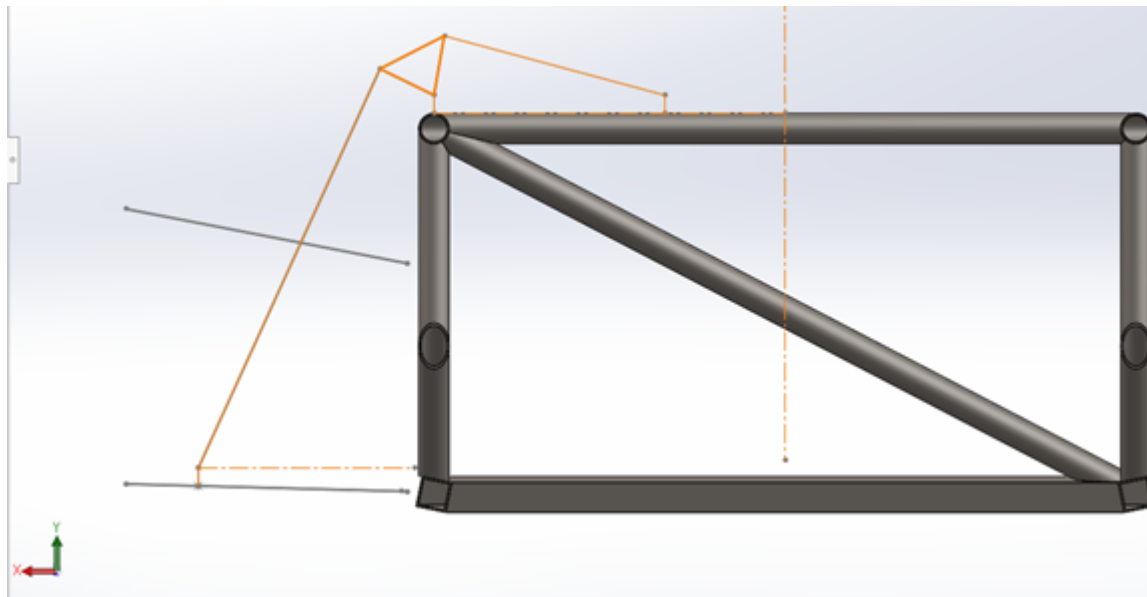


Figure B.31: Rear rocker and push rod location with respect to chassis

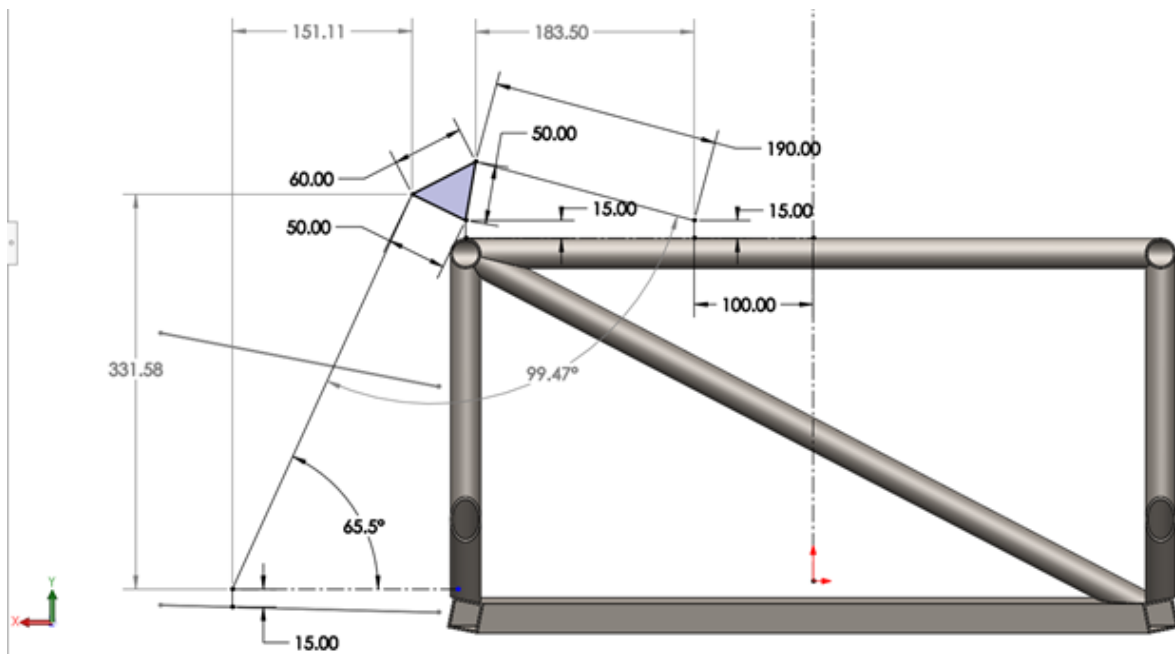


Figure B.32: Rear rocker and pushrod dimensions

From the figure above, the angles and values for each member are shown. The angle between the pushrod and shock absorber is seen to be 99.47° , which is within the optimized range ($80\text{-}120^\circ$). It should be noted that the mounting points are offset 15 mm from the connection points to the chassis as an approximation of where the mounts will be. The distance from the shock-chassis mount to the vertical center-line of the chassis is set to be 100 mm. The shock absorber length is set as 190 mm in an uncompressed state. From this, the rocker is dimensioned and a pushrod to shock angle in the X-Y plane is determined. The pushrod angle with the horizontal in the X-Y plane θ is determined to be 65.5° as seen in the figure above.

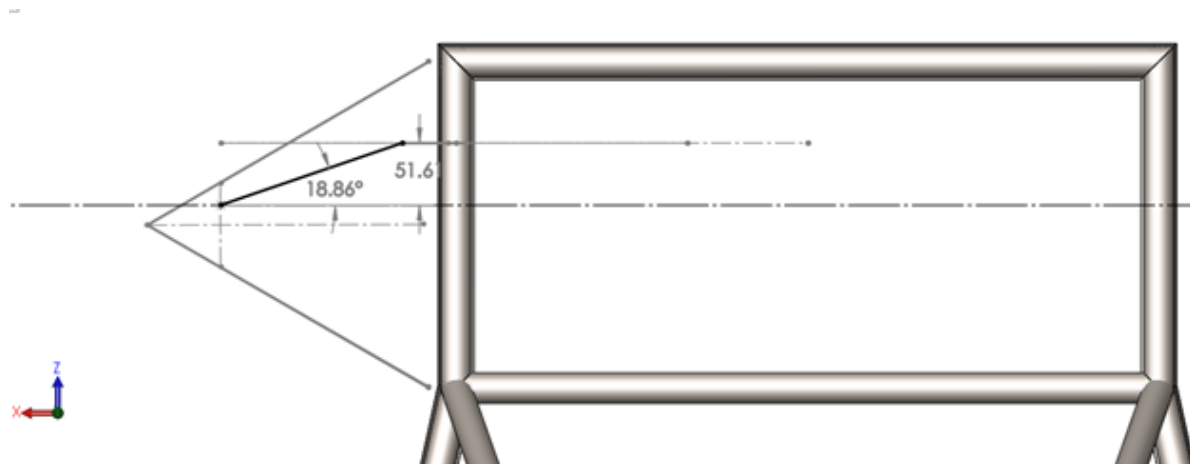


Figure B.33: Rear pushrod location determination

After setting the rocker dimensions and shock absorber location, a line can be made from the rocker-pushrod attachment point (point H), to the point where the pushrod connects to the LCA (point G). Since the rear pushrod is offset from the wishbone centerline, an additional angle with the horizontal in the X-Z plane must be found to get the pushrod location, which is 18.86° .

From all these steps, the pushrod length can be determined with a trigonometric relationship. The value for this pushrod length is found in the figure below using the SolidWorks measuring tool since the components are now all plotted in 3D space.

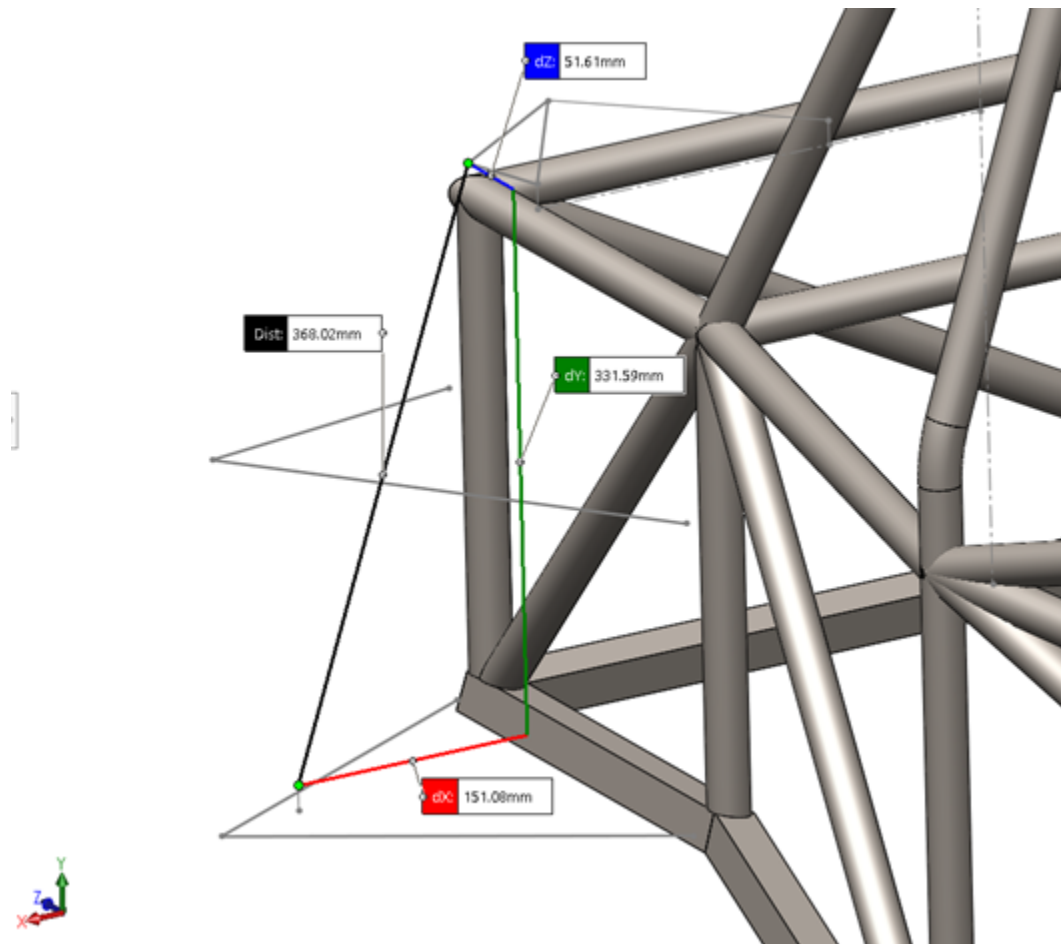


Figure B.34: Rear pushrod dimensions

Spring Analysis Springs must be used when designing shock absorbs as they are vital in absorbing any sudden forces the vehicle may encounter on a track. Helical compression springs are compressed when forces are applied to it. They regain their original positions once these forces are removed.

B.11.3 Description of Inputs and Outputs

The maximum force experienced on the front tire was found under high speed cornering conditions, which resulted in a reaction force by the push-rod of 1366.5 N. The spring will be designed to be able to support this force. The force applied when the spring is at its un-stretched length is 0 N.

B.11.4 Justification of Inputs, constants and Parameters

The spring will a peened spring with squared ends. Peened springs will be used as they have much better fatigue life properties and higher endurance strengths. The spring has squared ends as it allows for better load transfer.

The spring is expected to have a minimum of 3 to 15 active coils. The spring index is recommended to be in the range of 4 and 12.

B.11.5 Assumptions, Simplifications and Materials

The mean coil diameter D is defined as the average of the inside and outside coil diameters. Whilst, d is defined as the wire diameter.

A set of RC1 Shocks from Fox has a coil diameter D of D=38.1 mm and a wire diameter d=7.5 mm. Since this shock will be similar to the type chosen for the FSAE car it can be assumed that an initial mean coil diameter of D=50 mm and wire diameter of d=8 mm. The values of D and d are assumed for the first iteration and will be subject to change during parameterization.

$$ID = D - d = 50\text{mm} - 8\text{mm} = 42\text{mm} \quad (\text{B.138})$$

$$OD = D + d = 50\text{mm} + 8\text{mm} = 58\text{mm} \quad (\text{B.139})$$

The spring Material will be 302 Stainless wire. Which has the following properties: "Modulus of Elasticity = 6.89E+10 Pa, Shear Modulus = 2.60E+10 Pa, and an Ultimate Tensile Strength 1.077E+9 Pa which was calculated from $\frac{A}{d^m}$.

Front Spring Analysis

Having determined the minimum and maximum forces induced on the spring the amplitude and mean forces can then be determined:

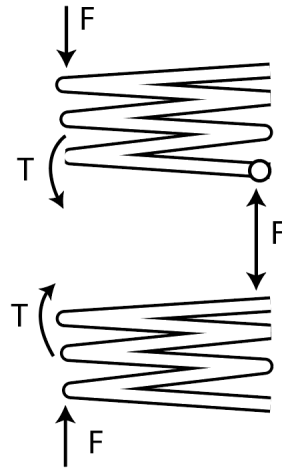


Figure B.35: FBD of Forces acting on spring

$$F_a = \frac{F_{max} - F_{min}}{2} = \frac{1366.5N - 0N}{2} = 683.25N \quad (\text{B.140})$$

$$F_m = \frac{F_{max} + F_{min}}{2} = \frac{1366.5N + 0N}{2} = 683.25N \quad (\text{B.141})$$

Hence, the deflection caused by F_{max} is

$$x_{max} = \frac{F_{max}}{K_s} = \frac{1366.5}{14885.62} = 0.0918m = 91.8mm \quad (\text{B.142})$$

Therefore, given the ultimate tensile strength of the material the torsional yield stress can be calculated as follows:

$$S_{sy} = 0.5 * UTS = 0.58 * 1077(MPa) = 624.66MPa \quad (B.143)$$

Defining our spring index as the ratio of the mean coil diameter over the wire diameter:

$$C = \frac{D}{d} = \frac{50}{8} = 6.25 \quad (B.144)$$

This spring index falls withing the expected range of 4 and 12.

For an as-wound spring the Solid force F_s which is the maximum force that must be resisted without set can be defined as follows:

$$F_s = (1 + \zeta) * F_{max} = (1 + 0.15) * (1366.56N) = 1571.54N \quad (B.145)$$

Where ζ the damping ratio selected for the spring must be greater than or equal to $\zeta=0.15$ to achieve robust linearity according to Shigley's

The number of coils can be determined through the following equation:

$$N_a = \frac{G * (d)^4}{8 * K_s * (D)^3} = \frac{(26 * 10^9) * (0.008)^4}{8 * 14885.62 * (.050)^3} = 7.15 turns \quad (B.146)$$

Thus, the number of active coils falls within the expected range of 3 to 15, rounding the number to 8 as square and ground ends are desired. The total number of coils can the be found to be:

$$N_t = N_a + 2 = 10 \quad (B.147)$$

The solid length of the spring can be determined as follows:

$$L_s = N_t * d = 10 * 8mm = 80mm \quad (\text{B.148})$$

The solid deflection can therefore be found

$$\delta_s = \frac{F_s}{K_s} = \frac{1571.54N}{14885.62\frac{N}{m}} = 0.105m = 105mm \quad (\text{B.149})$$

The free length is then:

$$L_f = L_s + \delta_s = 80mm + 105mm = 185mm \quad (\text{B.150})$$

Calculating for the shear stresses at amplitude the Bergsten correction factor K_B can be found and the equivalent shear stress at the solid length can be found:

$$K_B = \frac{4 * C + 2}{4C - 3} = \frac{4 * 6.25 + 2}{4 * 6.25 - 3} = 1.227 \quad (\text{B.151})$$

$$\tau_a = \frac{8 * F_a * D * K_B}{\pi * d^3} = \frac{8 * 1.227 * 683.28N * 50mm}{\pi * (8mm)^3} = 208.5MPa \quad (\text{B.152})$$

$$\tau_s = \frac{\tau_a * F_s}{F_a} = 208.5MPa * 1571.54N / 683.28N = 479.4MPa \quad (\text{B.153})$$

B.12 Chassis Impact Analysis Code

```
format long;
%Problem Characteristics
```

```
nnode = 18; %Number of Nodes
ndof_per_node = 3; %Number of degrees of freedom per node
nnode_per_element = 2; %Number of nodes per elements
nelem = 32; %Number of elements
nmat = 1; %Number of material types

%Elastic Modulus and Yield Stress of 4130 AISI Steel Tubes
Elastic_modulus = zeros(nmat,1);
Elastic_modulus(1,1) = 205000; %MPa

%Shear Modulus
Shear_modulus = zeros(nmat,1);
Shear_modulus(1,1) = 80000; %MPa

%Nodal coordinates in milimeters
Nodal_coordinates = zeros (nnode,2);

%First line is the nodal coordinate is the x coordinate
%Second line is the nodal coordinate is the y coordinate

Nodal_coordinates(1,1) = 0;
Nodal_coordinates(1,2) = 0;

Nodal_coordinates(2,1) = 0;
Nodal_coordinates(2,2) = 340;

Nodal_coordinates(3,1) = 439;
```

```
Nodal_coordinates(3,2) = 0;  
  
Nodal_coordinates(4,1) = 451.66;  
Nodal_coordinates(4,2) = 230;  
  
Nodal_coordinates(5,1) = 463.78;  
Nodal_coordinates(5,2) = 460.18;  
  
Nodal_coordinates(6,1) = 878;  
Nodal_coordinates(6,2) = 597.38;  
  
Nodal_coordinates(7,1) = 878;  
Nodal_coordinates(7,2) = 575.83;  
  
Nodal_coordinates(8,1) = 878;  
Nodal_coordinates(8,2) = 277;  
  
Nodal_coordinates(9,1) = 878;  
Nodal_coordinates(9,2) = 0;  
  
Nodal_coordinates(10,1) = 1357;  
Nodal_coordinates(10,2) = -51.5;  
  
Nodal_coordinates(11,1) = 1836;  
Nodal_coordinates(11,2) = -103;  
  
Nodal_coordinates(12,1) = 1836;  
Nodal_coordinates(12,2) = 275;
```

```
Nodal_coordinates(13,1) = 1836;
Nodal_coordinates(13,2) = 327.09;

Nodal_coordinates(14,1) = 1836;
Nodal_coordinates(14,2) = 1076;

Nodal_coordinates(15,1) = 2250.37;
Nodal_coordinates(15,2) = 276.37;

Nodal_coordinates(16,1) = 2249;
Nodal_coordinates(16,2) = -29;

Nodal_coordinates(17,1) = 2520;
Nodal_coordinates(17,2) = -29;

Nodal_coordinates(18,1) = 2520;
Nodal_coordinates(18,2) = 275;

%Connectivity table indicated the nodes that belong to each element
Connect_table = zeros(nelem,nnode_per_element + 1);

    %First line is node i that belongs to the element
    %Second line is node j that belongs to the element
    %Third line is the material flag

Connect_table(1,1) = 1;
Connect_table(1,2) = 2;
Connect_table(1,3) = 1;
```

```
Connect_table(2,1) = 2;  
Connect_table(2,2) = 5;  
Connect_table(2,3) = 1;  
  
Connect_table(3,1) = 2;  
Connect_table(3,2) = 4;  
Connect_table(3,3) = 1;  
  
Connect_table(4,1) = 1;  
Connect_table(4,2) = 4;  
Connect_table(4,3) = 1;  
  
Connect_table(5,1) = 1;  
Connect_table(5,2) = 3;  
Connect_table(5,3) = 1;  
  
Connect_table(6,1) = 5;  
Connect_table(6,2) = 4;  
Connect_table(6,3) = 1;  
  
Connect_table(7,1) = 4;  
Connect_table(7,2) = 3;  
Connect_table(7,3) = 1;  
  
Connect_table(8,1) = 5;  
Connect_table(8,2) = 7;  
Connect_table(8,3) = 1;  
  
Connect_table(9,1) = 4;
```

Connect_table(9,2) = 7;

Connect_table(9,3) = 1;

Connect_table(10,1) = 4;

Connect_table(10,2) = 8;

Connect_table(10,3) = 1;

Connect_table(11,1) = 4;

Connect_table(11,2) = 9;

Connect_table(11,3) = 1;

Connect_table(12,1) = 3;

Connect_table(12,2) = 9;

Connect_table(12,3) = 1;

Connect_table(13,1) = 7;

Connect_table(13,2) = 6;

Connect_table(13,3) = 1;

Connect_table(14,1) = 7;

Connect_table(14,2) = 8;

Connect_table(14,3) = 1;

Connect_table(15,1) = 8;

Connect_table(15,2) = 9;

Connect_table(15,3) = 1;

Connect_table(16,1) = 7;

Connect_table(16,2) = 12;

```
Connect_table(16,3) = 1;

Connect_table(17,1) = 8;
Connect_table(17,2) = 12;
Connect_table(17,3) = 1;

Connect_table(18,1) = 9;
Connect_table(18,2) = 12;
Connect_table(18,3) = 1;

Connect_table(19,1) = 9;
Connect_table(19,2) = 10;
Connect_table(19,3) = 1;

Connect_table(20,1) = 10;
Connect_table(20,2) = 11;
Connect_table(20,3) = 1;

Connect_table(21,1) = 11;
Connect_table(21,2) = 12;
Connect_table(21,3) = 1;

Connect_table(22,1) = 12;
Connect_table(22,2) = 13;
Connect_table(22,3) = 1;

Connect_table(23,1) = 13;
Connect_table(23,2) = 14;
Connect_table(23,3) = 1;
```

```
Connect_table(24,1) = 14;  
Connect_table(24,2) = 15;  
Connect_table(24,3) = 1;
```

```
Connect_table(25,1) = 12;  
Connect_table(25,2) = 15;  
Connect_table(25,3) = 1;
```

```
Connect_table(26,1) = 11;  
Connect_table(26,2) = 15;  
Connect_table(26,3) = 1;
```

```
Connect_table(27,1) = 11;  
Connect_table(27,2) = 16;  
Connect_table(27,3) = 1;
```

```
Connect_table(28,1) = 15;  
Connect_table(28,2) = 16;  
Connect_table(28,3) = 1;
```

```
Connect_table(29,1) = 16;  
Connect_table(29,2) = 17;  
Connect_table(29,3) = 1;
```

```
Connect_table(30,1) = 15;  
Connect_table(30,2) = 17;  
Connect_table(30,3) = 1;
```

```
Connect_table(31,1) = 15;
Connect_table(31,2) = 18;
Connect_table(31,3) = 1;

Connect_table(32,1) = 17;
Connect_table(32,2) = 18;
Connect_table(32,3) = 1;

%Radii of tubes in mm
OutterradiustubeA = 12.5;
InnerradiustubeA = (12.5 - 2.5);

OutterradiustubeB = 12.7;
InnerradiustubeB = (12.7 - 1.6);

OutterradiustubeC = 12.7;
InnerradiustubeC = (12.7 - 1.2);

%Width of square tubes in mm
OuterWidthtubeB = 25.4;
InnerWidthtubeB = (25.4-3.2);
OuterWidthtubeC = 25.4;
InnerWidthtubeC = (25.4-2.4);

%Moment of inertia of tubes (I)
InertiaPipeA = (pi/4)*((OutterradiustubeA^4)-(InnerradiustubeA^4));
InertiaPipeB = (pi/4)*((OutterradiustubeB^4)-(InnerradiustubeB^4));
InertiaPipeC = (pi/4)*((OutterradiustubeC^4)-(InnerradiustubeC^4));
InertiaSquareB = ((OuterWidthtubeB^4)/12)-((InnerWidthtubeB^4)/12);
```

```
InertiaSquareC = ((OuterWidthtubeC^4)/12)-((InnerWidthtubeC^4)/12);  
  
%Polar moment of inertia of tubes (J)  
PolarpipeA = (pi/2)*((OutterradiustubeA^4)-(InnerradiustubeA^4));  
PolarpipeB = (pi/2)*((OutterradiustubeB^4)-(InnerradiustubeB^4));  
PolarPipeC = (pi/2)*((OutterradiustubeC^4)-(InnerradiustubeC^4));  
PolarsquareB = ((OuterWidthtubeB^4)/6)-((InnerWidthtubeB^4)/6);  
PolarsquareC = ((OuterWidthtubeB^4)/6)-((InnerWidthtubeB^4)/6);  
  
%Assigning an outer radius to each element  
Tube_outer_radius = zeros(nelem,nmat);  
Tube_outer_radius(1,1) = OutterradiustubeB;  
Tube_outer_radius(2,1) = OutterradiustubeB;  
Tube_outer_radius(3,1) = OutterradiustubeB;  
Tube_outer_radius(4,1) = OutterradiustubeB;  
Tube_outer_radius(5,1) = OuterWidthtubeB;  
Tube_outer_radius(6,1) = OutterradiustubeB;  
Tube_outer_radius(7,1) = OutterradiustubeB;  
Tube_outer_radius(8,1) = OutterradiustubeB;  
Tube_outer_radius(9,1) = OutterradiustubeB;  
Tube_outer_radius(10,1) = OutterradiustubeB;  
Tube_outer_radius(11,1) = OutterradiustubeB;  
Tube_outer_radius(12,1) = OuterWidthtubeB;  
Tube_outer_radius(13,1) = OutterradiustubeA;  
Tube_outer_radius(14,1) = OutterradiustubeA;  
Tube_outer_radius(15,1) = OutterradiustubeA;  
Tube_outer_radius(16,1) = OutterradiustubeB;  
Tube_outer_radius(17,1) = OutterradiustubeB;  
Tube_outer_radius(18,1) = OutterradiustubeB;
```

```
Tube_outer_radius(19,1) = OuterWidthtubeB;
Tube_outer_radius(20,1) = OuterWidthtubeB;
Tube_outer_radius(21,1) = OutterradiustubeA;
Tube_outer_radius(22,1) = OutterradiustubeA;
Tube_outer_radius(23,1) = OutterradiustubeA;
Tube_outer_radius(24,1) = OutterradiustubeB;
Tube_outer_radius(25,1) = OutterradiustubeB;
Tube_outer_radius(26,1) = OutterradiustubeB;
Tube_outer_radius(27,1) = OuterWidthtubeB;
Tube_outer_radius(28,1) = OutterradiustubeB;
Tube_outer_radius(29,1) = OuterWidthtubeB;
Tube_outer_radius(30,1) = OutterradiustubeB;
Tube_outer_radius(31,1) = OutterradiustubeB;
Tube_outer_radius(32,1) = OutterradiustubeB;

%Assigning an inner radius to each element
Tube_inner_radius = zeros(nelem,nmat);
Tube_inner_radius(1,1) = InnerradiustubeB;
Tube_inner_radius(2,1) = InnerradiustubeB;
Tube_inner_radius(3,1) = InnerradiustubeB;
Tube_inner_radius(4,1) = InnerradiustubeB;
Tube_inner_radius(5,1) = InnerWidthtubeB;
Tube_inner_radius(6,1) = InnerradiustubeB;
Tube_inner_radius(7,1) = InnerradiustubeB;
Tube_inner_radius(8,1) = InnerradiustubeB;
Tube_inner_radius(9,1) = InnerradiustubeB;
Tube_inner_radius(10,1) = InnerradiustubeB;
Tube_inner_radius(11,1) = InnerradiustubeB;
Tube_inner_radius(12,1) = InnerWidthtubeB;
```

```
Tube_inner_radius(13,1) = InnerradiustubeA;
Tube_inner_radius(14,1) = InnerradiustubeA;
Tube_inner_radius(15,1) = InnerradiustubeA;
Tube_inner_radius(16,1) = InnerradiustubeB;
Tube_inner_radius(17,1) = InnerradiustubeB;
Tube_inner_radius(18,1) = InnerradiustubeB;
Tube_inner_radius(19,1) = InnerWidthtubeB;
Tube_inner_radius(20,1) = InnerWidthtubeB;
Tube_inner_radius(21,1) = InnerradiustubeA;
Tube_inner_radius(22,1) = InnerradiustubeA;
Tube_inner_radius(23,1) = InnerradiustubeA;
Tube_inner_radius(24,1) = InnerradiustubeB;
Tube_inner_radius(25,1) = InnerradiustubeB;
Tube_inner_radius(26,1) = InnerradiustubeB;
Tube_inner_radius(27,1) = InnerWidthtubeB;
Tube_inner_radius(28,1) = InnerradiustubeB;
Tube_inner_radius(29,1) = InnerWidthtubeB;
Tube_inner_radius(30,1) = InnerradiustubeB;
Tube_inner_radius(31,1) = InnerradiustubeB;
Tube_inner_radius(32,1) = InnerradiustubeB;

%Assigning a moment of inertia to every element
Tube_inertia = zeros(nelem,nmat);
Tube_inertia(1,1) = InertiaPipeB;
Tube_inertia(2,1) = InertiaPipeB;
Tube_inertia(3,1) = InertiaPipeB;
Tube_inertia(4,1) = InertiaPipeB;
Tube_inertia(5,1) = InertiaSquareB;
Tube_inertia(6,1) = InertiaPipeB;
```

```
Tube_inertia(7,1) = InertiaPipeB;
Tube_inertia(8,1) = InertiaPipeB;
Tube_inertia(9,1) = InertiaPipeB;
Tube_inertia(10,1) = InertiaPipeB;
Tube_inertia(11,1) = InertiaPipeB;
Tube_inertia(12,1) = InertiaSquareB;
Tube_inertia(13,1) = InertiaPipeA;
Tube_inertia(14,1) = InertiaPipeA;
Tube_inertia(15,1) = InertiaPipeA;
Tube_inertia(16,1) = InertiaPipeB;
Tube_inertia(17,1) = InertiaPipeB;
Tube_inertia(18,1) = InertiaPipeB;
Tube_inertia(19,1) = InertiaSquareB;
Tube_inertia(20,1) = InertiaSquareB;
Tube_inertia(21,1) = InertiaPipeA;
Tube_inertia(22,1) = InertiaPipeA;
Tube_inertia(23,1) = InertiaPipeA;
Tube_inertia(24,1) = InertiaPipeB;
Tube_inertia(25,1) = InertiaPipeB;
Tube_inertia(26,1) = InertiaPipeB;
Tube_inertia(27,1) = InertiaSquareB;
Tube_inertia(28,1) = InertiaPipeB;
Tube_inertia(29,1) = InertiaSquareB;
Tube_inertia(30,1) = InertiaPipeB;
Tube_inertia(31,1) = InertiaPipeB;
Tube_inertia(32,1) = InertiaPipeB;

%Assigning a polar moment of inertia to every element
Tube_polar = zeros(nelem,nmat);
```

```
Tube_polar(1,1) = PolarpipeB;  
Tube_polar(2,1) = PolarpipeB;  
Tube_polar(3,1) = PolarpipeB;  
Tube_polar(4,1) = PolarpipeB;  
Tube_polar(5,1) = PolarsquareB;  
Tube_polar(6,1) = PolarpipeB;  
Tube_polar(7,1) = PolarpipeB;  
Tube_polar(8,1) = PolarpipeB;  
Tube_polar(9,1) = PolarpipeB;  
Tube_polar(10,1) = PolarpipeB;  
Tube_polar(11,1) = PolarpipeB;  
Tube_polar(12,1) = PolarsquareB;  
Tube_polar(13,1) = PolarpipeA;  
Tube_polar(14,1) = PolarpipeA;  
Tube_polar(15,1) = PolarpipeA;  
Tube_polar(16,1) = PolarpipeB;  
Tube_polar(17,1) = PolarpipeB;  
Tube_polar(18,1) = PolarpipeB;  
Tube_polar(19,1) = PolarsquareB;  
Tube_polar(20,1) = PolarsquareB;  
Tube_polar(21,1) = PolarpipeA;  
Tube_polar(22,1) = PolarpipeA;  
Tube_polar(23,1) = PolarpipeA;  
Tube_polar(24,1) = PolarpipeB;  
Tube_polar(25,1) = PolarpipeB;  
Tube_polar(26,1) = PolarpipeB;  
Tube_polar(27,1) = PolarsquareB;  
Tube_polar(28,1) = PolarpipeB;  
Tube_polar(29,1) = PolarsquareB;
```

```
Tube_polar(30,1) = PolarpipeB;
Tube_polar(31,1) = PolarpipeB;
Tube_polar(32,1) = PolarpipeB;

%Local stiffness matrices
Keloc = Local_stiffness(Nodal_coordinates,Connect_table,Tube_outer_radius,Tube_inner_ra

%Rotation matrices to switch between local and global coordinates
R = Rotation(Nodal_coordinates,Connect_table);

%Global stiffness matrices
Ke = Global_stiffness(Keloc,R);

%Assemblage matrix
Ka = Assemblage_matrix(nnode,ndof_per_node,Connect_table,Ke);

%External force vector
Fa = zeros(nnode*ndof_per_node,1);

Frontimpact = -19826.38; %Newtons
Fa(19,1) = (Frontimpact/5);
Fa(22,1) = (Frontimpact/5);
Fa(25,1) = (Frontimpact/5);
Fa(31,1) = (Frontimpact/5);
Fa(34,1) = (Frontimpact/5);

%Boundary conditions appropiate for a front impact test
BC = zeros(nnode,ndof_per_node);
```

```
%fix the rear bulkhead, 1 means fixed
BC(1,1:3) = 1;
BC(2,1:3) = 1;
BC(18,1:3) = 1;
BC(17,1:3) = 1;

% Modifying Ka into KaSol and Fa into FaSol to get solution
beta = max(max(Ka))*10e9;
KaSol = Ka;
FaSol = Fa;
for i = 1:nnode
    for j = 1:ndof_per_node
        if BC(i,j) == 1
            KaSol((i-1)*ndof_per_node + j,(i-1)*ndof_per_node + j) = Ka((i-1)*ndof_per_node + j,(i-1)*ndof_per_node + j);
            FaSol((i-1)*ndof_per_node + j,1) = beta*0;
        end
    end
end

%Global displacement calculation
U = KaSol\FaSol;

%Processing of result
Reaction_forces = [];
Ulocal = zeros(2*ndof_per_node,nelem);
Uglobal = zeros(2*ndof_per_node,nelem);
Flocal = zeros(2*ndof_per_node,nelem);
```

```
axial_stress = zeros(nelem,1);

Ua = U;
Fa = Ka*Ua;
x = 1;
for i = 1:nnode
    for j = 1:ndof_per_node
        if BC(i,j)==1
            Reaction_forces(x,1) = Fa((i-1)*ndof_per_node + j,1);
            x = x+1;
        end
    end
end

%Parameters to be used when calculating the stiffness matrices
A = Cross_sectional_of_element(Tube_outer_radius,Tube_inner_radius);
L = Length_of_elements(Nodal_coordinates,Connect_table);
E = Elastic_modulus_of_elements(Elastic_modulus,Connect_table);
G = Shear_modulus_of_elements(Shear_modulus,Connect_table);
I = Moment_Inertia_of_elements(Tube_inertia);
J = Polar_moment_of_inertia(Tube_polar);
Kglobal = Global_stiffness(Keloc,R);
%Rotating local displacement and external force vectors to global coordinates
for i = 1:nelem
    Rot = R(:,:,i);
    for j = 1:ndof_per_node
        Uglobal(j,i) = Ua((Connect_table(i,1) - 1)*ndof_per_node + j,1);
        Uglobal(ndof_per_node + j,i) = Ua((Connect_table(i,2) - 1)*ndof_per_node + j,1);
    end

```

```
Ulocal(:,i) = Rot*Uglobal(:,i);
Flocal(:,i) = Keloc(:,:,i)*Ulocal(:,i);
%calculating stresses in each element
axial_stress(i,1) = max(Flocal(2,i))/A(i,1); %axial stress
shear_stress_yaxis(i,1) = (max(Flocal(1,i)))/A(i,1); %y axis shear stress
torsional_stress(i,1) = (max(Flocal(3,i)))*Tube_outer_radius(i,1))/Tube_polar(i,1);
bending_stress_yaxis(i,1) = (max(Flocal(3,i)))*Tube_outer_radius(i,1))/Tube_inertia;
end

%Organizing required stresses in a vector
stresses = zeros(1,4);

stresses(1,1) = max(axial_stress); %Tensile stress
stresses(1,2) = max(abs(shear_stress_yaxis(i,1))); %x Shear stress
stresses(1,3) = max(abs(torsional_stress(i,1))); %Torsional stress
stresses(1,4) = max(abs(bending_stress_yaxis(i,1))); %z Bending stress

%Calculating safety factors and organizing in a vector
SF = zeros(1,4);

SF(1,1) = abs(435/(stresses(1,1))); %Axial stress safety factor
SF(1,2) = 435/stresses(1,2); %Y Shear Stress safety factor
SF(1,3) = 435/stresses(1,3); %Torsional Stress safety factor
SF(1,4) = 435/stresses(1,4); %Y Bending Stress safety factor

%Calculating the parameter that are used to calculate the stiffness matrix
%Area of element calculation
function A = Cross_sectional_of_element(Tube_outer_radius,Tube_inner_radius)
[nelem,~] = size(Tube_inner_radius);
```

```
A = zeros(nelem,1);
for i = 1:nelem
    A(i,1) = pi*((Tube_outer_radius(i,1)^2)-(Tube_inner_radius(i,1)^2));
end
end

function L = Length_of_elements(Nodal_coordinates,Connect_table)
[nelem,~] = size(Connect_table);
L = zeros(nelem,1);
for i = 1:nelem
    L(i,1) = sqrt((Nodal_coordinates(Connect_table(i,1),1) - Nodal_coordinates(Conn
end
end

%Elastic modulus of elements
function E = Elastic_modulus_of_elements(Elastic_modulus,Connect_table)
[nelem,~] = size(Connect_table);
E = zeros(nelem,1);
for i = 1:nelem
    E(i,1) = Elastic_modulus(1,1);
end
end

%Shear modulus of elements
function G = Shear_modulus_of_elements(Shear_modulus,Connect_table)
[nelem,~] = size(Connect_table);
G = zeros(nelem,1);
for i = 1:nelem
    G(i,1) = Shear_modulus(1,1);
```

```
    end
```

```
end
```

```
%Moment of inertia of elements
```

```
function I = Moment_Inertia_of_elements(Tube_inertia)
```

```
    [nelem,~] = size(Tube_inertia);
```

```
    I = zeros(nelem,1);
```

```
    for i = 1:nelem
```

```
        I(i,1) = Tube_inertia(i,1);
```

```
    end
```

```
end
```

```
%Polar moment of Inertia of elements
```

```
function J = Polar_moment_of_inertia(Tube_polar)
```

```
    [nelem,~] = size(Tube_polar);
```

```
    J = zeros(nelem,1);
```

```
    for i = 1:nelem
```

```
        J(i,1) = Tube_polar(i,1);
```

```
    end
```

```
end
```

```
%3D Local stiffness matrix calculation
```

```
function Keloc = Local_stiffness(Nodal_coordinates,Connect_table,Tube_outer_radius,Tube
```

```
    [nelem,~] = size(Connect_table);
```

```
    Keloc = zeros(6,6,nelem); %each element is characterized by a 12x12 matrix
```

```
A = Cross_sectional_of_element(Tube_outer_radius,Tube_inner_radius);
```

```
L = Length_of_elements(Nodal_coordinates,Connect_table);
```

```
E = Elastic_modulus_of_elements(Elastic_modulus,Connect_table);
G = Shear_modulus_of_elements(Shear_modulus,Connect_table);
I = Moment_Inertia_of_elements(Tube_inertia);
J = Polar_moment_of_inertia(Tube_polar);

for i = 1:nelem

    %first row
    Keloc(1,1,i) = (A(i,1)*E(i,1))/L(i,1);
    Keloc(1,4,i) = -(A(i,1)*E(i,1))/L(i,1);

    %second row
    Keloc(2,2,i) = (12*E(i,1)*I(i,1))/L(i,1)^3;
    Keloc(2,3,i) = (6*E(i,1)*I(i,1))/L(i,1)^2;
    Keloc(2,5,i) = -Keloc(2,2,i);
    Keloc(2,6,i) = Keloc(2,3,i);

    %third row
    Keloc(3,2,i) = (6*E(i,1)*I(i,1))/L(i,1)^2;
    Keloc(3,3,i) = (4*E(i,1)*I(i,1))/L(i,1);
    Keloc(3,5,i) = -Keloc(3,2,i);
    Keloc(3,6,i) = Keloc(3,3,i)/2;

    %fourth row
    Keloc(4,1,i) = -(A(i,1)*E(i,1))/L(i,1);
    Keloc(4,4,i) = (A(i,1)*E(i,1))/L(i,1);

    %fifth row
    Keloc(5,2,i) = -(12*E(i,1)*I(i,1))/L(i,1)^3;
```

```
Keloc(5,3,i) = -(6*E(i,1)*I(i,1))/L(i,1)^2;
Keloc(5,5,i) = -Keloc(6,2,i);
Keloc(5,6,i) = Keloc(6,3,i);

%sixth row
Keloc(6,2,i) = (6*E(i,1)*I(i,1))/L(i,1)^2;
Keloc(6,3,i) = (2*E(i,1)*I(i,1))/L(i,1);
Keloc(6,5,i) = -Keloc(3,2,i);
Keloc(6,6,i) = Keloc(3,3,i)*2;
end

end

function R = Rotation(Nodal_coordinates,Connect_table)
[nelem,~] = size(Connect_table);
R = zeros(6,6,nelem);
L = Length_of_elements(Nodal_coordinates,Connect_table);
for i = 1:nelem
    %l
    R(1,1,i) = (Nodal_coordinates(Connect_table(i,2),1) - Nodal_coordinates(Connect_table(i,1),1));
    %m
    R(1,2,i) = (Nodal_coordinates(Connect_table(i,2),2) - Nodal_coordinates(Connect_table(i,1),2));
    R(2,1,i) = -R(1,2,i);
    R(2,2,i) = R(1,1,i);
    R(3,3,i) = 1;
    R(4,4,i) = R(1,1,i);
    R(4,5,i) = R(1,2,i);
    R(5,4,i) = -R(1,2,i);
    R(5,5,i) = R(1,1,i);
    R(6,6,i) = 1;
```

```

R(:,:,i) = R(:,:,i)/L(i,1);
end
end

%Global stiffness matrix calculation
function Kglobal = Global_stiffness(Keloc,R)
[sizeKglobal,~,nelem]=size(Keloc);
Kglobal = zeros(sizeKglobal,sizeKglobal,nelem);
for i = 1:nelem
    Rotate = R(:,:,i);
    Kglobal(:,:,:,i) = Rotate'*Keloc(:,:,:,i)*Rotate;
end
end

function Ka = Assemblage_matrix(nnode,ndof_per_node,Connect_table,Kglobal)
Ka = zeros(nnode*ndof_per_node,nnode*ndof_per_node);
[~,~,nelem]=size(Kglobal);
for ii = 1:nnode
    for jj = 1:nnode
        for k = 1:nelem
            if ii == Connect_table(k,1) && jj == Connect_table(k,1)
                for i = 1:ndof_per_node
                    for j = 1:ndof_per_node
                        Ka((ii - 1)*ndof_per_node + i,(jj - 1)*ndof_per_node + j) =
                    end
                end
            elseif ii == Connect_table(k,2) && jj == Connect_table(k,2)

```

```
        for i = 1:ndof_per_node
            for j = 1:ndof_per_node
                Ka((ii - 1)*ndof_per_node + i,(jj - 1)*ndof_per_node + j) =
            end
        end
    elseif ii == Connect_table(k,1) && jj == Connect_table(k,2)
        for i = 1:ndof_per_node
            for j = 1:ndof_per_node
                Ka((ii - 1)*ndof_per_node + i,(jj - 1)*ndof_per_node + j) =
            end
        end
    elseif ii == Connect_table(k,2) && jj == Connect_table(k,1)
        for i = 1:ndof_per_node
            for j = 1:ndof_per_node
                Ka((ii - 1)*ndof_per_node + i,(jj - 1)*ndof_per_node + j) =
            end
        end
    end
end
end
end
end
```